ISSN 1881-7815 Online ISSN 1881-7823

BST BioScience Trends

Volume 6, Number 2
April, 2012

IRCA BSSA

IACMHR

www.biosciencetrends.com

BST
BioScience Trends

ISSN: 1881-7815
Online ISSN: 1881-7823
CODEN: BTIRCZ
Issues/Year: 6
Language: English
Publisher: IACMHR Co., Ltd.

BioScience Trends is one of a series of peer-reviewed journals of the International Research and Cooperation Association for Bio & Socio-Sciences Advancement (IRCA-BSSA) Group and is published bimonthly by the International Advancement Center for Medicine & Health Research Co., Ltd. (IACMHR Co., Ltd.) and supported by the IRCA-BSSA and Shandong University China-Japan Cooperation Center for Drug Discovery & Screening (SDU-DDSC).

BioScience Trends devotes to publishing the latest and most exciting advances in scientific research. Articles cover fields of life science such as biochemistry, molecular biology, clinical research, public health, medical care system, and social science in order to encourage cooperation and exchange among scientists and clinical researchers.

BioScience Trends publishes Original Articles, Brief Reports, Reviews, Policy Forum articles, Case Reports, News, and Letters on all aspects of the field of life science. All contributions should seek to promote international collaboration.

Editorial Board

Editorial Office

Pearl City Koishikawa 603,
2-4-5 Kasuga, Bunkyo-ku,
Tokyo 112-0003, Japan
Tel: +81-3-5840-8764
Fax: +81-3-5840-8765
E-mail: office@biosciencetrends.com

BioScience Trends

Editorial and Head Office

Pearl City Koishikawa 603, 2-4-5 Kasuga, Bunkyo-ku,
Tokyo 112-0003, Japan

Tel: +81-3-5840-8764, Fax: +81-3-5840-8765
E-mail: office@biosciencetrends.com
URL: www.biosciencetrends.com

Editorial Board Members

CONTENTS

Volume 6, Number 2, 2012

Policy Forum

48 - 51 **Intractable and rare diseases research in Asia.**
Peipei Song, Jianjun Gao, Yoshinori Inagaki, Norihiro Kokudo, Wei Tang

Brief Report

52 - 56 **Influence of hapten density on immunogenicity for anti-ciprofloxacin antibody production in mice.**
Kun Hu, Xuanyun Huang, Yousheng Jiang, Junqiang Qiu, Wei Fang, Xianle Yang

Original Articles

57 - 62 **Study pattern of snoring and associated risk factors among medical students.**
Vatsal Singh, Saurabh Pandey, Abhijeet Singh, Rishabh Gupta, Rajendra Prasad, Mahendra Pal Singh Negi

63 - 69 **Effect of CXCR4 inhibitor AMD3100 on alkaline phosphatase activity and mineralization in osteoblastic MC3T3-E1 cells.**
Jing Luan, Yazhou Cui, Yongying Zhang, Xiaoyan Zhou, Genglin Zhang, Jinxiang Han

70 - 80 **Analysis of cytotoxicity induced by proinflammatory cytokines in the human alveolar epithelial cell line A549.**
Mitsuaki Muroya, Kyungho Chang, Kanji Uchida, Masahiko Bougaki, Yoshitsugu Yamada

81 - 88 **N-terminal PEGylation of human serum albumin and investigation of its pharmacokinetics and pulmonary microvascular retention.**
Ting Zhao, Yang Yang, Aizhen Zong, Haining Tan, Xinlei Song, Shuo Meng, Chunxia Song, Guangli Pang, Fengshan Wang

CONTENTS (*Continued*)

89 - 97 **Protective effect of *Lysimachia christinae* against acute alcohol-induced liver injury in mice.**
Junming Wang, Yasu Zhang, Ying Cui, Ju Liu, Binfeng Zhang

Case Report

98 - 102 **Intrahepatic cholangiocarcinoma with intrahepatic biliary lithiasis arising 47 years after the excision of a congenital biliary dilatation: Report of a case.**
Suguru Yamashita, Junichi Arita, Takashi Sasaki, Junichi Kaneko, Taku Aoki, Yoshihumi Beck, Yasuhiko Sugawara, Kiyoshi Hasegawa, Norihiro Kokudo

Guide for Authors

Copyright

(This journal was partially supported by a Grant-in-Aid for Scientific Research from Japan Society for the Promotion of Science.)

Policy Forum

DOI: 10.5582/bst.2012.v6.2.48

Intractable and rare diseases research in Asia

Peipei Song, Jianjun Gao, Yoshinori Inagaki, Norihiro Kokudo, Wei Tang*

Department of Surgery, Graduate School of Medicine, The University of Tokyo, Tokyo, Japan.

Summary **Intractable and rare diseases are an important public health issue and a challenge to medical care. In recent years, much progress has been made in the United States (US), the European Union (EU), and some parts of Asia including Japan, South Korea, and Taiwan, involving specific legislation to encourage discovery and development of orphan drugs, patients' advocacy organizations to provide vast information on intractable and rare diseases and improve patients' access to healthcare, special research programs to strengthen basic and applied research on intractable and rare diseases, and so on. While China is also actively promoting regulation of intractable and rare diseases, but still lags far behind the US, EU, Japan, and other countries and regions with orphan drug legislation. Based on systematic analysis of the current status and future perspectives for intractable and rare diseases in Asia, we recommend that three important aspects of support from government, patients' advocacy organizations and rare disease registry networks, special research programs and global information exchange platform, should be given great attention in promoting the development of intractable and rare diseases research in Asian countries.**

Keywords: Orphan diseases, orphan drugs, legislation, regulation

1. Introduction

Rare diseases are rare and often debilitating or even life-threatening diseases or conditions with a prevalence of less than 0.65‰-1‰, as defined by the World Health Organization (WHO). Intractable diseases mainly refer to rare diseases that have resulted mostly from unidentifiable causes and/or lack of clearly established or curable treatments. Intractable and rare diseases are an important public health issue and a challenge to medical care. In recent years, much progress has been made especially in the United States (US) and the European Union (EU), involving specific legislation to encourage discovery and development of orphan drugs, patients' advocacy organizations to provide vast information on intractable and rare diseases and improve patients' access to healthcare, special research programs to strengthen basic and applied research on intractable and rare diseases, and so on. In Asia, Japan, South Korea, and Taiwan have established systematic economic and regulatory incentives to encourage development of drugs for intractable and rare diseases. China is also actively promoting regulation of intractable and rare diseases, but it has not been included in the national health system and special legislation on orphan drugs has not been established until now. We did a systematic analysis on current status and future perspectives for intractable and rare diseases in Asia (*1*), which showed that three important aspects should be given great attention in promoting development of intractable and rare diseases research in Asian countries (Figure 1).

2. The support from government

The first aspect is support from government. It should include not only specific legislation to encourage manufacturers to develop orphan drugs, but also a sound supply mechanism and reimbursement system to ensure access to orphan drugs for patients with intractable and rare diseases. In Western countries, specific legislation on orphan drugs was first established in the US in 1983, then Australia in 1997, and the EU in 1999. In Asian countries and

**Address correspondence to:*
Dr. Wei Tang, Department of Surgery, Graduate School of Medicine, The University of Tokyo, 7-3-1 Hongo, Bunkyo-ku, Tokyo 113-8655, Japan.
E-mail: tang-sur@h.u-tokyo.ac.jp

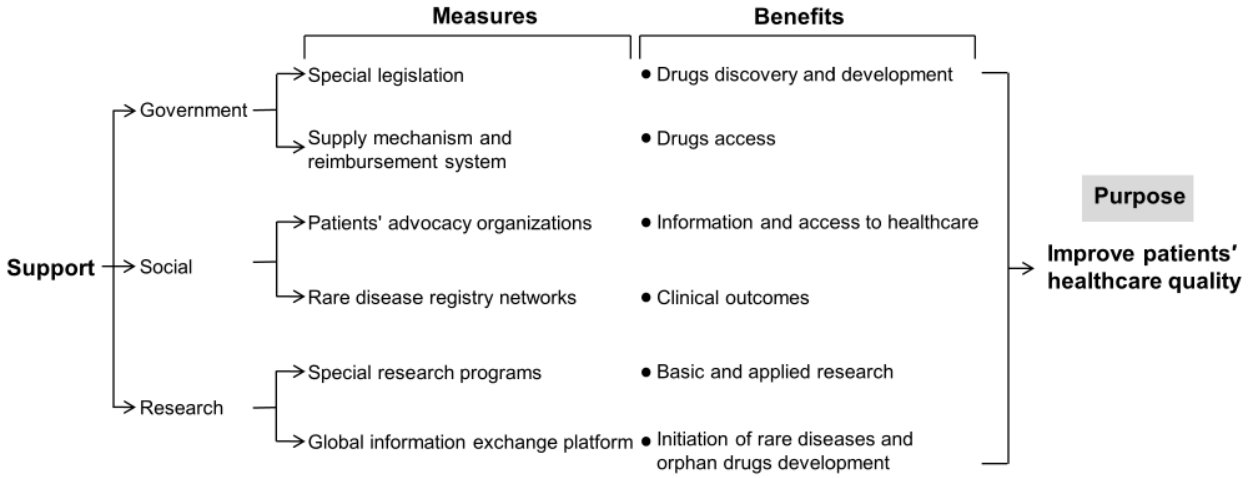

Figure 1. Three important supports in improving intractable and rare diseases in Asia.

regions, similar laws have also been established in Japan in 1993, Taiwan in 2000, and South Korea in 2003 (*2-4*). Incentives include financial subsidies, market exclusivity, tax credits, fee waivers, fast track approval, and protocol assistance, resulting in substantial improvements in treatment of patients with a range of intractable and rare diseases.

Furthermore, many measures for pricing and reimbursement have been taken to ensure access to orphan drugs for patients with intractable and rare diseases. For example, in Japan, the Japanese National Health Insurance (NHI) negotiates prices with pharmaceutical companies once a drug is approved for use, allowing a selling price of cost plus 10% for orphan drugs; 56 of 130 designated diseases in Japan are subject to reimbursement of medical expenses, with 30% of expenses paid by insurance companies and the rest paid by national and prefectures governments (*5*). In Taiwan, 77 approved orphan drugs and 40 special nutritional supplements can be imported, and the reimbursement cap is 70% of actual expenses but families that qualify for low-income status can receive reimbursement for up to 100% of drugs and nutritional supplements for patients (*6*). While China is actively preparing to regulate development of orphan drugs, but specific legislation on orphan drugs has not been established, current regulations only set forth general criteria to accelerate registration and approval of orphan drugs, detailed rules have not been implemented and incentives on orphan drugs imports have not been proposed until now. Moreover, although some regions, such as Shanghai and Shandong, have started to put out a trial use for reimbursement, the nationwide supply mechanism and reimbursement system have not been established, hampering access to orphan drugs for patients with intractable and rare diseases.

3. Social support

The second aspect is social support from patients' advocacy organizations and rare disease registry networks. It could provide quality information and a networking system to facilitate interaction among patients, clinicians, researchers, the pharmaceutical industry, and governmental bodies. Major patients' advocacy organizations in Western countries, such as the National Organization for Rare Disorders (NORD) in the US and the European Organization for Rare Diseases (EURORDIS) in Europe, can provide vast information on intractable and rare diseases and improve patients' access to healthcare. In Asia, many patients' advocacy organizations have also been established, such as the Japanese Intractable Disease Information Center (*http://www.nanbyou.or.jp*), the South Korean Organization for Rare Diseases (*http://www.kord.or.kr*), the Taiwan Foundation for Rare Disorders (TFRD) (*http://www.tfrd.org.tw*), the Hemophilia Home of China (HHC) (*http://www.xueyou.org/china*), and so on.

In recent years, progress has been made in dissemination of knowledge and information by established patients' advocacy organizations worldwide, but clinical studies on orphan drugs still encounter challenges due to the small size of the trial population and the fact that patients are often geographically dispersed. It is necessary to establish a global system for patient registration in order to promote epidemiological and basic research and improve the clinical outcome for patients with intractable and rare diseases (*7*). In Western countries, some web-based resources have been established, such as the Rare Diseases Clinical Research Network (RDCRN) in the US and the Orphanet in Europe, with the purpose of facilitating collaboration on clinical

outcomes as well as sharing advanced experience to minimize delays in access to orphan drugs for patients with intractable and rare diseases. In Asian countries, there are also many explorations on rare disease registry networks, for example, in China, a patients' advocacy organization of the China-Dolls Care and Support Association started voluntary registration in May 2010 and has registered 30 rare diseases with 3,000 cases, about 1,000 of which are osteogenesis imperfecta (*8*). Moreover, a comprehensive online database for registration of rare diseases cases has been created in 2012 *(http://www.chinards.com*), clinical data on around 50 types of rare diseases will be registered (*9*).

4. Support from special research

The third aspect is support from special research programs and the global information exchange platform. Special research programs strengthening basic and applied research on intractable and rare diseases would benefit patients with better diagnosis and more treatment choices. In Western countries, many special research centers or projects have been established to support research on rare diseases and development of orphan drugs, such as the Office of Rare Diseases Research (ORDR) in the US, and the Rare Disease Task Force (RDTF) in the EU. In Asian countries, the Specified Disease Treatment Research Program was established in Japan in 1972 with the support of the Ministry of Health, Labor, and Welfare, and 130 diseases have been the subject of special research programs and research grants from government sources expanded to 10 billion yen in 2010 (*10*). In South Korea, the Research Center for Rare Diseases (RCRD) was established in 2008 with the support of the Ministry of Family Affairs, Health and Welfare. The Center oversees 3 collaborative research projects, 9 single-center research projects, and 7 clinical research networks in order to provide a foundation for research on rare diseases and orphan drugs. While in China, research support comes mainly from the National Natural Science Foundation of China (NSFC). Data showed that 366 projects (involving 32 rare diseases) were funded by the NSFC from 1999 to 2007 with total funding of 89.358 million RMB and annual funding of about 10 million RMB, compared to just 1/10th of similar funding in the US (*11*).

Furthermore, the acquisition and diffusion of scientific knowledge and research results is the vital basis for identification of diseases, and most importantly, for research into new diagnostic and therapeutic procedures. So it is urgently needed to establish the global information exchange platform to promote information exchange among researchers active in the field of rare diseases and various difficult and complicated diseases research in the world. It is interestingly noted that there is a positive relationship between the number of published papers on a particular rare disease and the likelihood of initiation of rare diseases and orphan drugs development programs (*12*), but in contrast, few professional journals covering the topic of intractable and rare diseases have been established worldwide. In this context, the unique international professional journal in Asia − *Intractable & Rare Diseases Research* (*http://www.irdrjournal.com*), was launched in 2012, with the purpose of cultivating a global medical and drug information network on intractable and rare disease research, especially developing an Asian information exchange platform, to improve the quality of life for patients with intractable and rare diseases.

5. Conclusion

In conclusion, intractable and rare diseases are an important public health issue and a challenge to medical care. In recent years, much progress has been made in some parts of Asia, including Japan, South Korea, and Taiwan, in promoting the development of intractable and rare diseases research as well as improving the healthcare quality for patients with those diseases. China is also actively promoting the regulation of intractable and rare diseases, but still lags far behind the US, EU, Japan, and other countries and regions with orphan drug legislation. Three important aspects of the support from government, patients' advocacy organizations and rare disease registry networks, special research programs and global information exchange platform, should be given great attention in promoting the development of intractable and rare diseases research, especially for China and other countries in Asia.

Acknowledgements

This work was supported by the Center for Medical Standards Research, IRCA-BSSA Group.

References

1. Song PP, Gao JJ, Inagaki Y, Kokudo N, Tang W. Rare diseases, orphan drugs, and their regulation in Asia: Current status and future perspectives. Intractable Rare Dis Res. 2012; 1:3-9.
2. Villa S, Compagni A, Reich MR. Orphan drug legislation: Lessons for neglected tropical diseases. Int J Health Plann Manage. 2009; 24:27-42.
3. Taruscio D, Capozzoli F, Frank C. Rare diseases and orphan drugs. Ann Ist Super Sanita. 2011; 47:83-93.
4. Rinaldi A. Adopting an orphan. EMBO Rep. 2005; 6:507-510.
5. Japan Intractable Diseases Information Center. What is an intractable disease? *http://www.nanbyou.or.jp*

(accessed March 7, 2012).
6. Taiwan Foundation for rare disorders. About rare diseases. *http://www.tfrd.org.tw* (accessed March 9, 2012).
7. Forrest CB, Bartek RJ, Rubinstein Y, Groft SC. The case for a global rare-diseases registry. Lancet. 2011; 377:1057-1059.
8. Zhang YJ, Wang YO, Li L, Guo JJ, Wang JB. China's first rare-disease registry is under development. Lancet. 2011; 378:769-770.
9. Han JX, Cui YZ, Zhou XY. Rare diseases research in China: Opportunities, challenges, and solutions. Intractable Rare Dis Res. 2012; 1:10-12.
10. Kodama T, Tomita N. Global movement for diagnosis and treatment of rare/intractable diseases. Journal of the National Institute of Public Health. 2011; 60:105-111. (in Japanese)
11. Ding JX, Sun XD, Ji N, Shao WJ. The accessibility assessment on orphan drugs and legal system research in China and America. The Chinese Pharmaceutical Journal. 2011; 46:1129-1132. (in Chinese)
12. Tang W, Makuuchi M. Intractable and rare diseases research. Intractable Rare Dis Res. 2012; 1:1-2.

(*Received March 28, 2012; Accepted April 9, 2012*)

Brief Report

DOI: 10.5582/bst.2012.v6.2.52

Influence of hapten density on immunogenicity for anti-ciprofloxacin antibody production in mice

Kun Hu[1], Xuanyun Huang[2], Yousheng Jiang[1], Junqiang Qiu[1], Wei Fang[1], Xianle Yang[1,*]

[1] *Shanghai Ocean University, Shanghai, China;*
[2] *East China Sea Fishery Research Institute, Chinese Academy of Fishery Sciences, Shanghai, China.*

Summary **To generate antibodies against small molecules, it is necessary to couple them as haptens to large carriers such as proteins. However, the immunogenicity of the conjugates usually has no linear correlation with the hapten-protein ratio, which may lead to large variations in the character of the desired antibodies. In the present study, ciprofloxacin (CPFX) was coupled to bovine serum albumin (BSA) in five different proportions using a modified carbodiimide method. The conjugates were characterized qualitatively by spectrophotometric absorption and electrophoresis methods. Mass spectrometry and the trinitrobenzene sulfonic acid method were adopted to assay the density of conjugates quantitatively. As a result, CPFX-BSA conjugates with various hapten densities (21-30 molecules per carrier protein) were obtained. After immunization in mice, ELISA tests showed that the antisera titer increased gradually with the increase of hapten density. The antibody obtained from the mice showed high sensitivity toward CPFX. These results revealed the relationship between hapten density and immunogenicity as well as an optimized conjugation approach for immunization purposes.**

Keywords: Hapten density, conjugation, immunogenicity, ciprofloxacin

1. Introduction

A small hapten (molecular weight < 1,000) is usually not immunogenic by itself (*1,2*). It is well-known that immunogenicity can be acquired when a hapten is coupled with a macromolecule carrier, such as a protein, peptide or synthetic amino acid (*3*). A hapten is generally coupled to a carrier protein through the ε-amino group. The carrier protein can increase both the strength and specificity of the antibody response efficiently. The coupling ratio of the hapten-protein is usually important for the properties of the antibody induced by the modified hapten. In most cases, increasing of the coupling ratio can enhance the strength and specificity of the immune responses (*4*). On the other hand, the higher coupling ratio may decrease the activity of antibodies. The possible relationship between the immunogenicity and the hapten-protein ratio may cause large variations in the character of the desired antibodies. Screening an optimal hapten density for the conjugation is significant to improve the binding efficiency of hapten-protein conjugation (*5*).

Ciprofloxacin (CPFX) is an antibacterial agent applied as a veterinary medicine. The CPFX residues in consumed animal tissues raise potential risks for development of drug-resistance and chronic adverse effects in public health (*6*). The maximum residue limits (MRLs) of CPFX in food stuffs of animal origin were established by the European Union (*7*). Antibody-antigen reactions were extensively used to detect and quantify the CPFX residue in biological fluids. Such immunoassays were developed for determination of protein antigens as well as small molecule haptens. The central problem of fast detection by immunoassays was the availability of a specific antibody with high titer.

Although there are reports about CPFX conjugation (*1,8*), the varying hapten density leads to the unstable character of the antibodies to a great extent. Hence, the optimized coupling ratio of CPFX-bovine serum

**Address correspondence to:*
Dr. Xianle Yang, Shanghai Ocean University, 999 Hucheng-huan Road, Lingang New City, Shanghai 201306, China.
E-mail: xlyang@shou.edu.cn

albumin (BSA) has still not been attained. In our previous studies, a monoclonal antibody (mAb) against small hapten-CPFX with high affinity and specificity was produced and was used for rapid CPFX immunoassays in food stuff of animal origin (*9*). Furthermore, with the CPFX-specific mAbs, an indirect competitive enzyme-linked immunosorbent assay (ELISA) was developed for the sensitive and specific detection of CPFX residues in fishery products (*10*).

In this study, CPFX as a hapten was covalently attached to BSA by a modified carbodiimide method using 1-ethl-3-carbodiimide methiodide (EDC) (*1,8*). To generate the anti-CPFX antibody, the hapten density was optimized to improve the binding efficiency. It could be a benefit to the approach for preparing antibodies with good titre and sensitivity, which was significant for the CPFX immunoassay.

2. Materials and Methods

2.1. *Chemicals and animals*

CPFX (content ≥ 98.5%) was purchased from Zhejiang Guobang Pharmaceutical Co., Ltd. (Shangyu, Zhejiang, China). BSA was obtained from Dingguo Biotechnology Co., Ltd. (Beijing, China). Trinitrobenzene sulfonic acid (TNBS) was from Sigma-Aldrich (St Louis, MO, USA). EDC (purity ≥ 99.3%) was obtained from Yanchang Confident Biochemical Technology Co., Ltd. (Shanghai, China). Chemical reagents such as NaCl and K_2HPO_4 were from Guoyao Chemical Reagent Co., Ltd. (Shanghai, China). All the chemical reagents and solutions used in this paper were analytical grade. The buffer was prepared with double distilled water.

Individual Balb/c mice were purchased from the Second Military Medical University (Shanghai, China). All mice were housed under controlled conditions and received food and water *ad libitum*. All animal experiments were performed in accordance with the guidelines of Regulation on Animal Experimentation and were approved by State Scientific and Technological Commission, State Council, China.

2.2. *Coupling of the CPFX hapten and carrier protein*

The conjugates of BSA and CPFX were synthesized by a modified carbodiimide method using EDC (*11*). The conjugation reaction was performed with five different molecular ratios of BSA and CPFX (1:160, 1:320, 1:480, 1:640, and 1:800). CPFX was mixed with BSA (2 mg/mL) and EDC (60 mg/mL) while the reaction was carried out in phosphate buffer solution (pH 5.0) and incubated at 28°C for 2 h. The mixture was dialyzed against the same buffer for 2 days and then freeze-dried. The CPFX-BSA conjugates C1, C2, C3, C4, and C5 (see Table 1 for the molecular ratios) obtained were stored at –20°C until use.

2.3. *Spectrophotometric analysis*

The numbers of free Lys residue ε-amino groups in BSA conjugates were determined by the TNBS method (*12*). Conjugate samples (0.2 mg each) were dissolved in 1 mL of 0.1 M sodium carbonate solution and then 0.5 mL of 0.01% TNBS solution was added. After incubation for 2 h at 37°C, 0.5 mL of 10% sodium dodecyl sulfate (SDS) solution and 0.25 mL of 1 M hydrochloric acid solution were added to terminate the reaction. The absorbance was measured at 335 nm. The number of amino groups left on the BSA molecule after the coupling reaction was determined by the difference of optical density (OD) values between the control group and the coupling group.

CPFX-BSA conjugates (C1-C5) were scanned from 250 nm to 350 nm using a Spectronic UV-Vis Spectrophotometer (Thermo Fisher Scientific Inc., Madison, WI, USA). The resolution length range and scanning speed were 1 nm and 1 nm/sec, respectively.

2.4. *Gel electrophoresis analysis*

Apparent molecular size of CPFX-BSA conjugates was analyzed by SDS-polyacrylamide gel electrophoresis (SDS-PAGE) using a PowerPac 300 type electrophoresis apparatus (Bio-Rad Laboratories, Hercules, CA, USA). The conjugates (C1-C5) were dissolved in sample buffer (10 mM Tris, 1 mM EDTA, 2.5% SDS, and 5% mercaptoethanol, pH 8.0) with a final concentration of 1 mg/mL. After heating at 100°C for 5 min, 10 μL of each sample was loaded. The samples were separated at 80 V in the stacking gel and 100 V in a 12% separating gel. The protein samples were stained for 4 h using the Coomassie Brilliant Blue staining method and then de-stained by de-staining solution until the background was transparent.

2.5. *Mass spectrometry analysis*

The Agilent 1100 hp LCQ DECA Liquid Chromatography Mass Spectrum (Agilent Technologies, Santa Clara, CA, USA) was used to determine the molecular weights of the conjugates. The conjugates were dissolved in methanol and 10 μL of each was collected for injection. The chromatographic conditions were as follows. For gradient elution, ratios of mobile phases A and B (phase A, 20 mM sodium acetate + 0.018% triethylamine + 0.3% tetrahydrofuran, pH 7.2; phases B, 100 mM sodium acetate/acetonitrile/methyl alcohol (20:40:40, v/v/v, pH 7.2)) were 95:5 (v/v) during 0-5 min and gradually changed to 5:95 (v/v) during 5-17 min. The chromatography was performed at 25°C with a flow rate of 0.2 mL/min using a Zorbax 300SB-C18 column (Agilent Technologies). The workstation was operated in positive-ion linear mode with the following parameters:

Table 1. Determination of hapten density of CPFX-BSA conjugates by chemical TNBS method and mass spectrometry analysis

Conjugates	BSA-CPFX mole ratios in the reaction mixture	Chemical TNBS method		Mass spectrometry analysis		ΔM/Mh[a] (hapten density)
		Observed amount of amino group consumed (%)	Calculated amount of amino group consumed (moles/BSA molecule)	Observed molecular mass (Da)	Mass variation (ΔM)	
Control	1:0	0	0 (0)	66,210	0	0 (0)
C1	1:160	36.2	21.7 (22)[b]	73,015	6,805	20.6 (21)[b]
C2	1:320	41.5	24.9 (25)	74,202	7,992	24.1 (25)
C3	1:480	41.5	24.9 (25)	74,622	8,412	25.4 (26)
C4	1:640	47.1	28.2 (28)	75,216	9,006	27.2 (28)
C5	1:800	49.9	29.9 (30)	76,100	9,890	29.9 (30)

[a] Mh indicates molecular weight of CPFX hapten, Mh = 331.1; [b] Values in parentheses indicate deduced moles of CPFX binding on each BSA molecule.

20 kV accelerating voltages, 100 nsec extraction delay, and 500 m/z low mass gate (*13*). The molecular weight of the sample was analyzed with Data Explore™ software (Applied Biosystems, Carlsbad, CA, USA).

2.6. *Immunization*

The female 4 weeks old Balb/c mice were kept in the sterile room with feeding every day. CPFX-BSA conjugates (150 μg each) and Freund's complete adjuvants were mixed in the ratio of 1:1 to immunize the Balb/c mice. The antigen sample with adjuvant was intraperitoneally injected into the mice and boosted after two weeks. One week later, the mice were immunized again in the same way without adjuvant. After 10 days, a part of the blood sample was collected to determine the antisera titer by ELISA, and then 150 μg each of CPFX-BSA conjugate was injected into the mice by tail intravenous injection. Three days later, the blood sample of the mice was collected and kept at 4°C overnight. The sample was centrifuged at 7,000 rpm for 10 min. The supernatant was collected to determine the titer and lyophilized.

2.7. *ELISA*

A hundred μL of CPFX-conjugated ovalbumin, which was prepared in our laboratory (*10*), with a concentration of 400 ng/mL was added into wells of an ELISA plate (Dingguo Biotechnology Co., Ltd.) and incubated at 37°C for 1 h. After coating, the wells were washed 3 times (3 min each) with phosphate buffer containing 0.5% Tween-20 (washing solution). The wells were blocked with 200 μL 5% milk and stored at 4°C overnight. Two additional wells were filled with 100 μL buffer to serve as a control for nonspecific binding. After blocking, 100 μL of immunized mice sera (antisera) were added to the wells and incubated for 1 h at 37°C. After rinsing with washing solution, 100 μL of goat anti-mouse IgG conjugated with horseradish peroxidase (HRP) (1:6,000) was added and incubated for 0.5 h at 37°C. After washing 3 times, color development was initiated by adding 100 μL of 3,3',5,5'-tetramethylbenzidine (TMB)/H_2O_2 and, 10 min later, stopped by adding 50 μL of 2 M H_2SO_4. The absorbance was determined at 450 nm with a BioTek EL311 micro-plate reader (BioTek, Winooski, VT, USA).

2.8. *Detection of the sensitivity of antisera by indirect competitive ELISA*

The procedure of indirect competitive ELISA was similar to the ELISA process with some modifications. After blocking, 50 μL of suitably diluted antisera was added to each well and 50 μL samples of various concentrations of CPFX solution (2, 4, 6, 8, and 10 ng/mL) were added. The subsequent steps were the same as described above.

3. Results and Discussion

CPFX-BSA conjugates with various hapten densities were synthesized as described in Materials and Methods. In UV scanning spectra (250-350 nm), the maximum absorption peaks of BSA, CPFX, and CPFX-BSA conjugates were at 280, 270, and 275 nm, respectively, and the higher binding molar ratios of the carrier hapten-protein (C1-C5) correlated with stronger UV absorbance (data not shown). SDS-PAGE analysis of the conjugates (C1-C5) revealed that the molecular weights of the conjugates were larger than that of BSA (data not shown). These results suggest the success of the coupling reaction between CPFX and BSA.

The amount of free amino acid residues on the BSA molecule before and after coupling reaction was determined using the TNBS method and the amount of CPFX binding to the carrier BSA was calculated. With mass spectrometry analysis, the density of the hapten bound to the carrier protein was also determined by comparing the variations of molecular weight. As shown in Table 1, hapten densities of the conjugates increased gradually with increase of the hapten-protein molar ratios.

Next, mice were immunized with the conjugates C1-C5 and the antisera titer was determined by ELISA

as described in Materials and Methods. As shown in Figure 1A, the titer rose according to the increase of the ratio between carrier protein and hapten and reached 5.76×10^5 at the ratio of 1:800 (C5). In contrast, the antisera titer with different hapten density did not show a significant difference (data not shown). The sensitivity of the antibody produced by the coupling reaction was determined by the ELISA method. The standard dilution curve analysis of the antibody prepared by the conjugate C5 exhibited good sensitivity up to a level of ng/mL (Figure 1B). By indirect competitive ELISA, the IC_{50} value was 10.7 ng/mL (data not shown).

To acquire immunogenicity, the hapten needs to be coupled with a macromolecule (such as a carrier protein) and become a complete antigen. Generally, small molecules can covalently bind to a carrier protein. Different coupling methods are chosen and designed based on the different functional groups of the hapten. By the traditional EDC method, the conjugation efficiency for CPFX is not high enough as expected and the max value of hapten densities can reach 16 (*1*). In the traditional method, NHS is used as the activating group and can promote the carboxyl group to couple with the amino group (*1,8*), while the modified one without NHS can lead to a higher coupling efficiency. Unlike other fluoroquinolones, CPFX is abundant in amino and carboxyl groups. To couple CPFX, NHS may not be necessary for this reaction. In this method, the extra hapten and EDC were removed by extensive dialysis to ensure the accuracy of the following analysis. BSA is widely used as a carrier protein, because it contains various amino residues on the surface. Compared to tyrosine, tryptophan and imidazole residues, the lysine residue epsilon amino group allows CPFX hapten to couple much more easily by a covalent bond (*1*).

The production of the conjugates can be confirmed by SDS-PAGE. The greater amount of protein molecule bound by the hapten and the larger molecular weight of the conjugate correspond with the shorter migration distance. Electrophoresis analysis can analyze the process of conjugate coupling. Compared with the molecular weight of BSA (66 kDa) (*14*), the differences between different conjugates are very slight (3 kDa) (data not shown). As a result, the differences between the migration distances of the conjugates (C1-C5) were not significant. The hapten density of the conjugates can be calculated more precisely by comparing the molecular weight variations of the conjugates with mass spectrometry. There are 59 lysine residues in the BSA molecule (*14*), in which 26 residues exist on the surface (*5*). The results show that the number of CPFX molecules did not increase linearly with the increase of the reaction ratio between CPFX and BSA; however, the number of CPFX bound to each BSA molecule can reach as high as 30 (Table 1). It can be explained that the BSA molecule exists in an isomeric structure with high helicity in the environment at pH 5.0 (*15*). This structure contains a part of lysine, which normally exists in the inner part of the protein, exposed on the surface of the carrier protein molecule. Another explanation could be that the hapten can couple with other amino residues besides lysine.

The maximum absorption wavelength in the spectrogram can be used as the basis for the characteristic group analysis of the conjugates. Compared to the characteristic absorption peaks of the carrier protein and hapten, the ones of the conjugates (C1-C5) were shifted (data not shown). The results, which indicate the presence of distinctive groups in the

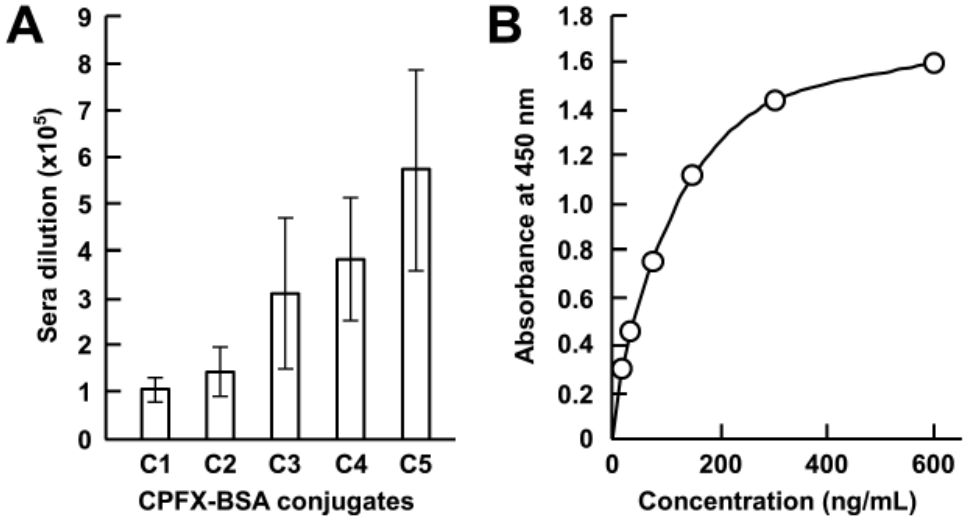

Figure 1. Qualitative analysis of the antibodies generated by various CPFX-BSA conjugates. (A) Titers of antiserum against CPFX obtained from mice immunized with CPFX-BSA conjugates with various hapten densities. Mice were immunized with C1, C2, C3, C4, and C5 having average hapten densities of 21, 25, 26, 28, and 30, respectively. **(B)** Standard dilution curve analysis of antibody generated by the conjugate C5.

conjugates, could confirm the specific binding of BSA and CPFX. The UV spectra of the conjugates suggested that the increase of the hapten-protein ratio caused the absorbance of the conjugate to increase gradually. This also validated the conclusion that the hapten density increased with the increase of hapten-protein ratio.

The amount of hapten bound to the carrier protein is an important factor which affects the quantity and quality of the antibody produced by the conjugate. However, the titer and affinity of the antibody did not increase linearly with the increase of the amount of the hapten bound to carrier protein (*1*). Generally, the binding affinity was optimal when 15 to 30 hapten molecules had bound to the surface of the carrier protein (*5*). The greater amount of hapten bound to the carrier protein, the higher, stronger and more specific antibody titer was produced by their conjugates. However, the immune reaction induced by the conjugate bound with less hapten was slow while the antibody produced by it had a higher affinity. The acquirement of optimal hapten density was important for the conjugate in the preparation of antibody. In addition, the antisera displayed better sensitivity than previously published (*2*). These findings could contribute to improving immunoassay methods.

In conclusion, the protein-hapten mole ratio could increase the hapten density of conjugates, which has a great influence on the immunogenicity of CPFX. An optimum molar ratio of CPFX-BSA conjugates could induce antibodies with good sensitivity, which was suitable to be applied for immunization purposes.

Acknowledgements

This study was supported by the 863 Program (Grant No. 2011AA10A216) and Special Fund for Agro-scientific Research in the Public Interest (Grant No. 201203085).

References

1. Erlanger BF. The preparation of antigenic hapten-carrier conjugates: A survey. Methods Enzymol. 1980; 70:85-104.
2. Duan JH, Yuan ZH. Development of an indirect competitive ELISA for ciprofloxacin residues in food animal edible tissues. J Agric Food Chem. 2001; 49:1087-1089.
3. Fuentes M, Palomo JM, Mateo C, Venteo A, Sanz A, Fernández-Lafuente R, Guisan JM. Optimization of the modification of carrier proteins with aminated haptens. J Immunol Methods. 2005; 307:144-149.
4. Marco MP, Gee S, Hammock BD. Immunochemical techniques for environmental analysis II. Antibody production and immunoassay development. Trends Analyt Chem. 1995; 14:415-425.
5. Singh KV, Kaur J, Varshney GC, Raje M, Suri CR. Synthesis and characterization of hapten-protein conjugates for antibody production against small molecules. Bioconjug Chem. 2004; 15:168-173.
6. Hernandez M, Aguilar C, Borrull F, Calull M. Determination of ciprofloxacin, enrofloxacin and flumequine in pig plasma samples by capillary isotachophoresis-capillary zone electrophoresis. J Chromatogr B Analyt Technol Biomed Life Sci. 2002; 772:163-172.
7. Diario Oficial de las Comunidades Europeas (DOCE), August 18, 1990. Council Regulation No. 2377/90 L224, 991, 2601.
8. Zhou Y, Li Y, Wang Z, Tan J, Liu Z. Synthesis and identification of the antigens for ciprofloxacin. Chinese Journal of Veterinary Science. 2006; 26:200-203. (in Chinese)
9. Jiang Y, Huang X, Hu K, Yu W, Yang X, Lv L. Production and characterization of monoclonal antibodies against small hapten-ciprofloxacin. Afr J Biotechnol. 2011; 10:14342-14347.
10. Hua K, Huang X, Jiang Y, Fang W, Yang X. Monoclonal antibody based enzyme-linked immunosorbent assay for the specific detection of ciprofloxacin and enrofloxacin residues in fishery products. Aquaculture. 2010; 310:8-12.
11. Huang X, Hu K, Fang W, Jin Y, Yang X. Preparation of ciprofloxacin-carrier protein conjugation and identification of its products. Journal of Shanghai Fishery University. 2008; 17:585-590. (in Chinese)
12. Habeeb AF. Determination of free amino groups in proteins by trinitrobenzenesulfonic acid. Anal Biochem. 1966; 14:328-336.
13. Pingbo Z, Yamamoto K, Wang Y, Banno Y, Fujii H, Miake F, Kashige N, Aso Y. Utility of dry gel from two-dimensional electrophoresis for peptide mass fingerprinting analysis of silkworm protein. Biosci Biotechnol Biochem. 2004; 68:2148-2154.
14. Hirayma K, Akashi S, Furuya M, Fukuhara K. Rapid confirmation and revision of the primary structure of bovine serum albumin by ESIMS and Frit-FAB LC/MS. Biochem Biophys Res Commun. 1990; 173:639-646.
15. Rosenoer VM, Oratz M, Rothschild MA, eds. Albumin Structure, Function and Uses. Pergamon, New York, USA, 1977.

(*Received September 19, 2011; Revised November 29, 2011; Re-revised February 22, 2012; Accepted March 9, 2012*)

Original Article

DOI: 10.5582/bst.2012.v6.2.57

Study pattern of snoring and associated risk factors among medical students

Vatsal Singh[1], Saurabh Pandey[1], Abhijeet Singh[1], Rishabh Gupta[1], Rajendra Prasad[1,*], Mahendra Pal Singh Negi[2]

[1] *Department of Pulmonary Medicine, CSM Medical University, Lucknow, Uttar Pradesh, India;*
[2] *Institute for Data Computing and Training, Lucknow, Uttar Pradesh, India.*

Summary **Snoring can impair lifestyle and cause late cardiopulmonary complications. Early detection of snoring and timely intervention during adolescence can avoid complications. A single center prospective cross-sectional study was conducted in 548 undergraduate 17-25 years old undergraduate medical students of CSM Medical University, Lucknow, who were interviewed on the basis of the modified Berlin Questionnaire along with their room-partners describing their snoring habits. Ninety-seven (17.7%) subjects were found to be snorers. Risk factors *viz.* day time sleepiness (European Stroke Scale (ESS) scores), smoking habits, alcohol intake, neck size and BMI were observed. The proportion of males, smokers, BMI, neck size and ESS scores were significantly ($p < 0.001$) higher in snorers than non snorers. Logistic regression found sex (OR = 5.73, 95% CI = 2.11-15.61), smoking (OR = 2.20, 95% CI = 0.97-5.62), BMI (OR = 3.16, 95% CI = 1.09-7.36) and neck size (OR = 2.03, 95% CI = 0.79-6.35) as significant ($p < 0.01$) independent risk factors for snoring. A clinically significant form of Sleep Disordered Breathing (Habitual snoring, ESS score ≥ 11 and BMI ≥ 25 kg/m^2) was suspected in 4 (0.7%) students. The findings of this study may also be validated in the general population. The study concluded that male undergraduate medical students are at a high risk for developing snoring habits.**

Keywords: Snoring, medical students, sleep disordered breathing, independent risk factors

1. Introduction

Snoring is a very common yet under recognized phenomenon in late adolescence. In recent years, snoring has been identified as not merely a nuisance factor for the co-sleeper but significantly associated with cardiopulmonary diseases. Epidemiologic investigation of snoring patterns has been hampered by difficulties in obtaining valid data from an adequate population based sample. Different sleep studies have reported a varied prevalence of snoring and related disorders among children and young adults (*1-3*). The variations arise due to laboratory constraints, different diagnostic criteria and association of other commonly found causative conditions, such as tonsillar hypertrophy, asthma, hypertension, gastro-esophageal reflux disorder and structural abnormalities in this age group (*4,5*).

Snoring may be only a symptom of a broad spectrum of obstructive respiratory abnormalities, clinically identified as Sleep Disordered Breathing (SDB) (*1*). SDB presents as partial respiratory tract obstruction as in Upper Airway Resistance Syndrome (UARS) or as complete obstruction resulting in Obstructive Sleep Apnea (OSA) with manifestations like snoring, episodes of hypopnea or apnea according to the extent and duration of obstruction (*6*). There are specific factors responsible for each of the clinical features of SDB which are not fully understood. Studies have indicated that habitual snoring is associated with hypertension, cardio-vascular disease and excessive daytime sleepiness (EDS) (*7*). Recurrent episodes of nocturnal asphyxia and arousal from sleep

**Address correspondence to:*
Dr. Rajendra Prasad, Department of Pulmonary Medicine, CSM Medical University, Lucknow 226003, Uttar Pradesh, India.
E-mail: rprasadkgmc@gmail.com

induce secondary physiological responses that may eventually produce cardiovascular, hemodynamic and neuropsychiatric manifestations (*8*). The behavioral problems may include excessive daytime sleepiness, aggressiveness, inattention, headache, poor memory and difficulty in socialization (*9*). Many underlying causes of SDB among adults such as obesity, start progressing during late adolescence. The effect of raised testosterone at puberty, which increases mass of pharyngeal muscles, cannot also be neglected. Therefore, there is an opportunity for intervention in development of SDB and related complications in the late adolescent age group.

Medical students typically start their education during late adolescence. There is sudden change from their active school life to a sedentary lifestyle. These students are exposed to risk factors of snoring like smoking and alcohol intake. Snoring might be the earliest manifestation of SDB in these students. There is a paucity of literature evaluating snoring habits among college students especially among medical students. Thus, in the present study, we have attempted to determine the pattern of snoring among the population of undergraduate medical students using a standardized questionnaire survey (*10,12-19*) and correlating the associated risk factors with snoring.

2. Materials and Methods

2.1. *Study population*

A single-center cross-sectional study was carried out in a sample of medical students of both genders ranging in age from 17 to 25 years between November 2010 and February 2011. Out of the 600 healthy individuals approached who qualified for the inclusion/exclusion criteria, 548 gave their consent and were included in the study. As inclusion criteria, we excluded subjects having systemic diseases like connective tissue disorders, chronic liver diseases, asthma, pulmonary tuberculosis, chronic pharyngitis, tonsillitis, immunosuppressive diseases, malignancies and heart diseases (except hypertension and vascular diseases).

2.2. *Procedure*

The subjects were interviewed on the basis of a predesigned standardized Berlin questionnaire (*10,12-19*) with some relevant modifications to elicit information from the subjects themselves and from their partners about the occurrence of snoring, cessation of breathing during sleep, tiredness, sleepiness while driving or any past history of hypertension. Often, people are unaware of their snoring habits themselves. Therefore, we used the standardized Berlin questionnaire which is designed to interview the room partners of the subjects. Sixty-five (11.86%) subjects whose partners were unavailable during the interview were contacted by telephone. The daytime sleepiness was also assessed using the Epworth Sleepiness Scale (ESS) (*11*). Some questions were also asked to evaluate possible risk factors for obstructive sleep apnea like smoking, alcoholism and use of sedatives or tranquillizers. Smoking status was defined if they smoked > 100 cigarettes in their lifetime and were still smoking or had given up less than one year ago (*20*) and alcoholism as daily intake of alcohol during the last one month. After getting a detailed clinical history, a relevant physical examination including height, weight, neck size and blood pressure was done. The neck size was measured at the level of cricoid cartilage. Blood pressure measurement was recorded in mm of Hg in a sitting and standing position after at least ten minutes of rest. Another recording was done after ten minutes along with any previous history of any anti-hypertensive medication in case the first recording was found to be abnormal. This was done in order to reduce the probability of a false risk group categorization.

2.3. *Statistical analysis*

Data were summarized as mean ± S.D. Groups were compared by independent Student's *t* test while discrete variables were compared by Fisher's exact test. Unadjusted binary logistic regression analysis was used to assess the effect of each independent predicator variable on snoring. The significant predictor variables were further analyzed by multivariate logistic regression analysis to assess the independent risk factor of snoring. Each regression model was adjusted for alcohol and hypertension. A $p < 0.05$ was considered statistically significant. MINITAB (Windows version 13.0) was used for analysis.

3. Results

3.1. *Basic characteristics*

3.1.1. *Subjects*

There were a total of 548 subjects. Of the total, 392 were males (71.53%) and 156 females (28.47%). The demographic profile of the study population has been described in Table 1.

3.1.2. *Snoring habits*

There were 97 (17.70%) snorers and 451 (82.29%) non-snorers in the study group. Among the snorers, as provided in Table 2, 16 (16.49%) snored louder than talking while 81 (83.50%) were non-loud snorers. The snoring frequency was more than 3-4 times per week in 19 (19.58%) subjects and less than 1-2 times per week in 78 (80.41%) subjects. Snoring of 39 (40.20%)

Table 1. Basic characteristics of subjects

Basic characteristics	*n* (%)
Mean Age (in years)	21.73 ± 1.81
Sex	
Male	392 (71.53%)
Female	156 (28.47%)
Mean neck size (in inch)	13.90 ± 1.23
Mean BMI (in kg/m^2)	21.95 ± 2.52
Mean ESS score	6.92 ± 3.11
Mean nocturnal sleeping hours	7.37 ± 1.10
Smoker	18 (3.28%)
Alcoholic	33 (6.02%)

Neck size was measured at the level of cricoid cartilage. BMI: Body Mass Index.

Table 2. Snoring habits of subjects

Snoring habits	*n* (%)
Snoring loudness	
Loud (more than talking)	16 (16.49%)
Non-loud (not more than talking)	81 (83.50%)
Snoring frequency	
≥ 3-4 times/week	19 (19.58%)
≤ 1-2 times/week	78 (80.41%)
Breathing quality	
Bothersome	39 (40.20%)
Non-bothersome	58 (59.79%)
Breathing pauses	
≥ 3-4 times/week	5 (5.15%)
≤ 1-2 times/week	18 (18.56%)
Never or almost never	39 (40.20%)
Not cared	35 (36.08%)

students bothered their partners while that of 58 (59.79%) did not. More than 3-4 breathing pauses during sleep were reported in 5 (5.15%) students, less than 1-2 times per week in 18 (18.56%), never or almost never in 39 (40.20%) while 35 (36.08%) students did not care to notice. In the overall population, there were 2.92% loud snorers, 3.47% habitual snorers, 7.12% bothered their partners and 0.91% had more than 3-4 breathing pauses per week during their sleep.

On comparing the risk factors between non-snorers and snorers (Table 3), the proportion of males, smokers, mean neck size, BMI and European Stroke Scale (ESS) scores in snorers was found significantly ($p < 0.001$) higher as compared to non-snores. However, the proportions (Y/N) of alcohol and hypertension did not differ ($p > 0.05$) between the two groups, *i.e.,* was found to be statistically the same.

3.1.3. *Daytime sleepiness*

Mean ESS score of the study population was 6.92 ± 3.11. Out of the 548 subjects, 44 (8.10%) reported morning tiredness more than 3-4 times per week, 172 (31.39%) had less than 1-2 times per week and 332 (60.58%) had never or almost never. Wake time tiredness was experienced more than 3-4 times per week by 89 (16.24%) subjects, less than 1-2 times per week by 153 (27.92%) subjects and never or almost never by 306 (55.84%) subjects. Drowsiness behind wheel more than 3-4 times per week was reported by 14 (2.55%) subjects, less than 1-2 times per week by 18 (3.28%) subjects, never or almost never by 230 (41.97%) subjects while 286 (52.19%) subjects did not drive.

Table 3. Basic characteristics of snorers versus non-snorers

Characteristic	Non-snorers (*n* = 451)	Snorers (*n* = 97)
Sex		
Males	300 (66.52%)	92 (94.85%)
Females	151 (33.48%)	5 (5.15%)
Mean neck size (in inch)	13.82 ± 1.17	14.69 ± 1.40
Mean BMI (in kg/m^2)	21.69 ± 2.38	23.44 ± 2.56
Mean ESS score	6.78 ± 2.90	7.71 ± 3.70
Smoking	6 (1.33%)	12 (12.37%)
Hypertensive	5 (1.11%)	3 (3.09%)
Alcoholism	26 (5.76%)	7 (7.22%)

BMI: Body Mass Index.

3.1.4. *Blood pressure and BMI*

Of all subjects, 8 (1.46%) were hypertensive, 173 (31.57%) were pre-hypertensive and 367 (66.97%) were found to be normotensive as per the JNC7 criteria (*21*). Sixty-four (11.67%) subjects were considered as obese according to the Asian classification of WHO (*22*).

3.2. *Identification of risk factors*

The effect of sex, smoking, BMI, neck size and ESS scores on snoring was evaluated by using logistic regression analysis and is summarized in Table 4. Logistic regression analysis (unadjusted) found a significant ($p < 0.05$ or $p < 0.001$) effect of sex, smoking, BMI, neck size and ESS scores on snoring. On evaluating the effect of all significant variables on snoring together (adjusted), all variables showed a significant effect on snoring except ESS scores. In other words, among observed risk factors, sex, smoking, BMI and neck size were independent risk factors for snoring.

4. Discussion

We took undergraduate medical students as the sample population to estimate the prevalence and pattern of snoring among apparently healthy adolescent individuals. There is strong evidence of various pathophysiologies which suggest that sleep disturbed breathing starts manifesting during late adolescence. Hormonal changes, changes in neuromuscular tone and development of obesity are some of the contributions to this phenomenon. Obesity is proposed as an underlying cause as it is correlated with increased neck

Table 4. Unadjusted and adjusted identification of risk factors for snoring by logistic regression analysis

Predictor variables	Unadjusted			Adjusted		
	b	*p* value	OR (95% CI)	b	*p* value	OR (95% CI)
Sex (M)	2.16	$p < 0.001$	8.68 (3.44 to 21.87)	1.75	$p < 0.001$	5.73 (2.11 to 15.61)
Smoking (Y)	2.14	$p < 0.001$	3.12 (1.04 to 7.34)	1.59	$p < 0.005$	2.20 (0.97 to 5.62)
BMI	2.27	$p < 0.001$	4.31 (1.19 to 10.44)	0.19	$p < 0.001$	3.16 (1.09 to 7.36)
Neck size	0.55	$p < 0.001$	2.73 (1.42 to 9.10)	0.23	$p < 0.007$	2.03 (0.79 to 6.35)
ESS	0.09	$p < 0.011$	1.10 (1.02 to 1.18)	0.07	$p < 0.054$	1.08 (1.00 to 1.16)

circumference and internal compression of pharynx by superficially located fat (*23*). Many cohort studies have revealed smoking and alcohol consumption as independent risk factors for SDB (*24*). Habits of smoking and alcohol intake also commonly develop during adolescence.

Our results showed a 17.7% prevalence of snoring among the subjects. This is slightly lower than the prevalence reported by western studies (25.7% and 28.7% by David *et al.* (*25*) and Angeles *et al*. (*26*), respectively). In another study, Balakrishnan *et al*. reported a lesser prevalence of 13.8% among adolescents (*27*). Overall, different studies state the prevalence of snoring in younger children in the range of 10-15% and 4-29% in adults (*28,29*). Similarly, in our earlier study we had found a 28.3% snoring prevalence among adults (*30*). We can decipher that prevalence of snoring increases from childhood to the adult age group with a steep rise during late adolescence. The fact that most of the independent risk factors like obesity, smoking and alcohol consumption are modifiable indicates the need to utilize the opportunity for intervention during adolescence. It should also be understood that the prevalence of snoring does not necessarily indicate the development of obstructive complications but these findings do highlight the need for awareness about possible complications.

Furthermore, habitual snoring even in the absence of SDB has been shown to be associated with EDS that adversely affects the performance and learning abilities of children (*31*). We found habitual snoring among 3.5% subjects which is comparable to 6% shown by Johnson and Roth (*32*). EDS was found among 63 (11.5%) subjects while in a study by Mahmoud *et al.*, EDS among adolescents was reported from 26.7% to 43% (*33*). Strikingly, 12 (63.2%) of the 19 habitual snorers in our study group had EDS. Habitual snorers have symptoms such as falling asleep while watching television or in public places in both genders (*34*). Shin *et al.* have also showed that habitual snoring correlates with an increasing degree of daytime sleepiness (*7*). This is thought to be related to sleep fragmentation as a result of partial upper airway obstruction during sleep, not necessarily with the presence of frank hypopnea or apnea (*35*). However, other factors like sleep deprivation due to demanding study or work schedules, together with irregular sleeping patterns common in this age group, may influence the results.

Among the 97 (17.7%) snorers in our study, there were 92 males and only 5 females. The gender drift could be due to the smaller female sample size but it may also be attributed to a hormonal influence on respiratory control and fat distribution. Male gender, large neck size, high BMI and smoking were identified as independent risk factors for snoring. Male gender and high BMI have also been proved as risk factors for snoring by other studies like by Bidad *et al.* (*2*) and David *et al.* (*25*). Similar to David *et al.*, alcohol consumption was not found to be associated with snoring in our study (*25*).

If we analyze to find the prevalence of clinically significant SDB, *i.e.,* suspicious for developing complications, defined as snoring at least 3-4 times per week, having excessive daytime sleepiness (ESS score ≥ 11) and obesity (BMI ≥ 25 kg/m^2), it was found in 4 (0.7%) subjects. Recently Amra *et al.* (*36*) and Johnson (*32*) have reported an SDB prevalence of 4.9% and 6% among adolescents in their respective studies. Though a clinically significant form of SDB was found to be comparatively lower than that of other studies, still its possibility cannot be underestimated.

Our cross-sectional study may have the limitation of sampling bias. However, the strength of associations found in our study show that the extent of effects of sampling error on results was minimized to a very low level. There is a possibility of under diagnosis of snoring when a standard full night polysomnography test is not administered. On the other hand, it may be better to assess snoring pattern over a period of time by subjective means rather than evaluating this symptom during a single night test. Uncertainties regarding the other causative factors were reduced by using extensive exclusion criteria. We attempted to remove the self-reporting bias by interviewing with their room partners. Nevertheless, the effect of unknown confounding factors cannot be excluded completely.

We conclude that the prevalence of snoring is high among the male population of late adolescent age group and is comparable to adults. The habit of snoring is frequently ignored as many people, including medical students, are unaware of the possible complications. Spreading information on snoring is necessary to encourage self-reporting. Also, it is important to

understand the pattern of snoring in addition to the causal associations, so as to identify the individuals at clinically significant risk for developing complications. The Berlin questionnaire is an effective and inexpensive modality for screening clinically significant snoring. Inclusion of more physical activities in the medical curriculum and avoidance of smoking should be promoted. Various treatment modalities like continuous positive airway pressure (CPAP), mandibular splints and other surgical interventions are available. Further, there is a need to study the impact of early diagnosis and intervention on the progression of snoring habits and associated co-morbidities.

References

1. Stoohs RA, Blum HC, Haselhorst M, Duchna HW, Guilleminault C. Normative data on snoring: A comparison between younger and older adults. Eur Respir J. 1998; 11:451-457.
2. Katayoon B, Shahab A, Asghar A, Narges G, Sorush Z, Moaieri H. Prevalence and correlates of snoring in adolescents. Iran J Allergy Asthma Immunol. 2006; 5:127-132.
3. Umana AN, Anah MU, Udonwa NE, Mgbe RB, Oyo-Ita V, Onoyon-Ita, Ukpong EE. Pattern of snoring among school children in Calabar, Nigeria. Nigerian Medical Practioner. 2007; 51:103-106.
4. Marcus CL, Omlin KJ, Basinki DJ. Normal polysomnographic values for children and adolescents. Am Rev Respir Dis. 1992; 146:1235-1239.
5. Carroll JL, Loughlin GM. Obstructive sleep apnoea ayndrome in infants and children: Clinical features and pathophysiology. In: Principals and Practice of Sleep Medicine in the Child. WB Saunders Company, Philadelphia, PA, USA, 1995; pp. 163-191.
6. Lugaresi E, Cirignotta F, Geraldi R, Montagna P. Snoring and sleep apnea: Natural history of heavy snorers disease. In: Guilleminault C, Partinen M, eds. Obstructive sleep apnea syndrome: Clinical research and treatment. Raven Press, New York, NY, USA, 1990; pp. 25-36.
7. Shin C, Joo S, Kim JK, Kim T. Prevalence and correlates of habitual snoring in high school students. Chest. 2003; 124:1709-1715.
8. Bradley TD, Phillipson EA. Pathogenesis and pathophysiology of the obstructive sleep apnea syndrome. Med Clin North Am. 1985; 69:1169-1185.
9. Caroll JL. Obstructive Sleep Disordered Breathing in Children: New controversies, new directions. Clin Chest Med. 2003; 24:261-282.
10. Nikolaus CN, Stoohs RA, Cordula MN, Kathryn C, Kingman RS. Using the Berlin questionnaire to identify patients at risk for the sleep apnea syndrome. Annals internal Medicine. 1999; 131:485-491.
11. Johns MW. A new method for measuring daytime sleeping, the Epworth sleepiness scale. Sleep. 1991; 14:540-545.
12. Cirignotta F, Alessandro RD, Partinen M. Prevalence of every night snoring and obstructive sleep apnoeas among 30-69 year old men in Bologna, Italy. Acta Psychiatr Scand. 1980; 79:366-372.
13. Redline S, Strohi KP. Recognition and consequences of obstructive sleep apnea hypopnea syndrome. Clin Chest Med. 1998; 19:1-19.
14. Kapuniai LE, Andrew DJ, Crowell DH, Pearce JW. Identifying sleep apnea from self-reports. Sleep. 1988; 11:430-436.
15. Flemons WW, Whitelaw WA, Brant R, Remmers JE. Likelihood ratios for a sleep apnea clinical prediction rule. Am J Respir Crit Care Med. 1994; 150 (5 Pt 1):1279-1285.
16. Flemons WW, Remmers JE. The diagnosis of sleep apnea: Questionnaires and home studies. Sleep. 1996; 19 (10 Suppl):S243-S247.
17. Kump K, Whalen C, Tishler PV, Browner, Ferrettee V, Strahi KP. Assessment of the validity and utility of a sleep-symptom questionnaire. Am J Respir Crit Care Med. 1994; 150:735-741.
18. Wu H, Yan-Go F. Self-reported automobile accidents involving patients with obstructive sleep apnea. Neurology. 1996; 46:1254-1257.
19. Maislin G, Pack AI, Kribbs NB, Smith PL, Schwartz AR, Kline LR. A survey screen for prediction of apnea. Sleep. 1995; 18:158-166.
20. West R, Hajek P, Stead L. Outcome criteria in smoking cessation trials: Proposal for a common standard. Addiction. 2005; 100:299-303.
21. Chobanian AV, Bakris GL, Black HR. Seventh report of the Joint National Committee on prevention, detection, evaluation and treatment of high blood pressure. Hypertension. 2003; 42:1206-1252.
22. World Health Organization, Western Pacific Region. The Asia-Pacific Perspective. Redefining obesity and its treatment. International Diabetes Institute, WHO/IASO/IOTF, Melbourne, Australia, 2000; pp. 15-21.
23. Stradling JR, Crosby JH. Predictors and prevalence of obstructive sleep apnoea and snoring in 1,001 middle aged men. Thorax. 1991; 46:85-90.
24. Young T, Finn L, Palta M. Chronic nasal congestion at night is a risk factor for snoring in a population-based cohort study. Arch Intern Med. 2001; 161:1514-1519.
25. David SC, Joseph KW, Alice SS, Dominic KL, Christopher KW, Roland CC. Prevalence of snoring and sleep-disordered breathing in a student population. Chest. 1999; 116:1530-1536.
26. Angeles SA, María FP, Francisco CG, Emilio GD, Soledad CG, Carmen CB, José CG. Sleep-related breathing disorders in adolescents aged 12 to 16 years: Clinical and polygraphic findings. Chest. 2001; 119:1393-1400.
27. Balakrishnan D, Thirunavukkarasu S, Edwin R, Virudhagirinathan BS. The prevalence of Snoring in the South Indian city of Chennai – Report of a population based survey (PEDEX). Presented in the First International ORL-HN conference of the National University of Singapore, 27-30 January 2005.
28. Teculescu DB, Caillier I, Perrin P. Snoring in French preschool children. Pediatr Pulmonol. 1992; 13:239-244.
29. Zamarrón C. Snoring and vascular diseases. An Med Interna. 1998; 15:669-671.
30. Prasad P, Garg R, Verma RK, Agarwal SP, Ahuja RC. A study on snoring habits in healthy population of Lucknow. Indian J Sleep Med. 2006; 1:37-40.
31. Ulfberg J, Carter N, Talback M. Excessive daytime sleepiness at work and subjective work performance in the general population and among heavy snorers and patients with obstructive sleep apnea. Chest. 1996;

110:659-663.
32. Johnson EO, Roth T. An epidemiologic study of sleep-disordered breathing symptoms among adolescents. Sleep. 2006; 29:1135-1142.
33. Mahmoud M, Babak G, Mir GB, Ebrahim A, Shahnaz K, Shervin S, Mahmoud RA. Sleep patterns and sleep problems among preschool and school-aged group children in a primary care setting. Iran J Ped. 2007; 17:213-221.
34. Ersu R, Arman AR, Save D, Karadag B, Karakoc F, Berkem M. Prevalence of snoring and symptoms of sleep-disordered breathing in primary school children in Istanbul. Chest. 2004; 126:19-24.
35. Guilleminault C, Stoohs R, Clerk A. A cause of excessive daytime sleepiness: The upper airways resistance syndrome. Chest. 1993; 104:781-787.
36. Amra B, Farajzadegan Z, Golshan M, Fietze I, Penzel T. Prevalence of sleep-related symptoms in a Persian population. Sleep Breath. 2011; 15:425-429.

(*Received August 30, 2011; Revised March 28, 2012; Accepted April 7, 2012*)

Original Article

DOI: 10.5582/bst.2012.v6.2.63

Effect of CXCR4 inhibitor AMD3100 on alkaline phosphatase activity and mineralization in osteoblastic MC3T3-E1 cells

Jing Luan, Yazhou Cui, Yongying Zhang, Xiaoyan Zhou, Genglin Zhang, Jinxiang Han*

Shandong Academy of Medical Sciences, Shandong Medical Biotechnological Center, Key Laboratory for Rare Disease Research of Shandong Province, and Key Laboratory for Biotech Drugs of the Ministry of Health, Ji'nan, Shandong, China.

Summary **The aim of the study was to investigate the effect of C-X-C chemokine receptor type 4 (CXCR4) inhibitor AMD3100 on the osteogenic differentiation of pre-osteoblastic cell line MC3T3-E1. In this study we found that blocking SDF-1/CXCR4 signaling with AMD3100 strongly suppressed osteogenic differentiation in MC3T3-E1 cells, as evidenced by an early decrease in the activity of alkaline phosphatase (ALP), and down-regulation of mRNA expression of the osteogenic master regulator Runx2, ALP, osteocalcin, and progressive ankylosis genes. Moreover, we found that the regulatory effect of AMD3100 might be mediated *via* intracellular STAT3 activation. However, AMD3100 exerted no significant effect on generation of matrix mineralization at the terminal stage of osteogenic induction. In conclusion, our results demonstrated an inhibitory role of AMD3100 in osteogenic differentiation of MC3T3-E1 cells, especially in the early stage, which provides novel insights into the effect of CXCR4 antagonists on modulation of osteogenesis.**

Keywords: SDF-1/CXCR4 signaling, AMD3100, MC3T3-E1, osteogenic differentiation, signal transducer and activator of transcription 3

1. Introduction

Stromal-derived factor 1 (SDF-1, also known as CXCL12) was initially identified as a bone marrow stromal cell-derived factor, which specially binds to a G-protein-coupled receptor, C-X-C chemokine receptor type 4 (CXCR4) (*1,2*). The SDF-1/CXCR4 signaling pathway has been found to be important for the process of cellular inflammatory, immune response, blood homeostasis *et al.* (*3,4*). AMD3100 (plerixafor), a CXCR4 antagonist, which can inhibit binding of SDF-1 to CXCR4 and subsequent signal transduction, has been used as an effective hematopoietic stem cell mobilization agent in patients with non-Hodgkin's lymphoma (NHL) and multiple myeloma (MM) (*5-8*). It has been proposed that AMD3100 may also play an important role in treatment of many other SDF-1/CXCR4-regulated pathological processes such as cancer, human immunodeficiency virus infection, rheumatoid arthritis, atherosclerosis, and asthma (*9-13*).

Recent studies have suggested the SDF-1/CXCR4 pathway is involved in bone remodeling and osteoblast differentiation (*14-16*). Kitaori *et al.* (*17*) found that SDF-1/CXCR4 signaling has a critical role in recruitment of mesenchymal stem cells (MSC) to the fracture site during skeletal repair *in vivo*. Zhu *et al.* (*15*) and Hosogane *et al.* (*16*) showed that SDF-1/CXCR4 participated in the process of bone morphogenetic protein 2 (BMP-2)-induced osteogenic differentiation of primary MSCs or MSC cells lines *in vivo*. Therefore, special attention has been given to learn about the efficacy or toxicity of AMD3100 on osteogenesis.

Until now, only a few studies have demonstrated the effect of AMD3100 on osteogenesis of MSC at the early stage. The modulation of AMD3100 on differentiation of preosteoblasts, especially on mineralization has not been investigated. Therefore, in this study, we utilized the murine pre-osteoblastic cell line MC3T3-E1 to observe the effect of CXCR4 inhibitor AMD3100 on

**Address correspondence to:*
Dr. Jinxiang Han, Shandong Academy of Medical Sciences, Shandong Medical Biotechnological Center, Key Laboratory for Rare Disease Research of Shandong Province, China, and Key Laboratory for Biotech Drugs of the Ministry of Health, China, Ji'nan 250062, Shandong, China.
E-mail: samshjx@sina.com

activity of alkaline phosphatase (ALP; an early marker of osteogenesis), expression of osteogenic factors, and mineralization (*18*). Furthermore, the possible mechanism of AMD3100 on ALP regulation by the transcription factor – signal transducer and activator of transcription 3 (STAT3) was also investigated.

2. Materials and Methods

2.1. *Chemicals and antibodies*

Dexamethasone, L-ascorbic acid, β-glycerophosphate, and the CXCR4 antagonist AMD3100 were all obtained from Sigma (St. Louis, MO, USA). All cell culture media and supplements were from Gibco (Carlsbad, CA, USA). Reagents for reverse transcription and those for real-time PCR reactions were from Toyobo (Shanghai, China). Anti-STAT3 and anti-phospho-STAT3 (Tyr705) rabbit monoclonal antibodies were purchased from Cell Signaling Technology (Danvers, MA, USA). Secondary goat anti-rabbit IgG was obtained from Santa Cruz (Santa Cruz, CA, USA). Enhanced chemiluminescence (ECL) detection reagent was purchased from Millipore (Billerica, MA, USA).

2.2. *Cells and osteogenic induction*

MC3T3-E1 cells were acquired from the Cell Bank of Type Culture Collection of Chinese Academy of Sciences (Shanghai, China). For osteogenic induction, MC3T3-E1 cells were plated at a density of 1×10^4 cells/cm^2 in 24-well plates and maintained in Dulbecco's modified Eagle's medium (DMEM) supplemented with 10% fetal bovine serum (FBS) and 1% penicillin-streptomycin at 37°C under 5% (v/v) CO_2 in a humidified atmosphere. Osteoblast differentiation was induced by addition of 10 nM dexamethasone, 50 μg/mL L-ascorbic acid and 10 mM β-glycerophosphate as described previously (*19*). To block SDF-1/CXCR4 signaling in MC3T3-E1 cells, cells were incubated with the CXCR4 antagonist AMD3100 respectively at concentrations of 50, 100, 200, and 400 μM.

2.3. *ALP activity*

ALP activity was measured at 3, 6, and 9 days of osteogenic induction as described previously with minor modifications (*20*). Briefly, MC3T3-E1 cells were washed with one volume of phosphate-buffered saline (PBS) (pH 7.4) and lysed with addition of 100 μL/well of 25 mM Tris-HCl (pH 7.4) and 0.5% Triton X-100. Fifty microliter of cell lysate was incubated with 100 μL *p*-nitrophenyl phosphate at 37°C for 20 min. The reaction was stopped by addition of 50 μL NaOH (3 M) and absorbance was measured at 405 nm.

2.4. *Mineralization analysis*

Mineralization analysis was performed at 14 and 21 days of osteogenic induction as described previously (*21*). MC3T3-E1 cells were washed with PBS and fixed with 4% paraformaldehyde. Then the cells were washed with PBS and stained with 0.5% (w/v) alizarin red S solution for 1 h. After washing with PBS, the stained cultures were photographed. Then the cells were incubated with 10% (w/v) cetylpyridium chloride at 37°C for 1 h, optical density of the supernatant was measured at 562 nm.

2.5. *Quantitative real-time polymerase chain reaction (RT-qPCR)*

RT-qPCR was used to measure expression of osteogenic markers including ALP, progressive ankylosis (Ank), runt-related gene 2 (Runx2), and osteocalcin (OCN) genes at 6 and 9 days of osteogenic induction. Total RNA was extracted from cells using Trizol reagent. One microgram of total RNA from each sample was reverse-transcribed, and levels of target gene expression were quantified in real-time PCR detection system with a LightCycler 480 thermocycler (Roche Applied Science, Mannheim, Germany). Relative expression of target genes was calculated based on ΔCT values, which are differences in the number of threshold cycles between the target gene and the housekeeping gene glyceraldehyde 3-phosphate dehydrogenase (GAPDH). The primer sequences of target genes that were analyzed in this study are listed in Table 1.

2.6. *Western-blot*

For Western-blot analysis, MC3T3-E1 cells at 3, 6, 9, and 14 days of osteogenic induction were collected, and then whole cell lysate was obtained and the amount of total cellular protein was determined using the Bradford assay (*15,22*). Equal loading of 30 μg aliquots of total protein from each sample were fractionated on 12% sodium dodecyl sulfate polyacrylamide gel electrophoresis (SDS-PAGE), and the following

Table 1. Quantitative real-time PCR primer sequences

Target genes	Primer sequences
ALP	Forward: 5'-TGGCTCTGCCTTTATTCCCTAGT-3' Reverse: 5'-AAATAAGGTGCTTTGGGAATCTGT-3'
Ank	Forward: 5'-ATGAGTCAGCCACCGAG-3' Reverse: 5'-GGAGGAAAGAGACGACAGTT-3'
Runx2	Forward: 5'-GCCGGGAATGATGAGAACTA-3' Reverse: 5'-GGTGAAACTCTTGCCTCGTC-3'
OCN	Forward: 5'-GCCATCACCCTGTCTCCTAA-3' Reverse: 5'-GCTGTGGAGAAGACACACGA-3'
GAPDH	Forward: 5'-CATCCCAGAGCTGAACG-3' Reverse: 5'-CTGGTCCTCAGTGTAGCC-3'

antibodies were incubated: anti-STAT3 (1:2,000), anti-phospho-STAT3 (Tyr705) (1:2,000), and anti-β-actin (1:1,000). Primary antibodies were detected with goat anti-rabbit IgG conjugated to horseradish peroxidase. Blots were developed with enhanced chemiluminescence (ECL) and exposed to X-ray film.

2.7. *Statistics*

Measurements in each experiment were run in triplicate. For quantitative data, results are reported as the mean ± S.D. To determine the differences between groups, one-way analysis of variance (ANOVA) was carried out using SPSS software (version 17.0), with significance accepted at $p < 0.05$.

3. Results

3.1. *CXCR4 inhibitor AMD3100 suppressed ALP activity during the early stage of osteogenic differentiation in MC3T3-E1 cells*

As seen in Figure 1, with osteoblast induction, ALP activity increased and achieved a peak at 6 days, and decreased slightly at 9 days, which is consistent with the previous studies (*16*). When treated with CXCR4 antagonist AMD3100, ALP activity significantly decreased at 3, 6, and 9 days (48%, 49%, and 53% decreases at 50 μM AMD3100, respectively, and 29%, 56%, and 73% decreases at 100 μM AMD3100, respectively) (Figure 1). Furthermore, detection of ALP activity in MC3T3-E1 cells at 6 days also showed that treatment with CXCR4 antagonist AMD3100 decreased osteogenic media-induced ALP activity in a concentration-dependent manner (49%, 56%, 67%, and 77% decreases with 50, 100, 200, and 400 μM of AMD3100, respectively) (data not shown). Taken together, these data suggest that CXCR4 inhibitor AMD3100 significantly inhibited ALP activity during the early stage of osteogenic differentiation in MC3T3-E1 cells.

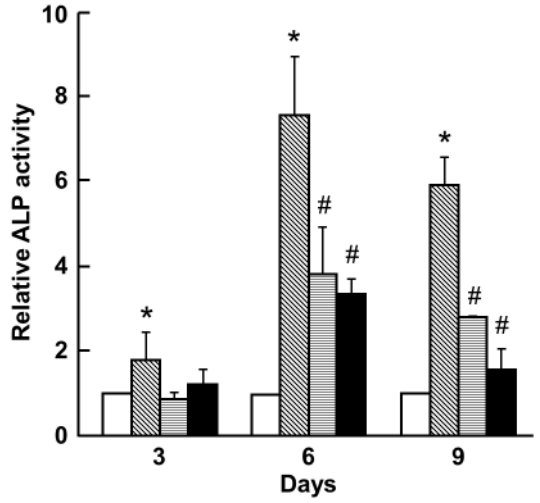

Figure 1. AMD3100 suppressed ALP activity during the early stage of osteogenic differentiation in MC3T3-E1 cells. MC3T3-E1 cells were treated with DMEM (open columns), osteogenic medium (shaded columns) and osteogenic medium supplemented with AMD3100 (horizontal and closed columns for 50 μM and 100 μM, respectively) and assessed for ALP activity at 3, 6, and 9 days (mean ± S.D., $n = 3$). * $p < 0.05$, *vs.* negative control group; # $p < 0.05$, *vs.* osteogenic induction group.

3.2. *CXCR4 inhibitor AMD3100 had no effect on matrix mineralization in MC3T3-E1 cells*

To evaluate calcium deposition in matrix, alizarin red staining was performed and quantified by a

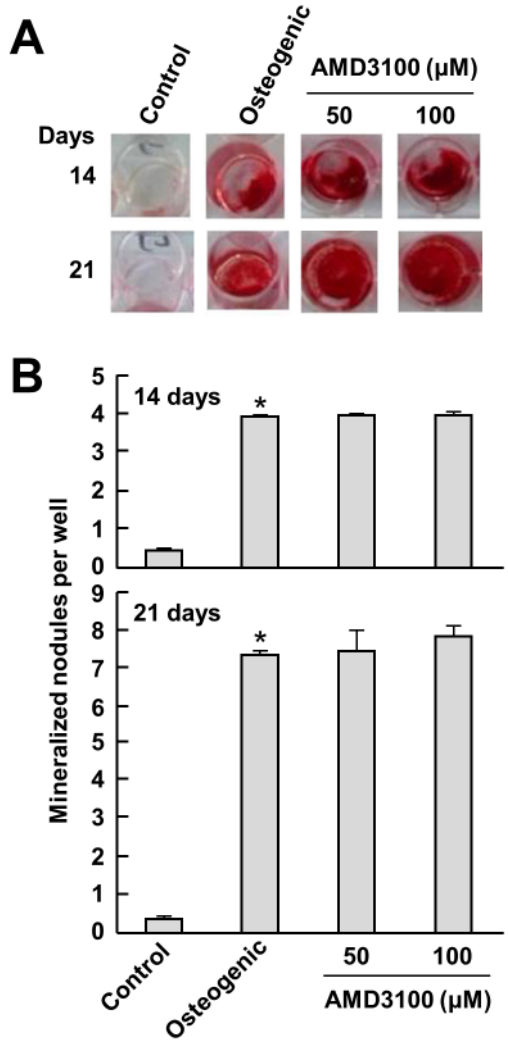

Figure 2. Effect of AMD3100 on matrix mineralization of MC3T3-E1 cells. (A) Typical observations for mineralization. Cells were cultured with DMEM, osteogenic medium and osteogenic medium supplemented with various concentrations of AMD3100 for 14 days (upper) and 21 days (lower). The resulting mineralization was assessed by Alzarin red S staining. **(B)** Quantitation of mineralization. Alzarin red S was solubilized in cell cultures of every group using cetylpyridinium chloride and quantified at 562 nm. Upper panel, 14 days; lower panel, 21 days. Data were mean ± S.D., $n = 3$. * $p < 0.05$, *vs.* negative control group.

colorimetric analysis based on solubilizing the red matrix precipitate with cetylpyridinium chloride at 14 and 21 days of osteoblast differentiation. Obvious matrix mineralization could be observed at 14 days of induction (upper panels in Figure 2A), and became extensive at 21 days as seen in Figure 2 (lower panels in Figure 2A). However, cetylpyridinium chloride analysis failed to detect minor increases or decreases in mineralization by treatment with AMD3100 at 50 and 100 μM (upper and lower panels in Figure 2B, respectively). These data suggest that CXCR4 inhibitor AMD3100 seemed to have no significant effect on generation of matrix mineralization at the terminal stage of osteogenic induction in MC3T3-E1 cells.

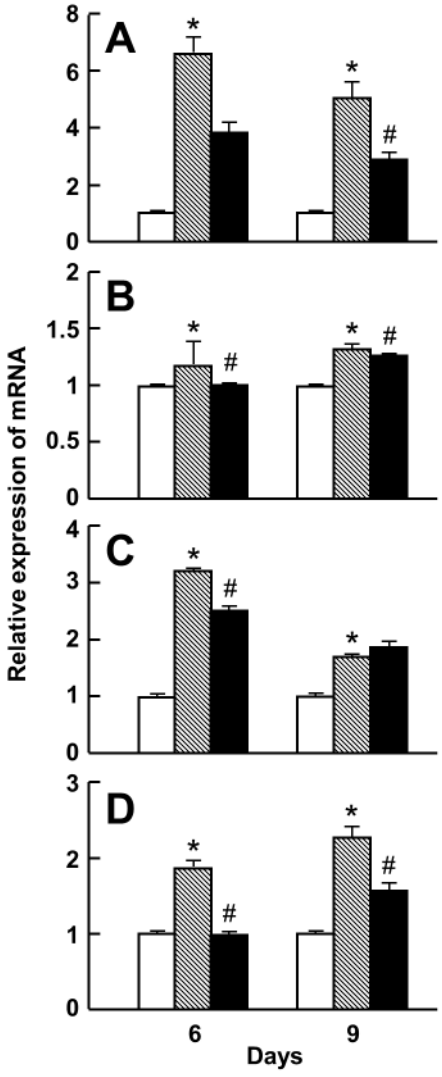

Figure 3. Effect of AMD3100 on osteoblast-specific marker genes expression in MC3T3-E1 cells. Cells were cultured with DMEM (open columns), osteogenic medium (shaded columns) and osteogenic medium supplemented with AMD3100 (400 μM) (closed columns) for 14 days, and then were harvested at 6 and 9 days during osteogenic differentiation for quantitative gene expression analysis of ALP **(A)**, Ank **(B)**, Runx2 **(C)**, and OCN **(D)**. Data were normalized to GAPDH expression and presented as fold difference relative to control cells cultured with DMEM (mean ± S.D., $n = 3$). * $p < 0.05$, *vs.* negative control group; # $p < 0.05$, *vs.* osteogenic induction group.

3.3. *Effect of CXCR4 inhibitor AMD3100 on osteoblast-specific marker genes expression in MC3T3-E1 cells*

The mRNA levels of four osteoblast-specific markers affected by CXCR4 inhibitor AMD3100 were determined by quantitative real time PCR analysis. As seen in Figure 3, compared with the osteogenic group, CXCR4 inhibitor AMD3100 (400 μM) suppressed the expression of both the early osteoblast differentiation markers (ALP and Runx2) and the late differentiation markers (Ank and OCN) at 6 and 9 days. Each difference reached a level of significance except for mRNA expression of Runx2 at 9 days.

3.4. *Effect of CXCR4 inhibitor AMD3100 on STAT3 in MC3T3-E1 cells*

To further understand mechanisms underlying the effect of AMD3100 on osteoblast differentiation, we examined the activation of STAT3 proteins in MC3T3-E1 cells treated with AMD3100 at 3 and 6 days of osteogenic induction. As seen in Figure 4, Western-blot results showed that osteogenic media stimulation increased the phosphorylation of STAT3 protein at 6 days compared with the control group, and treatment with CXCR4 antagonist AMD3100 almost abolished osteogenic media-induced STAT3 phosphorylation (Figure 4).

4. Discussion

In this study, we demonstrated that blocking the SDF-1/CXCR4 pathway could regulate osteogenic differentiation of pre-osteoblastic MC3T3-E1 cells. Our results demonstrate that CXCR4 inhibitor AMD3100 significantly inhibited the ALP activity during the early stage of osteogenic differentiation in MC3T3-E1 cells, but it seems to have no significant effect on generation of matrix mineralization at the terminal

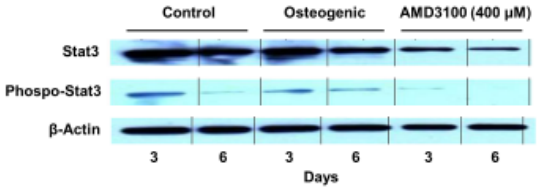

Figure 4. Blocking of SDF-1 signaling inhibited STAT3 expression during the early stage of osteogenic differentiation in MC3T3-E1 cells. Cells were treated with DMEM, osteogenic medium and osteogenic medium supplemented with AMD3100 (400 μM) for 6 days, and then levels of STAT3 and phospho-STAT3 were determined by Western-blot analysis.

stage of osteogenic induction in MC3T3-E1 cells. Meanwhile, ALP, Runx2, Ank, and OCN osteoblast-specific marker genes mRNA expression induced by the osteogenic media were decreased in MC3T3-E1 cells after treatment with AMD3100. Our results also show that the effect of AMD3100 on ALP might be mediated *via* inhibiting intracellular STAT3 activation at the early stage of osteogenic differentiation in MC3T3-E1 cells.

The high expression of SDF-1 by MSCs and osteoprogenitors indicates the intimacy between SDF-1 signaling and initiation of osteogenesis (*23*). High levels of SDF-1 have been detected in MSCs at the early stage of differentiation induced by dexamethasone or BMP2, while SDF-1's expression declines with cell maturation (*24*). Concomitantly, many studies revealed that abundant SDF-1 existing in osteoprecursors play an important role during postnatal bone development and bone regeneration (*25,26*). In this context, our detection that blocking of the SDF-1/CXCR4 signal axis inhibited osteogenic media-induced ALP activity and mRNA expression further suggested the involvement of SDF-1 signaling at the early stage of osteogenic fate determination of MC3T3-E1 cells, since ALP is expressed by MC3T3-E1 cells at the early phase of differentiation when committing to an osteogenic pathway. The result that CXCR4 inhibitor AMD3100 had no effect on matrix mineralization at the terminal stage of osteogenic differentiation in MC3T3-E1 cells may further prove the early role of SDF-1 signaling from another perspective.

The transcriptional regulation of osteoblast genes, such as ALP and OCN, takes place at their promoter regions *via* interaction with crucial transcription factors, such as Runx2, which is expressed at the earliest stage of osteogenic differentiation (*27*). In this context, our detection that blocking of SDF-1/CXCR4 signaling inhibited osteoinduced Runx2 expression further suggested the involvement of SDF-1/CXCR4 signaling in the osteogenic differentiation of MC3T3-E1 cells. Furthermore, our detection also showed that blocking SDF-1 signaling reduced expression of both the early osteoblast differentiation marker (ALP) and the late differentiation markers (Ank and OCN).

The finding of SDF-1 regulation of osteogenic differentiation led us to examine potential crosstalk between SDF-1 signaling and the osteogenic pathway in the context of promoting osteogenesis. The intracellular STAT3 pathway is the major sub pathway engaged in SDF-1 signaling, and studies have shown that STAT3 may play an important role in osteogenic differentiation (*28,29*). Moreover, Itoh *et al.* (*30*) detected that the interleukin-6 family-mediated STAT3 activation plays a critical role in osteoblast differentiation and bone formation. Our results that blocking of the SDF-1/CXCR4 axis inhibited the phosphorylation of STAT3 suggested involvement of STAT3 in mediating the SDF-1 effect on osteogenic differentiation in MC3T3-E1 cells. But, because of diverse species and cell types, the detailed mechanism involved in the STAT3 signaling-mediated osteogenesis still remains unknown (*31,32*). Mikami *et al*. (*31*) detected that a STAT3 siRNA suppressed the synergistic effect of BMP-2 and dexamethasone on ALP levels in mouse C3H10T1/2 pluripotent stem cells; but Levy *et al*. (*32*) indicated that eradication of STAT signaling considerably enhanced BMP-induced osteogenic differentiation of hMSCs, suggesting distinct roles of SDF-1 during different stages of differentiation in various cell types in response to different stimulants. Studies have shown that activation of the STAT3 pathway was rapid and transient (*32*). Similarly, our results show that blocking of SDF-1/CXCR4 signaling only had an effect on phosphorylation of STAT3 at the early stage of osteogenic differentiation in MC3T3-E1 cells. Furthermore, STAT3 and Runx2 are two of the major transcription factors that play essential roles in osteogenesis, they interact with each other in the nucleus, and Runx2 is a master regulator at the early phase of osteogenic differentiation; this interaction might affect osteogenic regulation (*33-35*). Further studies are needed to explain whether the interplay of STAT3 and Runx2 are involved in STAT3 signaling at the early stage of osteogenic differentiation.

In conclusion, our results indicate that blocking the SDF-1/CXCR4 pathway by AMD3100 exerts an inhibitory effect on the early osteogenic differentiation of MC3T3-E1 cells *via* the STAT3 pathway, but has no effect on generation of matrix mineralization at the terminal stage of osteogenic induction. These findings provide novel insights into the mechanisms underlying SDF-1/CXCR4 pathway inhibitors on osteogenic differentiation, which is helpful for re-evaluating their efficacy or toxicity on osteogenesis in the future.

Acknowledgements

This work was supported by the Key Project for Drug Research and Development from the Ministry of Science and Technology of China (Grant No. 2010ZX09401-302-5-07).

References

1. Zlotnik A, Yoshie O. Chemokines: A new classification system and their role in immunity. Immunity. 2000; 12:121-127.
2. D'Apuzzo M, Rolink A, Loetscher M, Hoxie JA, Clark-Lewis I, Melchers F, Baggiolini M, Moser B. The chemokine SDF-1, stromal cell-derived factor 1, attracts early stage B cell precursors *via* the chemokine receptor CXCR4. Eur J Immunol. 1997; 27:1788-1793.
3. Aiuti A, Tavian M, Cipponi A, Ficara F, Zappone E, Hoxie J, Peault B, Bordignon C. Expression of CXCR4, the receptor for stromal cell-derived factor-1 on fetal and adult human lympho-hematopoietic progenitors. Eur J

Immunol. 1999; 29:1823-1831.
4. Zhang XF, Wang JF, Matczak E, Proper JA, Groopman JE. Janus kinase 2 is involved in stromal cell-derived factor-1α-induced tyrosine phosphorylation of focal adhesion proteins and migration of hematopoietic progenitor cells. Blood. 2001; 97:3342-3348.
5. Wong RS, Bodart V, Metz M, Labrecque J, Bridger G, Fricker SP. Comparison of the potential multiple binding modes of bicyclam, monocylam, and noncyclam small-molecule CXC chemokine receptor 4 inhibitors. Mol Pharmacol. 2008; 74:1485-1495.
6. Martin C, Bridger GJ, Rankin SM. Structural analogues of AMD3100 mobilise haematopoietic progenitor cells from bone marrow *in vivo* according to their ability to inhibit CXCL12 binding to CXCR4 *in vitro*. Br J Haematol. 2006; 134:326-329.
7. De Clercq E. The AMD3100 story: The path to the discovery of a stem cell mobilizer (Mozobil). Biochem Pharmacol. 2009; 77:1655-1664.
8. Fricker SP, Anastassov V, Cox J, Darkes MC, Grujic O, Idzan SR, Labrecque J, Lau G, Mosi RM, Nelson KL, Qin L, Santucci Z, Wong RS. Characterization of the molecular pharmacology of AMD3100: A specific antagonist of the G-protein coupled chemokine receptor, CXCR4. Biochem Pharmacol. 2006; 72:588-596.
9. Uchida D, Onoue T, Kuribayashi N, Tomizuka Y, Tamatani T, Nagai H, Miyamoto Y. Blockade of CXCR4 in oral squamous cell carcinoma inhibits lymph node metastases. Eur J Cancer. 2011; 47:452-459.
10. Singh S, Srivastava SK, Bhardwaj A, Owen LB, Singh AP. CXCL12-CXCR4 signalling axis confers gemcitabine resistance to pancreatic cancer cells: A novel target for therapy. Br J Cancer. 2010; 103:1671-1679.
11. Hendrix CW, Flexner C, MacFarland RT, Giandomenico C, Fuchs EJ, Redpath E, Bridger G, Henson GW. Pharmacokinetics and safety of AMD-3100, a novel antagonist of the CXCR-4 chemokine receptor, in human volunteers. Antimicrob Agents Chemother. 2000; 44:1667-1673.
12. Lenoir M, Djerdjouri B, Perianin A. Stroma cell-derived factor 1α mediates desensitization of human neutrophil respiratory burst in synovial fluid from rheumatoid arthritic patients. J Immunol. 2004; 172:7136-7143.
13. Lukacs NW, Berlin A, Schols D, Skerlj RT, Bridger GJ. AMD3100, a CXCR4 antagonist, attenuates allergic lung inflammation and airway hyperreactivity. Am J Pathol. 2002; 160:1353-1360.
14. Otsuru S, Tamai K, Yamazaki T, Yoshikawa H, Kaneda Y. Circulating bone marrow-derived osteoblast progenitor cells are recruited to the bone-forming site by the CXCR4/stromal cell-derived factor-1 pathway. Stem Cells. 2008; 26:223-234.
15. Zhu W, Boachie-Adjei O, Rawlins BA, Frenkel B, Boskey AL, Ivashkiv LB, Blobel CP. A novel regulatory role for stromal-derived factor-1 signaling in bone morphogenic protein-2 osteogenic differentiation of mesenchymal C2C12 cells. J Biol Chem. 2007; 282:18676-18685.
16. Hosogane N, Huang Z, Rawlins BA, Liu X, Boachie-Adjei O, Boskey AL, Zhu W. Stromal derived factor-1 regulates bone morphogenetic protein 2-induced osteogenic differentiation of primary mesenchymal stem cells. Int J Biochem Cell Biol. 2010; 42:1132-1141.
17. Kitaori T, Ito H, Schwarz EM, Tsutsumi R, Yoshitomi H, Oishi S, Nakano M, Fujii N, Nagasawa T, Nakamura T. Stromal cell-derived factor 1/CXCR4 signaling is critical for the recruitment of mesenchymal stem cells to the fracture site during skeletal repair in a mouse model. Arthritis Rheum. 2009; 60:813-823.
18. Wang D, Christensen K, Chawla K, Xiao G, Krebsbach PH, Franceschi RT. Isolation and characterization of MC3T3-E1 preosteoblast subclones with distinct *in vitro* and *in vivo* differentiation/mineralization potential. J Bone Miner Res. 1999; 14:893-903.
19. Wang A, Ding X, Sheng S, Yao Z. Bone morphogenetic protein receptor in the osteogenic differentiation of rat bone marrow stromal cells. Yonsei Med J. 2010; 51:740-745.
20. Stephens AS, Stephens SR, Hobbs C, Hutmacher DW, Bacic-Welsh D, Woodruff MA, Morrison NA. Myocyte enhancer factor 2c, an osteoblast transcription factor identified by dimethyl sulfoxide (DMSO)-enhanced mineralization. J Biol Chem. 2011; 286:30071-30086.
21. Thouverey C, Strzelecka-Kiliszek A, Balcerzak M, Buchet R, Pikula S. Matrix vesicles originate from apical membrane microvilli of mineralizing osteoblast-like Saos-2 cells. J Cell Biochem. 2009; 106:127-138.
22. Kook SH, Hwang JM, Park JS, Kim EM, Heo JS, Jeon YM, Lee JC. Mechanical force induces type I collagen expression in human periodontal ligament fibroblasts through activation of ERK/JNK and AP-1. J Cell Biochem. 2009; 106:1060-1067.
23. Yu X, Huang Y, Collin-Osdoby P, Osdoby P. Stromal cell-derived factor-1 (SDF-1) recruits osteoclast precursors by inducing chemotaxis, matrix metalloproteinase-9 (MMP-9) activity, and collagen transmigration. J Bone Miner Res. 2003; 18:1404-1418.
24. Kortesidis A, Zannettino A, Isenmann S, Shi S, Lapidot T, Gronthos S. Stromal-derived factor-1 promotes the growth, survival, and development of human bone marrow stromal stem cells. Blood. 2005; 105:3793-3801.
25. Zhu W, Liang G, Huang Z, Doty SB, Boskey AL. Conditional inactivation of the CXCR4 receptor in osteoprecursors reduces postnatal bone formation due to impaired osteoblast development. J Biol Chem. 2011; 286:26794-26805.
26. Kumar S, Ponnazhagan S. Mobilization of bone marrow mesenchymal stem cells *in vivo* augments bone healing in a mouse model of segmental bone defect. Bone. 2012; 50:1012-1018.
27. Otto F, Thornell AP, Crompton T, Denzel A, Gilmour KC, Rosewell IR, Stamp GW, Beddington RS, Mundlos S, Olsen BR, Selby PB, Owen MJ. Cbfa1, a candidate gene for cleidocranial dysplasia syndrome, is essential for osteoblast differentiation and bone development. Cell. 1997; 89:765-771.
28. Huang C, Gu H, Zhang W, Manukyan MC, Shou W, Wang M. SDF-1/CXCR4 mediates acute protection of cardiac function through myocardial STAT3 signaling following global ischemia/reperfusion injury. Am J Physiol Heart Circ Physiol. 2011; 301:H1496-1505.
29. Nishimura R, Moriyama K, Yasukawa K, Mundy GR, Yoneda T. Combination of interleukin-6 and soluble interleukin-6 receptors induces differentiation and activation of JAK-STAT and MAP kinase pathways in MG-63 human osteoblastic cells. J Bone Miner Res. 1998; 13:777-785.
30. Itoh S, Udagawa N, Takahashi N, Yoshitake F, Narita H, Ebisu S, Ishihara K. A critical role for interleukin-6 family-mediated Stat3 activation in osteoblast

differentiation and bone formation. Bone. 2006; 39:505-512.
31. Mikami Y, Asano M, Honda MJ, Takagi M. Bone morphogenetic protein 2 and dexamethasone synergistically increase alkaline phosphatase levels through JAK/STAT signaling in C3H10T1/2 cells. J Cell Physiol. 2010; 223:123-133.
32. Levy O, Ruvinov E, Reem T, Granot Y, Cohen S. Highly efficient osteogenic differentiation of human mesenchymal stem cells by eradication of STAT3 signaling. Int J Biochem Cell Biol. 2010; 42:1823-1830.
33. Ogawa S, Satake M, Ikuta K. Physical and functional interactions between STAT5 and Runx transcription factors. J Biochem. 2008; 143:695-709.
34. Fan D, Chen Z, Chen Y, Shang Y. Mechanistic roles of leptin in osteogenic stimulation in thoracic ligament flavum cells. J Biol Chem. 2007; 282:29958-29966.
35. Ziros PG, Georgakopoulos T, Habeos I, Basdra EK, Papavassiliou AG. Growth hormone attenuates the transcriptional activity of Runx2 by facilitating its physical association with Stat3β. J Bone Miner Res. 2004; 19:1892-1904.

(*Received March 7, 2012; Revised April 12, 2012; Accepted April 16, 2012*)

Original Article

DOI: 10.5582/bst.2012.v6.2.70

Analysis of cytotoxicity induced by proinflammatory cytokines in the human alveolar epithelial cell line A549

Mitsuaki Muroya, Kyungho Chang*, Kanji Uchida, Masahiko Bougaki, Yoshitsugu Yamada

Department of Anesthesiology, Faculty of Medicine, The University of Tokyo, Tokyo, Japan.

Summary **Epithelial cell injury under hyperinflammatory conditions is critical in the development of septic acute lung injury (ALI). The aim of the present study is to analyze the cytotoxic effects of a mixture of proinflammatory cytokines in the human alveolar epithelial cell line A549. The cytotoxicity of proinflammatory cytokines were assessed in A549 cells by measuring lactate dehydrogenase released into the culture medium and by crystal violet staining of surviving cells. Activation of the caspase-dependent apoptotic pathway was evaluated by monitoring cleavage of cytokeratin 18 by caspases using enzyme-liked immunosorbent assay (ELISA). To estimate the cytotoxic signaling pathways responsible for epithelial injury, agents with antiinflammatory or antioxidative properties were extensively screened for cytoprotective effects in the inflammation-associated epithelial injury model. The present study revealed that inflammatory cytokines exerted cytotoxicity in A549 cells. A mixture of interleukin-1beta (IL-1β), tumor necrosis factor-alpha (TNF-α) and interferon-gamma (IFN-γ), designated as cytomix, augmented cytotoxicity compared with each individual cytokine. Treatment with glucocorticoid (dexamethasone), tetracycline-derived antiinflammatory antibiotics (minocycline or doxycycline), angiotensin II receptor blockers (losartan or telmisartan), or antioxidants (dimethyl sulfoxide, catalase) attenuated cytomix-induced cytotoxicity, including caspase activation. These results implied that inflammatory cytokines alone could cause alveolar epithelial injury in the pathophysiology of septic ALI. Caspase-dependent apoptosis was speculated to be one mechanism responsible for the cytokine-induced cytotoxicity. Agents with antiinflammatory or antioxidative properties such as glucocorticoid, tetracycline-derived antibiotics, angiotensin II receptor blockers, or direct antioxidants showed substantial effect in attenuating cytokine-induced cytotoxicity and may be candidates for treatment options.**

Keywords: Acute lung injury, sepsis, proinflammatory cytokine, epithelial cell injury, apoptosis

1. Introduction

Despite the broad repertoire of potent antibiotics and progress in intensive patient care, sepsis remains a life-threatening condition (*1*). Multiple organ dysfunctions are responsible for the high mortality rate of septic patients. Pulmonary, renal, cardiovascular and coagulation systems are susceptible to acute injury during septic sequelae and therefore resolution of vital organ dysfunctions is pivotal in management of patients with sepsis (*2*). Acute lung injury (ALI) and its more severe form, acute respiratory distress syndrome (ARDS), are characterized by hypoxemia and diffuse bilateral infiltrates in the lung (*3*). Although protective ventilatory strategies have been reported to improve patient survival (*4*), core information leading to decisive therapeutic intervention is still lacking. The pathophysiological basis of ALI consists of excessive and protracted alveolar inflammation accompanied by alveolar epithelial injury, including epithelial cell death (*5-7*). Thus, it is critical to clarify

**Address correspondence to:*
Dr. Kyungho Chang, Department of Anesthesiology, Faculty of medicine, The University of Tokyo, Hongo 7-3-1, Bunkyo-ku, Tokyo 113-8655, Japan.
E-mail: kchang-tky@umin.ac.jp

how the hyperinflammatory condition damages alveolar epithelial cells and to explore what pharmacological agents have potential to protect lung tissue.

In this study, we evaluated the cytotoxicity induced by a mixture of proinflammatory cytokines (IL-1β/TNF-α/IFN-γ), which have been suggested to play major roles in sepsis or ALI (*5,8-13*), in the human alveolar epithelial cell line A549. Then, to clarify the cytotoxic signaling pathways responsible for alveolar epithelial cell injury, various agents with antiinflammatory or antioxidative properties were screened for cytoprotective effects in an *in vitro* acute lung injury model (*9,14-17*).

2. Materials and Methods

2.1. *Cell culture and reagents*

Human lung carcinoma type II epithelium-like A549 cells, purchased from Riken BioResource Center Cell Bank (Tsukuba, Ibaraki, Japan), were grown in Dulbecco's Modified Eagle's Medium (DMEM; Sigma, St. Louis, MO, USA) with 10% heat-inactivated fetal bovine serum (FBS), 100 U/mL penicillin, 100 mg/mL streptomycin in 10 cm dishes at 37°C in a humidified atmosphere of 5% CO_2.

Reagents were purchased commercially as follows; human IL-1β, human high-mobility group box 1 (Humanzyme, Chicago, IL, USA); human TNF-α, human interleukin-6 (IL-6) (Prospec, Rehovot, Israel), human IFN-γ (Peprotech, Rocky Hill, NJ, USA); dexamethasone, minocycline, doxycycline, human Fas ligand (Enzo, Plymouth Meeting, PA, USA); losartan, telmisartan (LKT Laboratories, St. Paul, MN, USA); dimethyl sulfoxide (DMSO), catalase-polyethylene glycol (PEG), crystal violet (Sigma, St. Louis, MO, USA).

2.2. *Drug treatment*

A549 cells were seeded in 24-well tissue culture plates at 5×10^4 cells/well overnight. After cell attachment, the content of FBS in medium was decreased to 2% by medium change. Cells were pretreated for 1 h with agents which were expected to confer cytoprotection and then stimulated with proinflammatory cytokines. To recapitulate the severe inflammatory condition *in vitro* experiments, stimulation of cultured cells by combination of proinflammatory cytokines, such as IL-1β/TNF-α/IFN-γ (designated as cytomix for convenience) was employed (*15-17*). The concentration of these cytokines was mainly 10 ng/mL in the present study. This value was adopted with reference to other reports (*15-17*) and to our preliminary experiments. In fact, at this concentration, either IL-1β or TNF-α exerted substantial cytotoxicity in A549 cells. Control (ctrl) cells were treated with the corresponding vehicle alone. The concentration of vehicle DMSO or ethanol in the medium was kept ≤ 0.2% to minimize the effect of solvents.

2.3. *Cytotoxicity of cytokines against A549 cells*

The cytotoxicity of cytokines against A549 cells was evaluated after 24 h-60 h of cytokine stimulation depending on the purpose of the experiments. Cell morphologies were observed and photographed under a light microscope. Cytotoxicity was evaluated quantitatively by monitoring lactate dehydrogenase (LDH) concentration in culture medium and by crystal violet staining (*18,19*). LDH is abundant in the cytoplasm and is released into the culture medium accompanying damage of the cell membrane. Crystal violet solution can promptly fix and stain living cells on culture plates. Thus, LDH concentration reflects the total amount of damaged cells, while crystal violet staining reflects the total amount of surviving cells.

2.3.1. *LDH determination*

LDH concentration in culture medium was determined using a Cytotoxicity Detection Kit Plus (Roche Applied Science, Mannheim, Germany) according to the manufacturer's instructions. The samples were measured spectrophotometrically at a wavelength of 490 nm (with a reference wavelength of 620 nm). After subtracting the background control value (medium only), each sample value was represented in relation to the untreated control value.

2.3.2. *Crystal violet staining*

After aspiration of culture medium, surviving cells were fixed and stained with 0.5% crystal violet in 95% ethanol for 5 min and then washed with tap water several times. After photographs were taken, 1% sodium dodecylsulfate (SDS) solution was added to each well to elute the blue dye and the absorbance at 595 nm of the eluted samples was measured spectrophotometrically for quantitative evaluation. The values of samples stimulated with cytomix in the presence of pretreatment drugs were calibrated relative to that of the corresponding control with pretreatment drug only.

2.3.3. *Evaluation of caspase activity*

To explore the contribution of apoptosis to the cytokine-induced cytotoxicity of A549 cells, caspase activity was investigated. To this purpose, the levels of soluble caspase-cleaved cytokeratin 18 fragments were measured by M30 cytodeath ELISA (Peviva, Bromma, Sweden) according to the manufacturer's instructions. The M30 antibody recognizes a neo-epitope (Asp396) exposed after cleavage of cytokeratin 18 by effector caspase (caspase 3, 6, and 7) in human, monkey, and

bovine epithelial cells (*20,21*). After subtracting the background control value (empty blank), each sample value was represented in relation to the untreated control value.

2.4. *Statistical analysis*

Experiments were carried out in triplicate and repeated at least three times. Data are expressed as means ± standard error of mean (S.E.M.). Statistical significance of differences between means was determined with either by Student's *t* test or by analysis of variance followed by post hoc Tukey test for multiple comparisons. All statistical procedures were performed using Excel 2004 (Microsoft, USA) with the add-in software Statmate™ 2008 (ATMS, Japan). In all analyses, $p < 0.05$ was taken to indicate statistical significance.

3. Results

3.1. *Mixture of proinflammatory cytokines exerted cytotoxicity synergistically in A549 cells*

The cytotoxic effects of proinflammatory cytokines were investigated in A549 cells. Cytomix (a mixture of IL-1β/TNF-α/IFN-γ) induced cell death, a decrease in cell number, and morphological changes in A549 cells in a dose dependent manner (Figures 1A and 1B). The cytotoxicity became prominent 48 hours after cytomix challenge (Figure 1C). IL-1β decreased cell survival (Figures 2A and 2B) and significantly induced cell damage (Figure 2C). TNF-α showed similar cytotoxicity, although to a lesser extent than IL-1β at the same concentration. IFN-γ alone failed to show cytotoxicity at this concentration. However, adding IFN-γ to IL-1β/TNF-α significantly augmented the cytotoxicity compared to IL-1β/TNF-α alone. This cytotoxic synergism was thought to reflect the clinical observations in sepsis where multiple cytokines are responsible for biological toxic effects in cooperation (*22*).

To estimate the role of apoptosis in cytokine-induced cytotoxicity, the activity of caspases was evaluated by measurement of cleaved cytokeratin 18 released into the culture medium. Cytokeratin 18 is a cytoskeleton protein distributed in the cytoplasm of human epithelial cells. It is a substrate of activated effector caspases (caspase 3, 6, 7), and the amount of cleaved form in culture medium

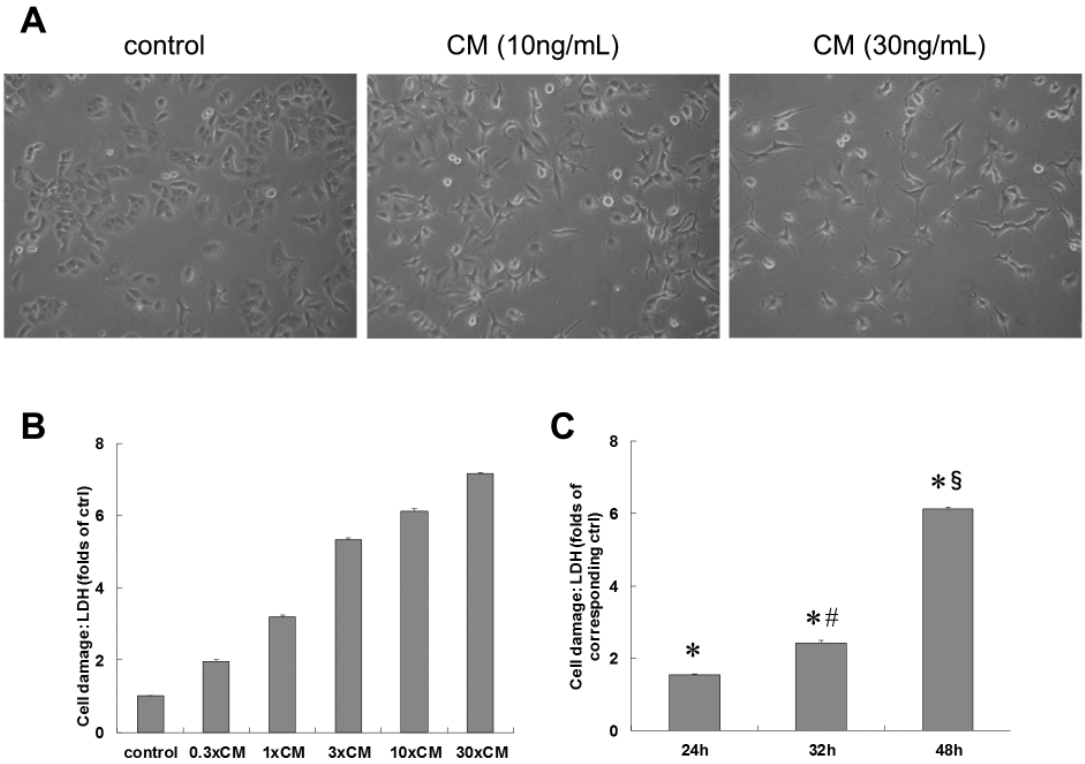

Figure 1. Cytomix induced cell death in A549 cells in a dose-dependent manner. (A) Light microscopic images of A549 cells stimulated with cytomix (CM: a mixture of IL-1β/TNF-α/IFN-γ) for 48 h. Dose dependent decrease in cell number and changes in morphology were observed. The original magnification of the images was 100×. **(B)** A549 cells were stimulated with cytomix at various concentrations. 1× CM stands for 1 ng/mL each of IL-1β, TNF-α, and IFN-γ. Cell damage was evaluated by monitoring the concentration of LDH in culture medium at 48 hours after cytomix challenge. Cytomix induced cell damage in a dose dependent manner in A549 cells. **(C)** A549 cells were stimulated with 10× CM. Cell damage was evaluated by LDH measurement at the indicated times after cytomix challenge. The cytotoxicity induced by cytomix became remarkable 48 h after cytomix challenge. Control cells were treated with the corresponding vehicle alone. Bar graph shows means ± S.E.M. * $p < 0.01$ *vs.* the corresponding control, $^{\#}$ $p < 0.01$ *vs.* 24 h, § $p < 0.01$ *vs.* 32 h.

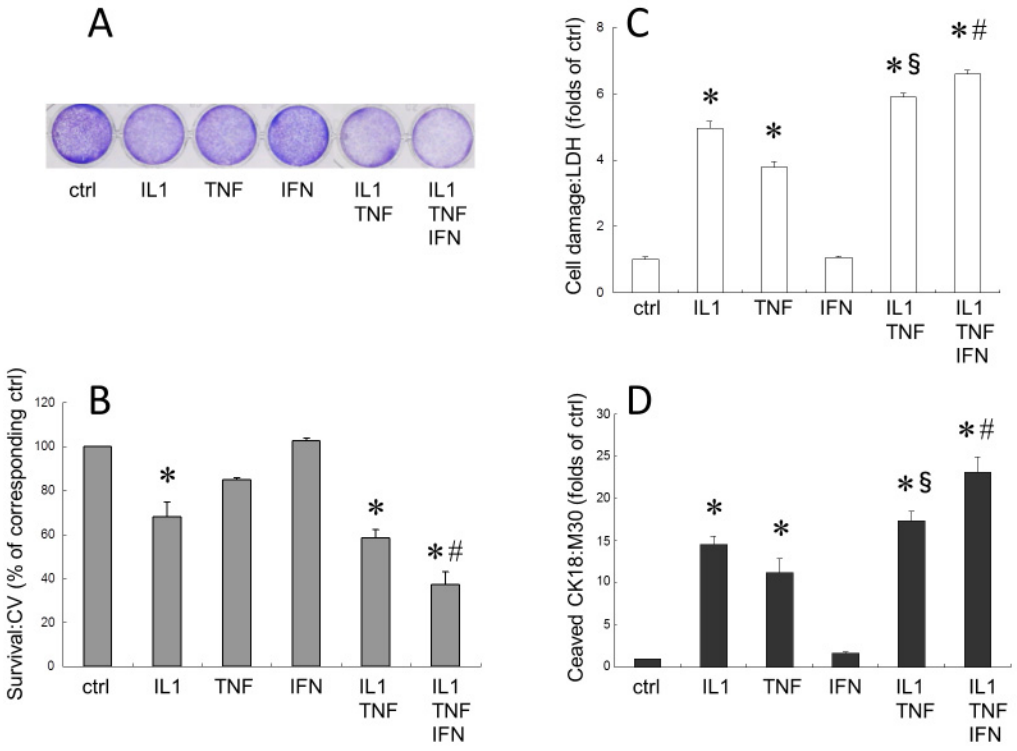

Figure 2. Mixture of proinflammatory cytokines exerted synergistic cytotoxicity in A549 cells. A549 cells were stimulated with proinflammatory cytokines, alone or in combination as indicated, for 48 h. The concentration of each cytokine was 10 ng/ml. The combination of IL-1β/TNF-α/IFN-γ was the most potent in terms of cytotoxicity. Bar graph shows means ± S.E.M. Control (ctrl) cells were treated with the corresponding vehicle alone. **(A)** Photographs showing crystal violet staining of residual cells in culture plates. **(B)** Quantitative analysis of crystal violet (CV) staining was performed as described in "Materials and Methods". * $p < 0.05$ *vs.* ctrl, # $p < 0.05$ *vs.* IL1/TNF. **(C)** Cell damage was evaluated by monitoring the concentration of LDH in culture medium. * $p < 0.01$ *vs.* control, § $p < 0.01$ *vs.* IL1, # $p < 0.05$ *vs.* IL1/TNF. **(D)** Caspase activation was estimated by the concentration of cleaved cytokeratin 18 in culture medium using an M30 cytodeath ELISA kit. * $p < 0.01$ *vs.* control, § $p < 0.01$ *vs.* IL1, # $p < 0.05$ *vs.* IL1/TNF.

is thought to reflect the extent of apoptotic cell death, as explained in the "Materials and Methods". Similar to LDH (Figure 2C), the amount of cleaved cytokeratin 18 was increased significantly by IL-1β or TNF-α but not by IFN-γ alone (Figure 2D). In addition, cytomix showed the most prominent increase in level of cleaved cytokeratin 18.

In addition to IFN-γ, to explore a more appropriate combination of inflammatory mediators, cytotoxicity of other inflammatory mediators, such as Fas ligand, IL-6, or high-mobility group box 1 (HMGB1), was also investigated because these mediators have been reported to play significant roles in sepsis (*14,21,23*). With contrast to IFN-γ, however, Fas ligand, IL-6, or HMGB1 failed to show cytotoxicity in A549 cells, either alone or in combination with IL-1β/TNFγ, up to 100 ng/mL (Figure S1) (*http://www.biosciencetrends.com/getabstract.php?id=532*).

3.2. *Pharmacological attenuation of cytomix-induced cytotoxicity in A549 cells*

Next, to search for cytoprotective agents that can suppress the cytotoxicity induced by cytomix, various agents with antiinflammatory or antioxidative properties were extensively screened using LDH measurements. Preliminary experiments revealed that treatment with glucocorticoid (dexamethasone), tetracycline-derived antiinflammatory antibiotics (minocycline or doxycycline), angiotensin II receptor blockers (losartan or telmisartan), or antioxidants (dimethyl sulfoxide, catalase) attenuated cytomix-induced cytotoxicity in a dose dependent manner (data not shown and Table S1 (*http://www.biosciencetrends.com/getabstract.php?id=532*)). On the other hand, pharmacological agents, which failed to attenuate cytokine-induced cytotoxicity in A549 cells, are listed in Table S2 (*http://www.biosciencetrends.com/getabstract.php?id=532*).

Dexamethasone is one of the most widely used drugs for various inflammatory diseases. For ALI, it has been repeatedly reappraised (*24,25*) although its clinical validity has not been established. Dexamethasone improved cell survival after cytomix stimulation in A549 cells (Figure 3A). Dexamethasone also markedly attenuated LDH leakage (Figure 3B) and cleavage of cytokeratin 18 (Figure 3C) induced by cytomix stimulation.

Tetracycline-derived antibiotics, such as minocycline

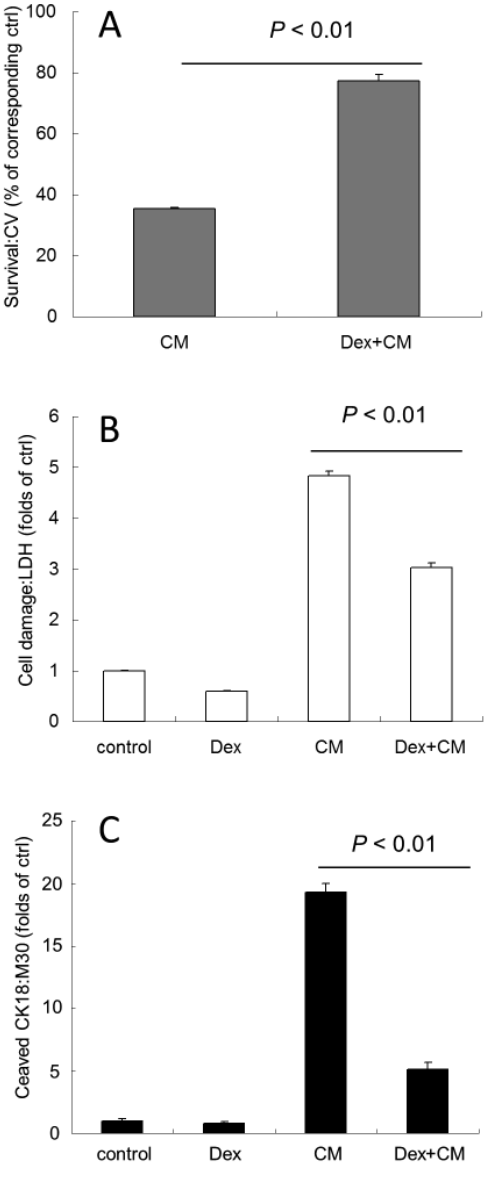

Figure 3. Dexamethasone attenuated cytomix-induced cytotoxicity in A549 cells. A549 was pretreated with dexamethasone (Dex: 1 μM) 1 h before cytomix (CM: a mixture of IL-1β/TNF-α/IFN-γ) stimulation. Forty eight hours after cytomix stimulation, cytotoxicity was evaluated as described in Materials and Methods. Control cells were treated with the corresponding vehicle alone. Bar graph shows means ± S.E.M. **(A)** Dexamethasone significantly recovered cell number in A549 cells stimulated with cytomix in crystal violet staining. **(B** and **C)** LDH and cleaved cytokeratin 18 in culture medium were also determined. Dexamethasone significantly decreased LDH **(B)** and cleaved cytokeratin 18 levels **(C)** in A549 cells stimulated with cytomix.

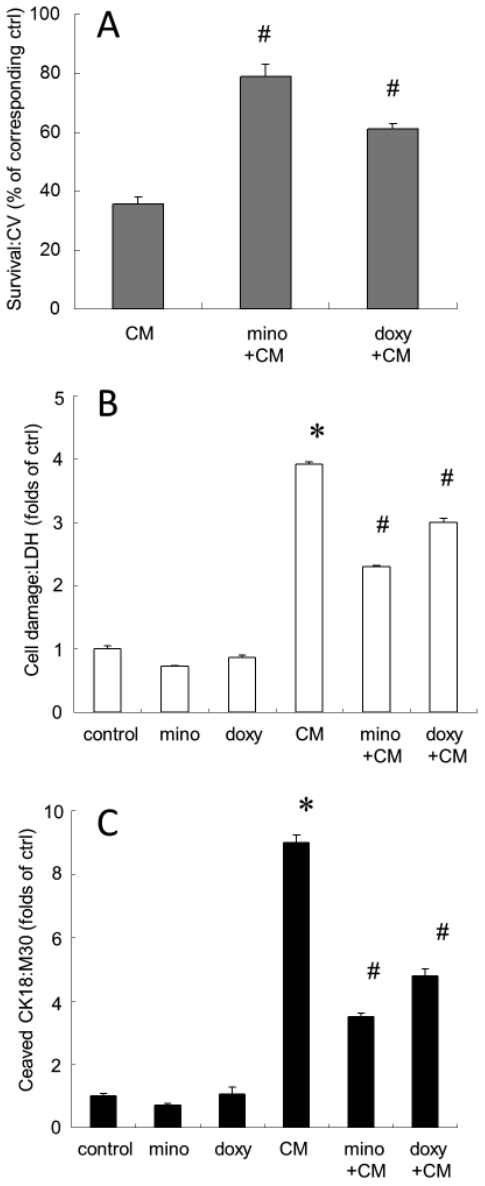

Figure 4. Tetracycline-derived antibiotics (minocycline and doxycycline) attenuated cytomix-induced cytotoxicity in A549 cells. A549 was pretreated with minocycline (mino: 100 μg/mL) or doxycyclie (doxy: 100 μg/mL) 1 h before cytomix (CM: a mixture of IL-1β/TNF-α/IFN-γ) stimulation. Forty eight hours after cytomix stimulation, cytotoxicity was evaluated as described in Materials and Methods. Control (ctrl) cells were treated with the corresponding vehicle alone. Bar graph shows means ± S.E.M. * $p < 0.01$ *vs.* control; # $p < 0.01$ *vs.* CM. **(A)** Minocycline or doxycycline significantly recovered cell number in A549 cells stimulated with cytomix in crystal violet staining. **(B** and **C)** LDH and cleaved cytokeratin 18 in culture medium were also determined. Minocycline or doxycycline significantly decreased LDH **(B)** and cleaved cytokeratin 18 levels **(C)** in A549 cells stimulated with cytomix.

or doxycycline, are known to have pleiotropic effects other than inhibiting growth of microorganisms, including antiinflammatory and cytoprotective properties (*17,26,27*). Minocycline or doxycycline was shown to attenuate the cytotoxicity induced by cytomix in A549 cells similar to dexamethasone (Figure 4) .

Angiotensin II receptor blockade has been shown to confer cytoprotection in cardiovascular tissues subjected to inflammation or ischemia/reperfusion injury (*28,29*). Some reports have argued that it is also a promising candidate for alleviating the pathophysiology of ALI (*30,31*). Losartan, the first angiotensin II receptor blocker (ARB) clinically applied, improved cell survival after cytomix stimulation in A549 cells (Figure 5A). In addition, it attenuated LDH leakage and cleavage of cytokeratin 18 induced by cytomix stimulation

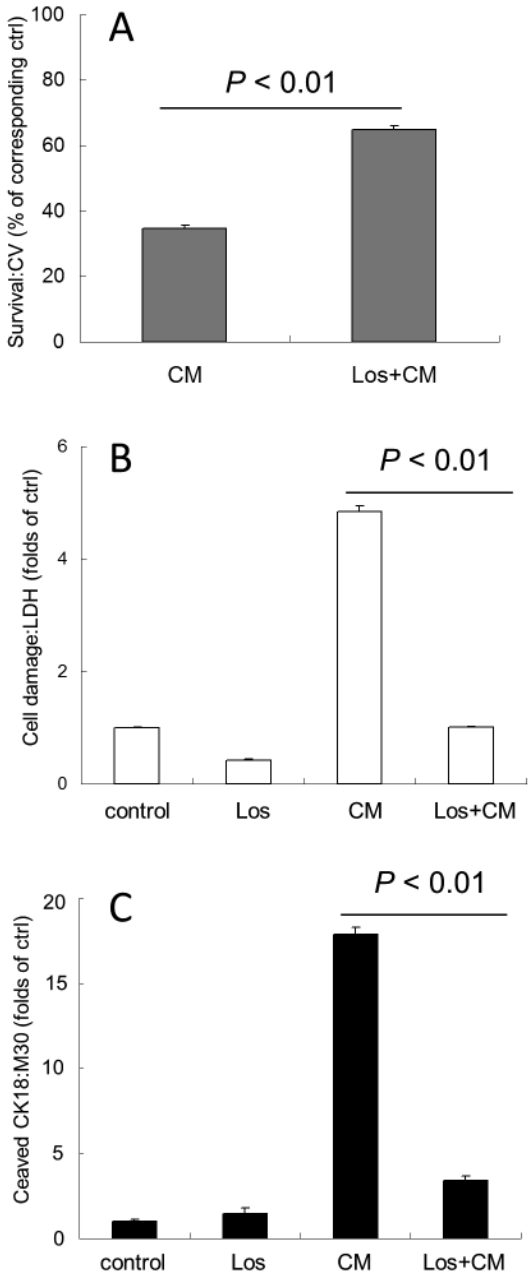

Figure 5. Losartan attenuated cytomix-induced cytotoxicity in A549 cells. A549 was pretreated with losartan (Los: 0.5 mM) 1 h before cytomix (CM: a mixture of IL-1β/TNF-α/IFN-γ) stimulation. Forty eight hours after cytomix stimulation, cytotoxicity was evaluated as described in "Materials and Methods". Control cells were treated with the corresponding vehicle alone. Bar graph shows means ± S.E.M. **(A)** Losartan significantly recovered cell number in A549 cells stimulated with cytomix in crystal violet staining. **(B** and **C)** LDH and cleaved cytokeratin 18 in culture medium were also determined. Losartan significantly decreased LDH **(B)** and cleaved cytokeratin 18 levels **(C)** in A549 cells stimulated with cytomix.

(Figures 5B and 5C). Telmisartan, another established ARB, showed similar cytoprotective effects in cytomix-stimulated A549 cells (data not shown).

Oxidative stress is potentially cytotoxic and has been implicated in the mechanisms of various diseases, including acute disease such as systemic inflammation or ischemia-reperfusion injury (*32,33*). There are a number of antioxidants with respective spectrum for neutralizing reactive oxygen species. DMSO, an important polar aprotic solvent, has antioxidant properties such as reducing lipid peroxidation (*34*). Catalase is a common enzyme found in nearly all living organisms that are exposed to oxygen, where it catalyzes the decomposition of hydrogen peroxide to water and oxygen (*35*). These antioxidants attenuated the cytotoxicity induced by cytomix in A549 cells, in terms of cell survival, cell damage, or cleavage of cytokeratin 18 (Figure 6).

3.3. *Dexamethasone or losartan still exerted cytoprotection with delayed treatment after challenge of cytomix in A549 cells*

Cytoprotcetive effects of dexamethasone or losartan were tested as therapeutic agents, meaning that drug administration began after cytomix challenge in A549 cells. Dexamethasone (Figures 7A and 7B) or losartan (Figures 7C and 7D) still conferred cytoprotection significantly with delayed administration up to 12 hours after cytomix challenge, although the degree of cytoprotection decreased compared to pretreatment.

4. Discussion

The main findings of the present study can be summarized as follows:

1. A mixture of proinflammatory cytokines (IL-1β/TNF-α/IFN-γ) exerted synergistic cytotoxic effects in the human alveolar epithelial cell line A549.

2. Cytokine-induced cytotoxicity was mediated at least partially by the caspase-dependent apoptotic signaling pathway.

3. Antiinflammatory agents, such as glucocorticoid (dexamethasone), tetracycline-derived antibiotics (minocycline, doxycycline), angiotensin II receptor blockers (losartan, telmisartan), or antioxidants (DMSO, catalase) showed prominent cytoprotective effects against the cytotoxicity induced by proinflammatory cytokines.

4. Dexamethasone or losartan still exerted cytoprotection following late treatment after challenge of cytomix in A549 cells.

IL-1β and TNF-α are postulated to be the two main proinflammatory cytokines involved in systemic inflammation (*7,11*). Either of these cytokines alone can induce clinical manifestations, such as hypotension, high fever, chills, and organ dysfunction, representative of sepsis (*22*). In the present study, these cytokines showed cytotoxicity in A549 cells. Although IFN-γ has not yet been regarded as essential in pathophysiology of sepsis like IL-1β or TNF-α, this study clearly showed that it enhanced the cytotoxicity of IL-1β and TNF-α. In fact, the importance of IFN-γ in the native

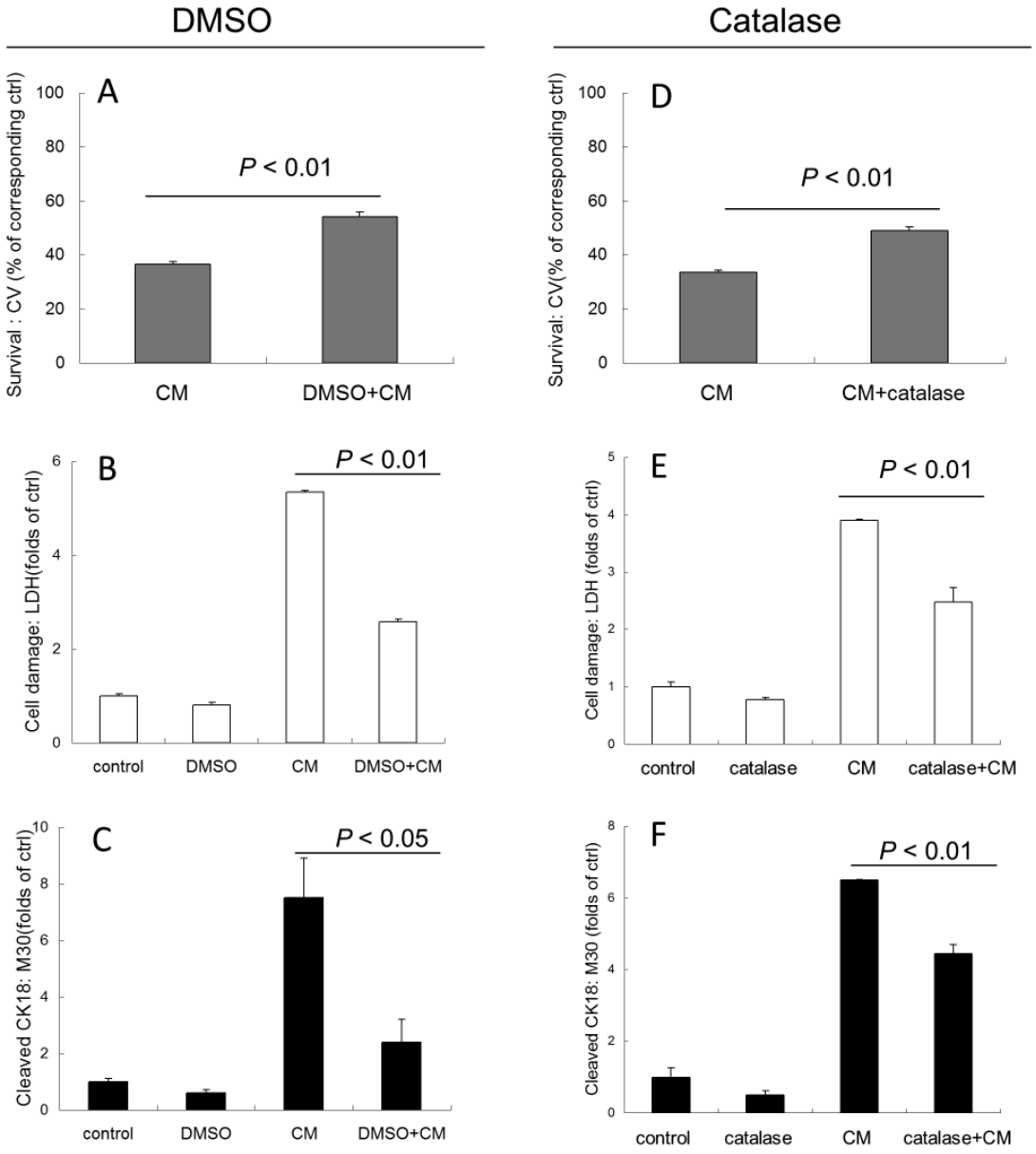

Figure 6. Antioxidants (DMSO or catalase) attenuated cytomix-induced cytotoxicity in A549 cells. A549 was pretreated with dimethyl sulfoxide (1% DMSO, **A-C**) or catalase conjugtated to polyethylene glycol (1,000 unit/mL, **D-F**) 1 h before cytomix (CM: a mixture of IL-1β/TNF-α/IFN-γ) stimulation. Forty eight hours after cytomix stimulation, cytotoxity was evaluated as described in "Materials and Methods". Control (ctrl) cells were treated with the corresponding vehicle alone. Bar graph shows means ± S.E.M. DMSO **(A)** or catalase **(D)** significantly recovered cell number in A549 cells stimulated with cytomix in crystal violet staining. LDH and cleaved cytokeratin 18 in culture medium were also determined. DMSO **(B and C)** or catalse **(E and F)** significantly decreased LDH and cleaved cytokeratin 18 levels in A549 cells stimulated with cytomix.

immune system has recently attracted a great deal of attention (*36*). For example, IFN-γ promotes innate immune response by activating macrophage, which plays major roles in eliminating infectious pathogens. IFN-γ enhances immune cell responsiveness to other inflammatory stimuli, such as toll-like receptor ligands and TNF. This phenomenon, termed as "priming", greatly augments toll-like receptor-induced expression of inflammatory mediators and immune effectors including multiple cytokines and chemokines, and profoundly affects biological outcomes of inflammation. In a murine model of sepsis induced by cecal ligation and puncture (CLP), late administration of anti-IFN-γ antibody enhanced survival (*37*). In fact, high levels of IFN-γ has been demonstrated in some populations with clinical systemic inflammation, especially in virus-associated ALI such as SARS (severe acute respiratory syndrome) (*8,10*). Multiple inflammatory mediators have been proved in the bloodstream and bronchoalveolar lavage fluid of patients with septic ALI (*10-13*). The observation that a mediator such as IFN-γ, which has minimal direct toxicity against

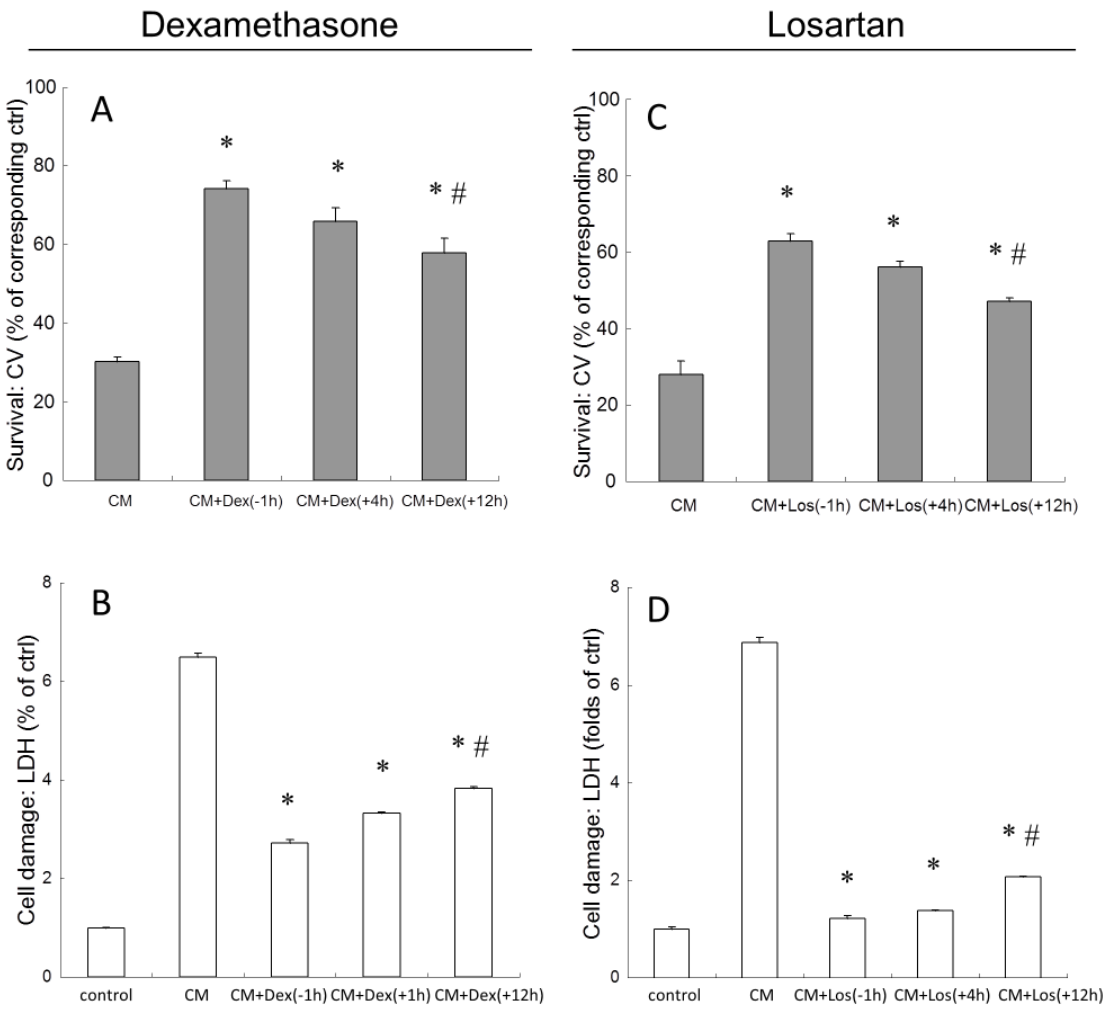

Figure 7. Dexamethasone or losartan still exerted cytoprotection with delayed treatment after cytomix challenge in A549 cells. A549 was stimulated with cytomix (CM: a mixture of IL-1β/TNF-α/IFN-γ). Co-treatement of either dexamethasone (1 μM or losartan (0.5 mM) was initiated 1 h before (−1 h), 4 h after (+4 h), or 12 h after (+12 h) cytomix stimulation. Sixty hours after cytomix stimulation, cytotoxicity was evaluated by crystal violet staining and LDH measurement. Dexamethasone **(A** and **B)** or losartan **(C** and **D)** still conferred cytoprotection significantly with delayed treatment up to 12 h after cytomix challenge, although the degree of cytoprotection decreased significantly compared to pretreatment (−1 h). Control (ctrl) cells were treated with the corresponding vehicle alone. Bar graph shows means ± S.E.M. * $p < 0.01$ *vs.* CM; # $p < 0.01$ *vs.* pretreatment (−1 h).

parenchymal cells, can exert synergistic cytotoxicity in combination with other mediators implies the complex pathophysiology of sepsis and suggests one reason for the failure of antiinflammatory strategies targeting a single mediator such as IL-1β or TNF-α (*38*).

Neutrophil recruitment and epithelial injury play pivotal roles in the development of ALI (*5-7,21*). A number of inflammatory mediators, such as proinflammatory cytokines, lipid mediators, complements, reactive oxygen species or neutrophil-derived ptoteases such as elastase (*39*), are postulated to be responsible for loss of epithelial integrity. However, there is little doubt that proinflammatory cytokines make a substantial contribution in initiating the pathological process of septic ALI. Thus, elucidation of the direct link between proinflammatory cytokines and epithelial injury, focusing on molecular mechanisms, is indispensable to understand the progression of septic ALI. The present study confirmed that human alveolar epithelial cells were damaged after challenge by proinflammatory cytokines. Cell death evoked by cytokine challenge was remarkable, and the increase in level of cleaved cytokeratin 18 strongly suggested the substantial involvement of caspase-dependent apoptosis. These results are compatible with other reports arguing that apoptosis pathways are activated in septic ALI experimentally or clinically (*5-7,11,40,41*).

As it has been established that hyperinflammatory status is the major pathophysiology of septic ALI, modifying inflammation should be highlighted as one of the central strategies for alleviating septic ALI. Although protective ventilatory strategies have been shown to lessen mortality in ALI patients (*4*), the way of directly downregulating inflammation itself has not been fully examined. In addition, there is increasing evidence that oxidative stress as well as nitrosative

stress prevails at sites of inflammation as adaptive responses of the host, such as antimicrobial strategies or stress-evoked signal transduction (*32,33*). As excessive oxidative stress in turn causes tissue damage of host cells, alleviation of oxidative stress can be a promising alternative to controlling inflammation-associated injury in septic ALI (*42,43*). In the present study, we screened agents with antiinflammatory or antioxidative properties for cytoprotective effects in the *in vitro* model mimicking alveolar hyperinflammation. We have demonstrated that antiinflammatory agents dexamethasone, tetracycline-derived antibiotics, or ARBs attenuated cytokine-induced cytotoxicity including caspase activation in A549 cells. In addition, antioxidants such as DMSO or catalase similarly attenuated cytokine-induced cytotoxicity. These agents have been referred to as cytoprotective in inflammation-associated conditions (*24-35*), although clinical validity has not been fully defined, especially in septic ALI. Further investigations are underway to clarify the mechanism of pharmacological attenuation of cytokine-induced cytotoxicity. It is widely accepted that inflammatory stimuli activate NF-kappaB pathway and MAP kinase pathway (*44*). Simultaneously, oxidative stress contributes to epithelial injury because catalase was effective in attenuating inflammation-associated cell death in the present results. Thus, we are now focusing on NF-kappaB pathways, MAP kinase pathways and sources of oxidative stress (such as mitochondria, NADPH oxidase, xanthine oxidase, inducible nitric oxide synthase, or arachidonic acid cascade), as cytotoxic signal pathways evoked by inflammatory stimuli (Figure 8).

The present study has some limitations. First, A549 is a cancer cell line and its intrinsic cell death pathways may differ from those of physiological human alveolar epithelial cells. Second, cytotoxic mediators employed here were IL-1β/TNF-α/IFN-γ and it is not clear whether this combination is optimal in simulating *in vivo* hyperinflammatory status. Third, the methods used to detect cell death in our experiments were limited. For example, the apoptotic component was estimated based on the level of cleaved cytokeratin 18 and was not confirmed directly by morphological evidence of apoptosis.

However, it is important to check the signaling pathway using human cells as well as using *in vivo* animal models. It is practically impossible to include all of inflammatory mediators as stimulants. The combination of IL-1β/TNF-α/IFN-γ has often been adopted to set up hyperinflammation *in vitro* and accepted in many medical journals (*15-17,45-48*). In the present study it exerted sufficient cytotoxicity with clinical relevance as discussed earlier. It is reported that in clinical septic patients, numerous cytokines, irrespective pro-, or anti-inflammatory, appear in an overlapping manner as long as inflammatory process

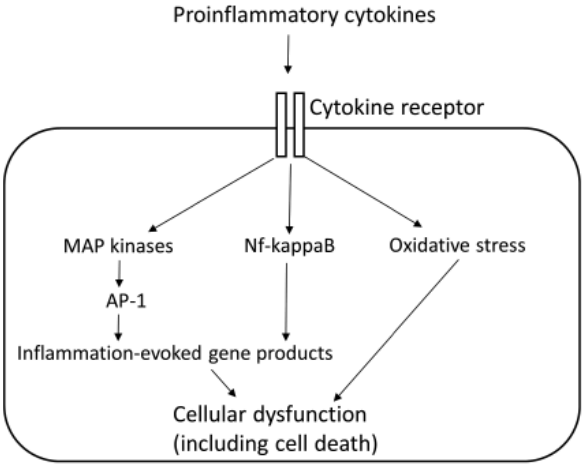

Figure 8. Proposed signaling pathways through which proinflammatory cytokines induce cytotoxicity in alveolar epithelial cells. Putative intracellular signaling components responsible for proinflammatory cytokine-induced cellular dysfunction are shown. It is postulated that cytoprotective agents will interfere in somewhere in the above-mentioned signaling pathways (see "Discussion"). MAP kinase: mitogen activated protein kinase; AP-1: activating protein-1.

continues (*49*). Thus, we postulate that IL-1β/TNF-α/IFN-γ is a minimum and appropriate mixture to simulate the status of clinical cytokine storm in *in vitro* system. Lastly, direct confirmation of apoptosis was not the main objective of this study. Apoptosis is now regarded as just one form of cell death patterns in the recent framework explaining the physiological cell death mechanism (*6*). Thus, evaluation of overall cytotoxicity is more important when differential demonstration of other cell death patterns, such as autophagy, necroptosis, or caspase-independent other programmed cell death, has not been well established yet.

In conclusion, inflammatory cytokines showed synergistic cytotoxic effects on A549 cells. Caspase-dependent apoptosis was speculated to be one mechanism responsible for the cytokine-induced cytotoxicity. Agents with antiinflammatory or antioxidative properties such as glucocorticoid, tetracycline-derived antibiotics, angiotensin II receptor blockers, or antioxidants showed substantial effect in attenuating cytokine-induced cytotoxicity. Further investigations to clarify the mechanisms of their beneficial effects will contribute to exploring new treatment options for ALI.

Acknowledgements

We thank Dr. Fumito Ichinose (Boston, MA, USA) and Dr. Masaomi Nangaku (Tokyo, Japan) for the critical reading of the paper and insightful suggestions. This work was supported in part by grants from the Ministry of Education, Culture, Sports, Science and Technology of Japan (No. 21592304 to K.C.).

References

1. Angus DC, Linde-Zwirble WT, Lidicker J, Clermont G, Carcillo J, Pinsky MR. Epidemiology of severe sepsis in the united states: Analysis of incidence, outcome, and associated costs of care. Crit Care Med. 2001; 29:1303-1310.
2. Dellinger RP, Levy MM, Carlet JM, *et al*. Surviving Sepsis Campaign: International guidelines for management of severe sepsis and septic shock. Intensive Care Med. 2008; 34:17-60.
3. Wheeler AP, Bernard GR. Acute lung injury and the acute respiratory distress syndrome: A clinical review. Lancet. 2007; 369:1553-1564.
4. Ventilation with lower tidal volumes as compared with traditional tidal volumes for acute lung injury and the acute respiratory distress syndrome. the acute respiratory distress syndrome network. N Engl J Med. 2000; 342:1301-1308.
5. Perl M, Lomas-Neira J, Chung CS, Ayala A. Epithelial cell apoptosis and neutrophil recruitment in acute lung injury-a unifying hypothesis? what we have learned from small interfering RNAs. Mol Med. 2008; 14:465-475.
6. Tang PS, Mura M, Seth R, Liu M. Acute lung injury and cell death: How many ways can cells die? Am J Physiol Lung Cell Mol Physiol. 2008; 294:L632-L641.
7. Martin TR, Hagimoto N, Nakamura M, Matute-Bello G. Apoptosis and epithelial injury in the lungs. Proc Am Thorac Soc. 2005; 2:214-220.
8. Theron M, Huang KJ, Chen YW, Liu CC, Lei HY. A probable role for IFN-gamma in the development of a lung immunopathology in SARS. Cytokine. 2005; 32:30-38.
9. Bastarache JA, Sebag SC, Grove BS, Ware LB. Interferon-gamma and tumor necrosis factor-alpha act synergistically to up-regulate tissue factor in alveolar epithelial cells. Exp Lung Res. 2011; 37:509-517.
10. Wong CK, Lam CW, Wu AK, Ip WK, Lee NL, Chan IH, Lit LC, Hui DS, Chan MH, Chung SS, Sung JJ. Plasma inflammatory cytokines and chemokines in severe acute respiratory syndrome. Clin Exp Immunol. 2004; 136:95-103.
11. Brabant D, Michael P, Bleiblo F, Saleh M, Narain R, Tai TC, Ramana CV, Parrillo JE, Kumar A, Kumar A. Septic sera induces apoptosis and DNA fragmentation factor 40 activation in fibroblasts. Biochem Biophys Res Commun. 2011; 412:260-265.
12. Meduri GU, Kohler G, Headley S, Tolley E, Stentz F, Postlethwaite A. Inflammatory cytokines in the BAL of patients with ARDS. persistent elevation over time predicts poor outcome. Chest. 1995; 108:1303-1314.
13. Wu CL, Lin LY, Yang JS, Chan MC, Hsueh CM. Attenuation of lipopolysaccharide-induced acute lung injury by treatment with IL-10. Respirology. 2009; 14:511-521.
14. Mizuta M, Nakajima H, Mizuta N, Kitamura Y, Nakajima Y, Hashimoto S, Matsuyama H, Shime N, Amaya F, Koh H, Ishizaka A, Magae J, Tanuma SI, Hashimoto S. Fas ligand released by activated monocytes causes apoptosis of lung epithelial cells in human acute lung injury model *in vitro*. Biol Pharm Bull. 2008; 31:386-390.
15. Fang X, Neyrinck AP, Matthay MA, Lee JW. Allogeneic human mesenchymal stem cells restore epithelial protein permeability in cultured human alveolar type II cells by secretion of angiopoietin-1. J Biol Chem. 2010; 285:26211-26222.
16. Bastarache JA, Wang L, Geiser T, Wang Z, Albertine KH, Matthay MA, Ware LB. The alveolar epithelium can initiate the extrinsic coagulation cascade through expression of tissue factor. Thorax. 2007; 62:608-616.
17. Raza M, Ballering JG, Hayden JM, Robbins RA, Hoyt JC. Doxycycline decreases monocyte chemoattractant protein-1 in human lung epithelial cells. Exp Lung Res. 2006; 32:15-26.
18. Ota H, Tokunaga E, Chang K, Hikasa M, Iijima K, Eto M, Kozaki K, Akishita M, Ouchi Y, Kaneki M. Sirt1 inhibitor, sirtinol, induces senescence-like growth arrest with attenuated ras-MAPK signaling in human cancer cells. Oncogene. 2006; 25:176-185.
19. Saotome K, Morita H, Umeda M. Cytotoxicity test with simplified crystal violet staining method using microtitre plates and its application to injection drugs. Toxicol In Vitro. 1989; 3:317-321.
20. Leers MP, Kölgen W, Björklund V, Bergman T, Tribbick G, Persson B, Björklund P, Ramaekers FC, Björklund B, Nap M, Jörnvall H, Schutte B. Immunocytochemical detection and mapping of a cytokeratin 18 neo-epitope exposed during early apoptosis. J Pathol. 1999; 187:567-572.
21. Perl M, Chung CS, Perl U, Lomas-Neira J, de Paepe M, Cioffi WG, Ayala A. Fas-induced pulmonary apoptosis and inflammation during indirect acute lung injury. Am J Respir Crit Care Med. 2007; 176:591-601.
22. Dinarello CA. Proinflammatory and anti-inflammatory cytokines as mediators in the pathogenesis of septic shock. Chest. 1997; 112 (6 Suppl):321S-329S.
23. Cohen J. The immunopathogenesis of sepsis. Nature. 2002; 420:885-891.
24. Peter JV, John P, Graham PL, Moran JL, George IA, Bersten A. Corticosteroids in the prevention and treatment of acute respiratory distress syndrome (ARDS) in adults: Meta-analysis. BMJ. 2008; 336:1006-1009.
25. Agarwal R, Nath A, Aggarwal AN, Gupta D. Do glucocorticoids decrease mortality in acute respiratory distress syndrome? A meta-analysis. Respirology. 2007; 12:585-590.
26. Nikodemova M, Duncan ID, Watters JJ. Minocycline exerts inhibitory effects on multiple mitogen-activated protein kinases and IkappaBalpha degradation in a stimulus-specific manner in microglia. J Neurochem. 2006; 96:314-323.
27. Wang AL, Yu AC, Lau LT, Lee C, Wu le M, Zhu X, Tso MO. Minocycline inhibits LPS-induced retinal microglia activation. Neurochem Int. 2005; 47:152-158.
28. Matsuhisa S, Otani H, Okazaki T, Yamashita K, Akita Y, Sato D, Moriguchi A,Imamura H, Iwasaka T. Angiotensin II type 1 receptor blocker preserves tolerance to ischemia-reperfusion injury in dahl salt-sensitive rat heart. Am J Physiol Heart Circ Physiol. 2008; 294:H2473-H2479.
29. Cianchetti S, Del Fiorentino A, Colognato R, Di Stefano R, Franzoni F, Pedrinelli R. Anti-inflammatory and anti-oxidant properties of telmisartan in cultured human umbilical vein endothelial cells. Atherosclerosis. 2008; 198:22-28.
30. Wang F, Xia ZF, Chen XL, Jia YT, Wang YJ, Ma B. Angiotensin II type-1 receptor antagonist attenuates LPS-induced acute lung injury. Cytokine. 2009; 48:246-253.
31. Imai Y, Kuba K, Rao S, *et al*. Angiotensin-converting enzyme 2 protects from severe acute lung failure. Nature.

2005; 436:112-116.
32. Dare AJ, Phillips AR, Hickey AJ, Mittal A, Loveday B, Thompson N, Windsor JA. A systematic review of experimental treatments for mitochondrial dysfunction in sepsis and multiple organ dysfunction syndrome. Free Radic Biol Med. 2009; 47:1517-1525.
33. Crimi E, Sica V, Williams-Ignarro S, Zhang H, Slutsky AS, Ignarro LJ, Napoli C. The role of oxidative stress in adult critical care. Free Radic Biol Med. 2006; 40:398-406.
34. Sanmartin-Suarez C, Soto-Otero R, Sanchez-Sellero I, Mendez-Alvarez E. Antioxidant properties of dimethyl sulfoxide and its viability as a solvent in the evaluation of neuroprotective antioxidants. J Pharmacol Toxicol Methods. 2011; 63:209-215.
35. Beckman JS, Minor RL Jr, White CW, Repine JE, Rosen GM, Freeman BA. Superoxide dismutase and catalase conjugated to polyethylene glycol increases endothelial enzyme activity and oxidant resistance. J Biol Chem. 1988; 263:6884-6892.
36. Hu X, Ivashkiv LB. Cross-regulation of signaling pathways by interferon-gamma: Implications for immune responses and autoimmune diseases. Immunity. 2009; 31:539-550.
37. Márquez-Velasco R, Martínez-Velázquez AX, Amezcua-Guerra LM, Flores-Guzmán F, Díaz-Quiñonez A, Massó F, Paniagua-Solís J, Bojalil R. Enhanced survival from CLP-induced sepsis following late administration of low doses of anti-IFNγF(ab')2 antibody fragments. Inflamm Res. 2011; 60:947-953.
38. Zeni F, Freeman B, Natanson C. Anti-inflammatory therapies to treat sepsis and septic shock: A reassessment. Crit Care Med. 1997; 25:1095-1100.
39. Misumi T, Tanaka T, Mikawa K, Nishina K, Morikawa O, Obara H. Effects of sivelestat, a new elastase inhibitor, on IL-8 and MCP-1 production from stimulated human alveolar epithelial type II cells. J Anesth. 2006; 20:159-165.
40. Hotchkiss RS, Nicholson DW. Apoptosis and caspases regulate death and inflammation in sepsis. Nat Rev Immunol. 2006; 6:813-822.
41. Matsuda N, Yamamoto S, Takano K, Kageyama S, Kurobe Y, Yoshihara Y, Takano Y, Hattori Y. Silencing of fas-associated death domain protects mice from septic lung inflammation and apoptosis. Am J Respir Crit Care Med. 2009; 179:806-815.
42. Koga H, Hagiwara S, Inomata M, Kono Y, Oyama Y, Kai S, Nishida T, Noguchi T. The new vitamin E derivative, ETS-GS, protects against cecal ligation and puncture-induced systemic inflammation in rats. Inflammation. 2011; 35:545-553.
43. El-Sayed NS, Mahran LG, Khattab MM. Tempol, a membrane-permeable radical scavenger, ameliorates lipopolysaccharide-induced acute lung injury in mice: A key role for superoxide anion. Eur J Pharmacol. 2011; 663:68-73.
44. Matsuda N, Hattori Y. Systemic inflammatory response syndrome (SIRS): Molecular pathophysiology and gene therapy. J Pharmacol Sci. 2006; 101:189-198.
45. Wang Q, Guo XL, Wells-Byrum D, Noel G, Pritts TA, Ogle CK. Cytokine-induced epithelial permeability changes are regulated by the activation of the p38 mitogen-activated protein kinase pathway in cultured Caco-2 cells. Shock. 2008; 29:531-537.
46. Berg S, Sappington PL, Guzik LJ, Delude RL, Fink MP. Proinflammatory cytokines increase the rate of glycolysis and adenosine-5'-triphosphate turnover in cultured rat enterocytes. Crit Care Med. 2003; 31:1203-1212.
47. Farley KS, Wang L, Mehta S. Septic pulmonary microvascular endothelial cell injury: Role of alveolar macrophage NADPH oxidase. Am J Physiol Lung Cell Mol Physiol. 2009; 296:L480-L488.
48. Sappington PL, Han X, Yang R, Delude RL, Fink MP. Ethyl pyruvate ameliorates intestinal epithelial barrier dysfunction in endotoxemic mice and immunostimulated Caco-2 enterocytic monolayers. J Pharmacol Exp Ther. 2003; 304:464-476.
49. Tamayo E, Fernández A, Almansa R, Carrasco E, Heredia M, Lajo C, Goncalves L, Gómez-Herreras JI, de Lejarazu RO, Bermejo-Martin JF. Pro- and anti-inflammatory responses are regulated simultaneously from the first moments of septic shock. Eur Cytokine Netw. 2011; 22:82-87.

(*Received February 7, 2012; Revised February 20, 2012; Accepted March 2, 2012*)

Original Article

DOI: 10.5582/bst.2012.v6.2.81

N-terminal PEGylation of human serum albumin and investigation of its pharmacokinetics and pulmonary microvascular retention

Ting Zhao[1], Yang Yang[1], Aizhen Zong[1], Haining Tan[2], Xinlei Song[1], Shuo Meng[1], Chunxia Song[3], Guangli Pang[4], Fengshan Wang[1,2,*]

[1] *Institute of Biochemical and Biotechnological Drugs, School of Pharmaceutical Sciences, Shandong University, Ji'nan, China;*
[2] *National Glycoengineering Research Center, Shandong University, Ji'nan, China;*
[3] *Marine College, Shandong University at Weihai, Weihai, China;*
[4] *Shandong Taibang Biological Products Co. Ltd., Taian, China.*

Summary **Human serum albumin (HSA) is used as an important plasma volume expander in clinical practice. In the present study, HSA was N-terminally PEGylated and a PEGylated HSA (PEG-HSA) carrying one chain of PEG (20 kDa) per HSA molecule was obtained. The purity, secondary structure and hydrodynamic radius of the modified protein were characterized using sodium dodecyl sulfate polyacrylamide gel electrophoresis, circular dichroism measurements, and dynamic light scattering, respectively. The pharmacokinetics in normal mice and vascular permeability of the PEG-HSA in a lipopolysaccharide-induced acute lung injury mice model were evaluated. The results showed that the biological half-life of the modified HSA was approximately 2.2 times of that of native HSA, and PEG-HSA had a lower vascular permeability which suggested that PEGylation of HSA could reduce extravasation into interstitial space. It can be inferred that due to the prolonged half-life time and enhanced vascular retention, the molecularly homogeneous PEG-HSA may be a superior candidate as a plasma volume expander in treating capillary permeability increase related illness.**

Keywords: Human serum albumin, N-terminal PEGylation, vascular permeability, pharmacokinetics

1. Introduction

Human serum albumin (HSA) is the major protein component of human plasma with a plasma content of 42 ± 3.5 g/L. It consists of a single non-glycosylated polypeptide chain of 585 amino acids forming a heart-shaped molecule with molecular weight of 66.5 kDa (*1*). HSA is responsible for 80% of the colloid osmotic pressure of plasma (25-33 mmHg). Because of this, its main clinical use is in maintaining colloid osmotic pressure and increasing circulating plasma volume. HSA is widely used to treat hypovolemia caused by traumatic shock, massive hemorrhage, burns, cirrhosis with ascites and hypoalbuminemia, with a usual dosage of 10 g/dose or more (*2*).

In spite of the many theoretical benefits of albumin infusion in critically ill patients, the clinical use of albumin is still controversial. It is reported that the loss rate of albumin to tissue spaces rose by more than 300% in patients with septic shock and the average increase occurring within 7 h of cardiac surgery was 100% (*3,4*). The transcapillary escape rate in cachectic cancer patients was twice that of healthy individuals (*5*). Increased vascular permeability is an important cause of the hypoalbuminemia commonly seen in acute and chronic disease (*6*). Under these conditions, correction of low plasma volume therefore becomes essential. However, the plasma expanding effect

**Address correspondence to:*
Dr. Fengshan Wang, Institute of Biochemical and Biotechnological Drugs, School of Pharmaceutical Sciences, Shandong University, Ji'nan 250012, China.
E-mail: fswang@sdu.edu.cn

of HSA is transient due to a continuous leakage of macromolecules into the interstitial space (*7*), such poor intravascular retention does not only lead to interstitial edema but also demands frequent HSA infusion to maintain the desired blood concentration (*8*).

In addition, commercial production of HSA is primarily based on fractionation of plasma obtained from blood donors, which is limited in supply but has high clinical demand globally. Many efforts have been made to develop a substitute for plasma-derived HSA (pdHSA) by means of gene manipulation techniques (*2,9*). However, due to the high dosage of HSA in clinical applications, there is still an unsettled problem concerning the establishment of techniques for high purity, low cost, industrial, large-scale production of recombinant HSA (rHSA). Therefore, at present, plasma is still the most important source of HSA as a plasma volume expander.

In the present study, we hypothesized whether an albumin alternative agent with properties of good intravascular retention and a long life time could be developed to solve the problems of interstitial edema and frequent infusion. Increasing the molecular weight of HSA may be a very good potential approach to make a modified HSA as a superior volume expander. We conjugated HSA with polyethylene glycol (PEG) in a site-specific manner by taking advantage of the differences between the p*Ka* values of the α-amino group of the N-terminal amino acid residue and the ε-amino groups of the Lys residues in the protein backbone. This N-terminal PEGylation could generate a chemically well-defined and molecularly homogeneous modified HSA product. The secondary structure and hydrodynamic radius was characterized. In addition, a pharmacokinetics study of native HSA and PEGylated HSA (PEG-HSA) was conducted using an iodine-125 (^{125}I) isotope tracing technique in mice, and vascular permeability was evaluated in a murine model of lipopolysaccharide (LPS)-induced lung injury.

2. Materials and Methods

2.1. *Materials*

Propionaldehyde-derivatized 20 kDa linear monofunctional PEG (mPEG) was purchased from Beijing Kaizheng Biotech Development Co., Ltd., Beijing, China. HSA was kindly provided by Shandong Taibang Biologic Products Co., Ltd., Taian, China. ^{125}I was purchased from the China Institute of Atomic Energy, Beijing, China. DEAE Sepharose Fast Flow was purchased from GE Healthcare Bio-Sciences, Piscataway, NJ, USA. LPS from *Escherichia coli* 055:B5 was a product of Sigma-Aldrich, St Louis, MO, USA. Other reagents and chemicals were of commercially available analytical grade. Circular dichroism (CD) spectra were measured using a Chirascan spectropolarimeter, Applied Photophysics, Surrey, UK. Dynamic light scattering (DLS) measurements were performed on a DAWN® HELEOS™ multi-angle laser light scattering photometer, Wyatt Technology, Santa Barbara, CA, USA. Histology examination was conducted with an inverted fluorescence microscope (Olympus, Tokyo, Japan).

2.2. *Animals*

Four to five week-old male Kunming mice weighing 18-20 g used in the experiments were supplied by the experimental animal center of Shandong University. The animals were housed in animal facilities accredited by the Shandong Council on Animal Care and treated in accordance with approved protocols. Animals were maintained in a specific pathogen-free environment that was temperature-controlled (23 ± 2°C) and humidity-controlled (60 ± 10%), under a 12:12 h light/dark cycle.

2.3. *Preparation of 20 kDa mPEG-propionaldehyde-modified HSA*

The reaction was carried out with stirring at 4°C for 36 h using 25 mg freeze-dried HSA at a 5 mg/mL protein concentration in 10 mM sodium phosphate buffer, pH 6.0, containing 20 mM sodium cyanoborohydride. The PEG-propionalde derivative (Mw = 20 kDa, 23 mg) was added to give a 3:1 molar ratio of PEG/protein.

The reaction mixture was stopped by diluting the mixture with 10 volumes of buffer A (10 mM phosphate buffer, pH 6.5) and applied to a DEAE Sepharose FF column (2.6 cm × 20 cm) which was initially equilibrated with buffer A. The column was washed with buffer A to remove unconjugated PEG and then, bound proteins were eluted with an ascending linear gradient up to 40% buffer B (10 mM phosphate buffer, pH 6.5 containing 1 M NaCl) over 5 column volumes. The elution was monitored at 280 nm. The fraction containing mono-PEGylated HSA was collected and desalted by ultrafiltration employing a membrane with a 30 kDa cut-off. Protein concentration was determined using a bicinchoninic acid (BCA) assay kit (Solarbio, Beijing, China) according to the manufacturer's instructions.

2.4. *Purity identification of PEGylated HSA using sodium dodecyl sulfate polyacrylamide gel electrophoresis (SDS-PAGE)*

Reaction mixtures and fractions from the DEAE column were analyzed by SDS-PAGE. Samples in loading buffer were incubated at 100°C for 5 min, and loaded on a 10% polyacrylamide Tris-glycine gel according to Laemmli (*10*). Electrophoresis was programmed using a two-step mode applying constant voltages of 80 V in the stacking gel and 130 V in the separation gel. After approximately

2 h, gels were stained with Coomassie Brilliant Blue R-250 overnight and destained afterwards. Gel images were scanned immediately after the destaining steps on a gel imaging system.

2.5. *Secondary structure analysis by far-UV CD measurement*

CD analysis was used to examine the secondary structural conformation of HSA and PEG-HSA. CD measurements were taken on an Applied Photophysics Chirascan spectropolarimeter using a 1 mm circular quartz cell at room temperature. The spectra were recorded in the far UV (190~260 nm) using 5 μM HSA solution or an equimolar quantity of PEGylated HSA in 50 mM phosphate buffer, pH 7.4 (*8*). The bandwidth was 1 nm and time-per-point was 1 sec.

2.6. *Hydrodynamic radius determination by DLS*

DLS was used to characterize the hydrodynamic radius (R_h) of HSA and PEG-HSA molecules. A linearly polarized gallium arsenide (GaAs) laser operating at 658 nm was used to illuminate the sample which was maintained at 25°C. Observations were made at a scattering angle of 99°. Scattering intensity data were processed using the instrumental software to obtain the R_h and size distribution of each sample. All calculations were based on the Stokes-Einstein equation: $R_h = k_BT/6\pi\eta_0D$ where R_h is the hydrodynamic radius, k_B is Boltzmann's constant, T is the absolute temperature, η_0 is the solvent viscosity, and D is the translational diffusion coefficient (*11*). The protein samples were prepared by dissolution of an appropriated amount of freeze-dried powder in saline and filtered through a 0.22 μm filter (Millipore, Billerica, MA, USA).

2.7. *Pharmacokinetic study*

HSA and PEG-HSA were iodinated with $Na^{125}I$ using iodogen (1,3,4,6-tetrachloro-3a,6a-diphenylglycoluri) methods as described previously (*12*). ^{125}I-labeled HSA and PEG-HSA solutions were administered as a single *i.v.* bolus injection in saline *via* the tail vein of Kunming mice. Blood samples (100 μL) were collected at 5, 20, and 45 min and at 1, 4, 8, 12, 24, 36, 48, 60, 72, 84, and 96 h post injection and plasma was harvested by centrifugation. ^{125}I-HSA or ^{125}I-PEG-HSA associated radioactivity in the plasma samples was determined after precipitation with 10% trichloroacetic acid (TCA) (*13*). The resultant TCA precipitates were counted for radioactivity using a Packard Cobra II Auto-Gamma Counter to determine the ^{125}I radioactivity associated with HSA. Pharmacokinetic parameters were evaluated using practical pharmacokinetic program version 97 (supplied by Chinese Pharmacological Society).

2.8. *Pulmonary microvascular permeability in the LPS-induced capillary leak model*

The vascular permeability of HSA and PEG-HSA was evaluated using LPS-induced capillary leak as a model system. Pulmonary capillary leak was induced by intranasal (*i.n.*) administration of 10 μg LPS in 50 μL saline, and 50 μL of saline solution alone was administrated to Kunming mice as a control (*14*). HSA and PEGylated HSA were labeled with fluorescein isothiocyanate (FITC) as described by Monsigny *et al*. (*15*). Mice were randomly allocated to three experimental groups: control group (saline + FITC-HSA), HSA-treated model group (LPS + FITC-HSA), and PEG-HSA-treated model group (LPS + FITC-PEG-HSA). FITC-labeled protein (0.42 mg/kg) were administered intravenously (*i.v.*) *via* a tail vein 20 min after the injection of LPS or saline. At 4 h post LPS administration, mice were anesthetized, and the thorax was opened, left atrium incised, and the lung was perfused *in situ* with isotonic saline *via* the pulmonary artery. Then the flushed pulmonary tissue was removed and fixed in 10% formalin for fluorescence micrograph studies. The fluorescence intensities of mice lung frozen sections were examined with an inverted fluorescence microscope using 40× objectives.

2.9. *Statistical analysis*

All data are expressed as mean ± S.D., except where otherwise noted. The data were statistically analyzed using student's *t*-test. Statistic analysis was performed using *3P97* (Chinese Academy of Sciences Mathematics Research Institute).

3. Results

3.1. *Preparation of 20 kDa mPEG-propionaldehyde-modified HSA*

The PEG-HSA conjugate was prepared by reductive alkylation between propionaldehyde derivatives of a 20 kDa mPEG molecule and the free α-amino group of the N-terminal amino acid residue of HSA. By taking advantage of the differences between the p*Ka* values of the α-amino group of the N-terminal amino acid residue and the ε-amino groups of the Lys residues in the protein backbone (*16*), the mPEG propionaldehyde was expected to be selectively conjugated to the N-terminal α-amino group of HSA and a homogeneous conjugate would be obtained. Figure 1 shows the results of SDS-PAGE analysis and DEAE Sepharose FF column chromatography for the products of the PEGylation reaction. SDS-PAGE analysis of native HSA and conjugation reaction mixture (lanes 2 and 3, respectively, in Figure 1A) showed that, compared with the lane of native HSA (Mw = 66.5 kDa) and the protein molecular

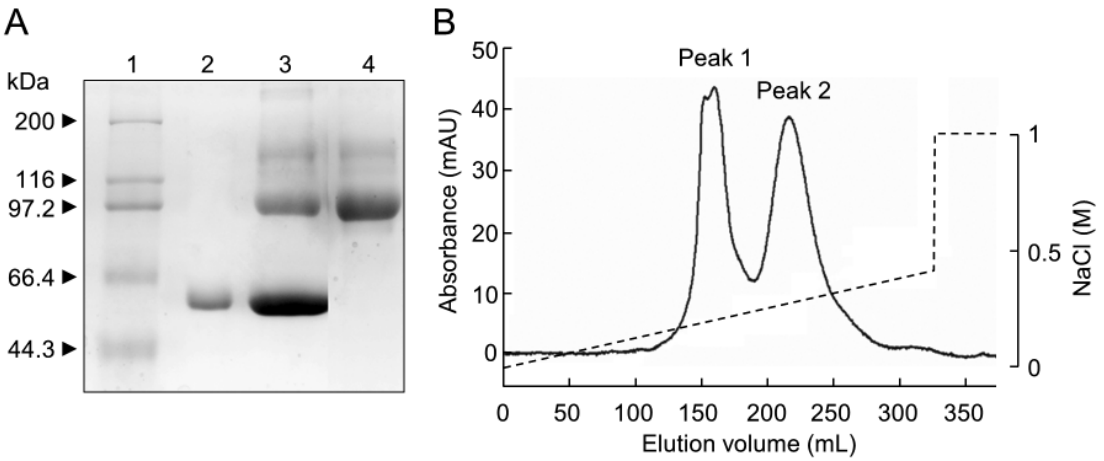

Figure 1. Purification of the PEGylated HSA. (A) SDS-PAGE analysis of column fractions. Gel was stained with Coomassie Brilliant Blue R-250. Lane 1, markers; lane 2, native HSA; lane 3, PEGylation reaction mixture; lane 4, peak 1 eluted from DEAE Sepharose FF column. Five micrograms of protein was applied in each lane. **(B)** Elution profile for DEAE Sepharose FF column chromatography of the HSA PEGylation reaction mixture. Solid line, absorbance at 280 nm; dashed line, NaCl concentration (M).

weight markers, a new protein band with an apparent molecular weight of about 100 kDa was observed in the reaction mixture lane. According to the molecular weight of the new protein, it could be inferred that only one PEG chain was attached onto each HSA molecule, and thus the mono-PEGylated HSA was predominantly produced by using mPEG-propionaldehyde. The modification rate was up to 35% as estimated by optical density scanning of the electrophoretic bands.

The PEGylated HSA was purified from non-PEGylated protein and unreacted PEG by ion exchange chromatography using a DEAE Sepharose FF column. As shown in Figure 1B, two major peaks were obtained with NaCl linear gradient elution. SDS-PAGE of the fractions showed a band with an apparent molecular weight of 90 kDa eluted at 0.18 M NaCl was PEG-HSA (lane 4 in Figure 1A, peak 1 in Figure 1B), whereas the unmodified PEG was eluted at 0.3 M NaCl (peak 2 in Figure 1B). The yield of the purified mono-PEGylated HSA was about 32%.

3.2. *Secondary structure analysis by far-UV CD measurement*

To obtain information of the secondary structure changes of PEG-HSA, CD measurements of HSA and PEG-HSA were performed in the far-UV region (Figure 2). The far-UV CD spectrum of the PEGylated HSA showed the same shape as that of native HSA. The result indicated that the PEG-HSA structure was almost identical to that of native HSA and PEGylation did not cause significant alteration of the secondary structure of HSA.

3.3. *Hydrodynamic radius determination by DLS*

The distribution of the hydrodynamic radius of HSA and PEG-HSA in saline obtained by DLS is shown in Figure 3. The protein concentration determined by BCA assay was 0.01 mg/mL. The hydrodynamic radius (R_h) distribution of PEG-HSA was more heterogeneous than that of native HSA due to polydispersity of the conjugated mPEG molecules. The calculated R_h of PEG-HSA was 50.7 nm, which was increased about 6.5 times as compared to that of the HSA molecule (R_h = 7.8 nm).

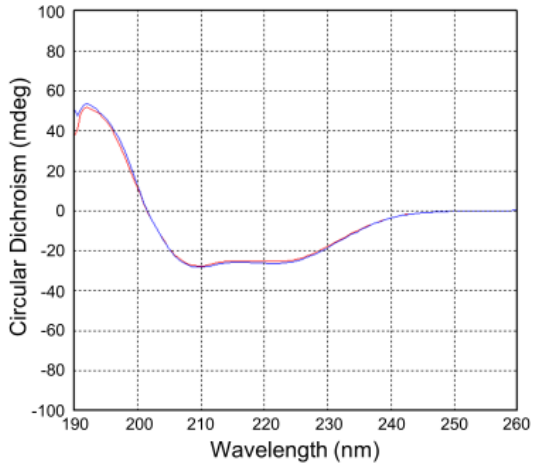

Figure 2. CD profiles of native HSA and PEG-HSA. CD spectra were recorded at room temperature with a 0.1 cm light path cuvette. All samples were dissolved in 50 mM phosphate buffer, pH 7.4. Red line, HSA; blue line, PEG-HSA.

3.4. *Pharmacokinetic study*

PEGylation of therapeutic peptides and proteins is a useful method for prolonging their circulation time in blood (*17*). The pharmacokinetics study of native HSA and PEG-HSA conjugate was conducted by the ^{125}I isotope tracing method. Blood levels of the proteins were measured from 5 min to 96 h post

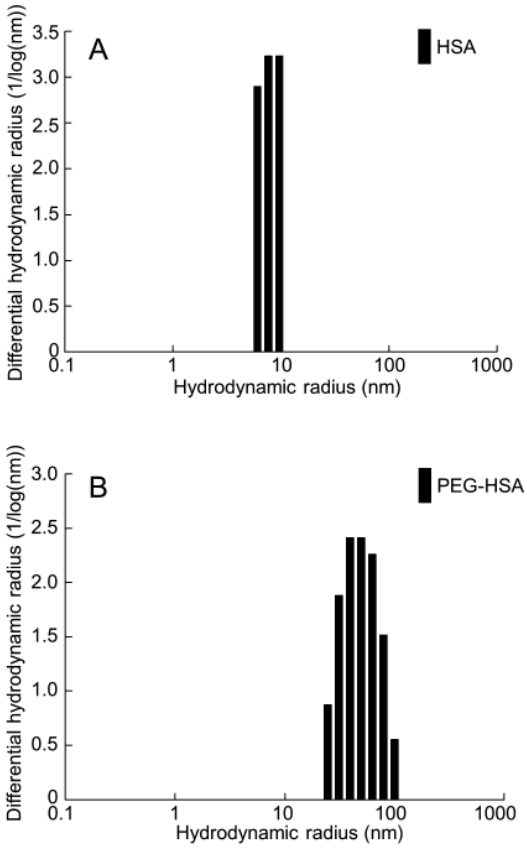

Figure 3. Hydrodynamic radius distribution of HSA and PEG-HSA. Hydrodynamic radius was determined by DLS at a concentration of 0.01 mg/mL of HSA **(A)** or PEG-HSA **(B)** in saline at 25°C.

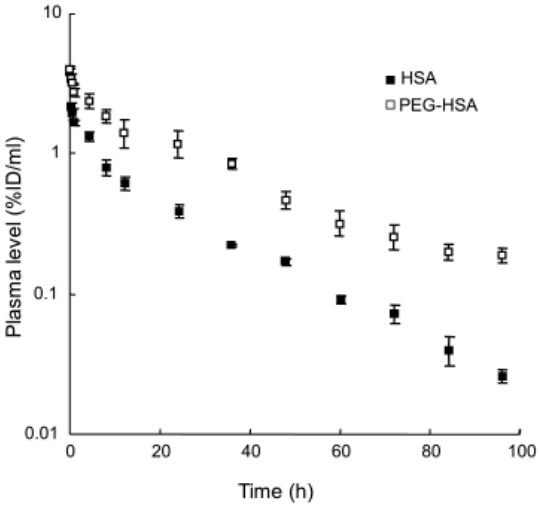

Figure 4. Plasma level of radiolabeled proteins after a single intravenous administration of ^{125}I-HSA or ^{125}I-PEG-HSA to normal mice. Closed symbol, ^{125}I-HSA; open symbol, ^{125}I-PEG-HSA. Data is expressed as a percentage of injected dose per milliliter plasma (%ID/mL) and each point represents the mean ± S.D. (n = 3).

Table 1. Pharmacokinetic parameters estimated by two-compartmental model analysis following a single *i.v.* bolus injection of ^{125}I-HSA or ^{125}I-PEG-HSA to mice.

Paramaters	HSA	PEG-HSA
$AUC_{0-\infty}$ (μg•h/mL)	2.79 ± 0.09	10.95 ± 1.06**
$t_{1/2\alpha}$ (h)	0.17 ± 0.08	0.82 ± 0.65
$t_{1/2\beta}$ (h)	10.3 ± 0.4	22.5 ± 1.7**
CL (mL/h)	0.39 ± 0.03	0.13 ± 0.01**
MRT (h)	22.6 ± 0.8	42.5 ± 3.4*
Vdss (mL)	5.62 ± 0.12	4.08 ± 0.44*

Data are expressed as mean ± S.D. (n = 3).* $p < 0.05$, ** $p < 0.01$, ^{125}I-PEG-HSA *vs.* ^{125}I-HSA.Abbreviations: HSA, human serum albumin; PEG-HSA, PEGylated HSA; AUC, area under the curve; CL, clearance; MRT, mean residence time; Vdss, steady state volume of distribution.

injection. The plasma radiolabeled HSA and PEG-HSA concentration versus time profiles following a single *i.v.* bolus injection in mice is shown in Figure 4, and the pharmacokinetic parameters for these two proteins using a two-compartment model are listed in Table 1. It can be seen in Figure 4, that the plasma concentrations of native HSA and PEG-HSA showed an exponential declining pattern after *i.v.* administration. The elimination of PEG-HSA was slower than that of native HSA. The half-life of the PEG-HSA (22.5 ± 1.7 h) was increased about 2.2 times, as compared to that of native HSA (10.3 ± 0.4 h). On the other hand, the ^{125}I-PEG-HSA showed a two-thirds decrease in clearance (CL), and a marked increase in the area under the plasma concentration-time curve (AUC) was observed. These results suggest that PEG-HSA has longer retention in blood circulation.

3.5. *Pulmonary microvascular permeability in LPS-induced capillary leak model*

Endotoxin, the bacterial LPS released from the bacterial cell wall, is considered to be an important eliciting factor in the development of acute lung injury (*18*). The increment of endothelial permeability is an indicator of lung injury in murine models (*19*). In this study, vascular permeability of native and PEGylated HSA was evaluated using a LPS-induced acute lung injury model. The extravasation of FITC-labeled protein into pulmonary tissue was used as an index of vascular permeability. As shown in Figure 5, under a fluorescent microscope, an increase in fluorescence intensity was observed in the HSA-treated model group compared with the control group, which meant the modeling succeeded. Meanwhile, a lower vascular permeability of FITC-PEG-HSA was observed compared to FITC-HSA. These results suggested that the PEGylation of HSA could reduce extravasation into lung parenchyma.

4. Discussion

HSA has been widely used for the treatment of shocks, burns, trauma, and various critical illnesses that result in albumin loss, but previous studies have produced conflicting results regarding the safety and efficacy of the use of albumin in critical illness with increased capillary permeability (*20,21*). Under such

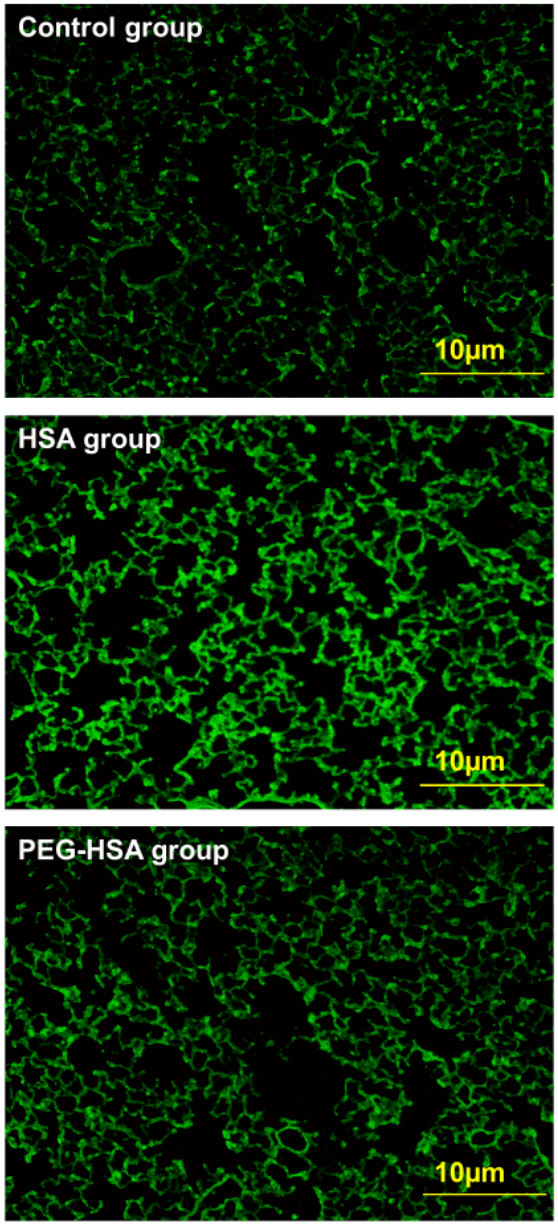

Figure 5. Typical fluorescence micrographs of pulmonary tissues at 4 h after LPS intranasal administration in acute lung injury mice. Vascular permeability of HSA and PEG-HSA was evaluated using a LPS-induced capillary leak model. Top, control group; middle, HSA-treated group; bottom, PEG-HSA-treated group. Bars, 10 μm.

conditions, the HSA infused as a plasma expander may be transported to tissue and bring on further edema. In this study, we modified HSA in a site-specific manner by covalent conjugation of commercial propionaldehyde-derivatized 20 kDa mPEG to the HSA molecule N-terminus. The structurally uniform PEG-HSA was easy to obtain and the preparation method was reproducible. As can be inferred from CD spectra, the structural characteristics of the PEGylated HSA are almost identical to that of native HSA (Figure 2), which indicated that PEGylation did not influence the secondary structure of HSA.

PEG conjugation is regarded as a valuable technique in applied biotechnology that makes protein drugs more water-soluble, non-aggregating, non-immunogenic and more stable to proteolytic digestion (*22*). PEG-propionaldehyde with a large molecular weight of 20 kDa was selected in order to endow the protein with a marked masking effect and a larger hydrodynamic radius. As each ethylene oxide unit of PEG binds 2-3 water molecules by hydrogen bonds, the PEG molecule acts as if it were five to ten times larger than a protein of comparable molecular weight (*23*). In our study, the hydrodynamic radius of PEG-HSA was increased by over 6.5 times, although the molecular weight of PEG-HSA was just 1.3 times that of native HSA (Figure 3, Table 1). The conjugation of HSA with the 20 kDa mPEG endows the HSA molecule with a great hydrated volume.

The pharmacokinetic analysis of PEG-HSA indicated that the PEGylated HSA showed a longer intravascular residence time (Figure 4). It has been reported that the mechanism of HSA breakdown involves endocytotic uptake into vesicles, which could fuse with lysosomes in endothelial cells (*24*). This process involves binding to the scavenger receptors (gp18 and gp30) on the endothelial surface membrane (*25*). Hence, it is likely that the degradation reduction effect of chemical modification of proteins is due to the masking effect of PEG attached to the surface of the HSA molecule, which can prevent recognition of the scavenger receptors, reticuloendothelial system and proteolytic enzymes.

Under normal physiological conditions, the HSA molecule distributes between the intravascular and extravascular compartments. Each day, 120~145 g of HSA is lost into the extravascular space and most of this is recovered back into the circulation by lymphatic drainage (*26*). Critical illness, such as sepsis, shock and major injury, breaks the distribution balance of HSA between the two compartments. The altered distribution is related to an increase in capillary leakage. In this situation, using exogenous albumin to increase the plasma albumin concentration seems beneficial, but it is argued that the infused albumin was inefficient in reducing liquid shift and may contribute to delayed pulmonary edema (*27*). In this study, we expected that increasing the molecular size of albumin by PEG modification could reduce the flow of albumin across capillary membranes under conditions with increased capillary leakage. LPS-induced acute lung injury was used to compare the pulmonary microvascular permeability properties of HSA and PEG-HSA. In this model, inflammatory cascade reactions induce increased microvascular permeability and capillary leakage, especially in pulmonary tissue (*23*). We observed a significant lower vascular permeability of the PEG-HSA at 4 h after injection (Figure 5), which indicated that increasing the molecular size of albumin by PEG modification could reduce transcapillary loss

of albumin molecules. Based on the hydrodynamic radius determination and pulmonary microvascular permeability measurement, it can be inferred that increasing the molecular weight of HSA by PEGylation may contribute to improvement of intravascular retention, and prevent intravascular fluid loss and interstitial liquid accumulation.

The results of the pharmacokinetic study and pulmonary microvascular permeability of N-terminal PEGylated HSA in this study are very similar to those of Cys34-specific PEGylated HSA as we described previously (*29*). The molecular weights of PEG reagents applied to these two conjugations targeting different modification sites were both 20 kDa. Many studies have shown that the *in vivo* behavior and biological properties of drug-PEG conjugates were markedly dependent on the molecular weight of the PEG conjugated (*30,31*). This information provides a reasonable explanation for our results. However, the PEGylation on the two modification sites (N-terminal amino group and sulfydryl group at Cys34) may have different influences on the drug binding functions of HSA, and this work is being carried out in our lab.

In conclusion, the present study offers a simple, reliable method to reduce vascular permeability and improve half-life in circulation of infused HSA, and consequently promotes intravascular retention and decreases administration frequency. Our main task in the future is investigation of pharmacodynamics of PEGylated HSA, optimization of modification strategies and *in vivo* safety evaluation of different modified products.

Acknowledgements

This work was supported by a grant from Department of Science & Technology of Shandong Province (No. 2010GSF10215).

References

1. Mingetti PP, Ruffner DE, Kuang WJ, Dennison OE, Hawkins JW, Beattie WG, Dugaiczyk A. Molecular structure of the human albumin gene is revealed by nucleotide sequence within q11e22 of chromosome 4. J Biol Chem. 1986; 261:6747-6757.
2. Kobayashi K. Summary of recombinant human serum albumin development. Biologicals. 2006; 34:55-59.
3. Groeneveld AB, Teule GJ, Bronsveld W, van den Bos GC, Thijs LG. Increased systemic microvascular albumin flux in septic shock. Intensive Care Med. 1987; 13:140-142.
4. Bradley JA, Cunningham KJ, Jackson VJ, Hamilton DNH, Ledingham IA. Serum protein levels in critically Ill surgical patients. Intensive Care Med. 1981; 7:291-295.
5. Waterhouse C, Fenninger LD, Keutmann EH. Nitrogen exchange and caloric expenditure in patients with malignant neoplasms. Cancer. 1951; 4:500-514.
6. Fleck A, Raines G, Hawker F, Trotter J, Wallace PI, Ledingham IM, Calman KC. Increased vascular permeability: A major cause of hypoalbuminaemia in disease and injury. Lancet. 1985; 1:781-784.
7. Marx G. Fluid therapy in sepsis with capillary leakage. Eur J Anaesthesiol. 2003; 20: 429-442.
8. Matsushita S, Chuang VT, Kanazawa M, Tanase S, Kawai K, Maruyama T, Suenaga A, Otagiri M. Recombinant human serum albumin dimer has high blood circulation activity and low vascular permeability in comparison with native human serum albumin. Pharm Res. 2006; 23:882-891.
9. Doweiko JP, Nompleggi DJ. Role of albumin in human physiology and pathophysiology. JPEN J Parenter Enteral Nutr. 1991; 15:207-211.
10. Laemmli UK. Cleavage of structural proteins during the assembly of the head of bacteriophage T4. Nature. 1970; 227:680-685.
11. Kathmann EEL, Davis DAD, McCormick CL. Synthesis and solution behavior of terpolymers of acrylic acid, acrylamide, and the zwitterionic monomer 3-[(2-acrylamido-2-methylpropyl)dimethylammonio]-1-propanesulfonate. Macromolecules. 1994; 27:3156-3161.
12. Fraker PJ, Speck JC Jr. Protein and cell membrane iodinations with a sparingly soluble chloroamide, 1,3,4,6-tetrachloro-3a,6a-diphrenylglycoluril. Biochem Biophys Res Commun. 1978; 80:849-857.
13. Cho HM, Rosenblatt JD, Kang YS, Iruela-Arispe ML, Morrison SL, Penichet ML, Kwon YG, Kim TW, Webster KA, Nechustan H, Shin SU. Enhanced inhibition of murine tumor and human breast tumor xenografts using targeted delivery of an antibody-endostatin fusion protein. Mol Cancer Ther. 2005; 4:956-967.
14. Szarka RJ, Wang N, Gordon L, Nation PN, Smith RH. A murine model of pulmonary damage induced by lipopolysaccharide *via* intranasal instillation. J Immunol Methods. 1997; 202:49-57.
15. Monsigny M, Roche AC, Midoux P. Uptake of neoglycoproteins *via* membrane lectin(s) of L1210 cells evidenced by quantitative flow cytofluorometry and drug targeting. Biol Cell. 1984; 51:187-196.
16. Kinstler O, Molineux G, Treuheit M, Ladd D, Gegg C. Mono-N-terminal poly(ethylene glycol)-protein conjugates. Adv Drug Deliv Rev. 2002; 54:477-485.
17. Cantin AM, Woods DE, Cloutier D, Dufour EK, Leduc R. Polyethylene glycol conjugation at Cys232 prolongs the half-life of alpha1 proteinase inhibitor. Am J Respir Cell Mol Biol. 2002; 27:659-665.
18. Zhang H, Sun GY. LPS induces permeability injury in lung microvascular endothelium *via* AT(1) receptor. Arch Biochem Biophys. 2005; 441:75-83.
19. Mizgerd JP, Skerrett SJ. Animals models of human pneumonia. AmJ Physiol Lung CellMol Physiol. 2008; 294:387-398.
20. Wilkes MM, Navickis RJ. Patient survival after human albumin administration. A meta-analysis of randomized, controlled trials. Ann Intern Med. 2001; 135:149-164.
21. Cochrane Injuries Group. Human albumin administration in critically ill patients: Systematic review of randomised controlled trials. Cochrane Injuries Group Albumin Reviewers. BMJ. 1998; 317:235-240.
22. Veronese F, Pasut G. PEGylation, successful approach to drug delivery. Drug Discov Today. 2005; 10:1451-1458.
23. Kozlowski A, Harris JM. Improvements in protein PEGylation: Pegylated interferons for treatment of

hepatitis C. J Controlled Release. 2001; 72:217-224.
24. Schnitzer JE, Oh P. Albondin-mediated capillary permeability to albumin. Differential role of receptors in endothelial transcytosis and endocytosis of native and modified albumins. J Biol Chem. 1994; 269:6072-6082.
25. Schnitzer JE, Bravo J. High affinity binding, endocytosis, and degradation of conformationally modified albumins. Potential role of gp30 and gp18 as novel scavenger receptors. J Biol Chem. 1993; 268:7562-7570.
26. Nicholson JP, Wolmarans MR, Park GR. The role of albumin in critical illness. Br J Anaesth. 2000; 85:599-610.
27. Manelli JC. Is albumin administration useful in critical care for burnt patients? Ann Fr Anesth Reanim. 1996; 15:507-513.
28. Groeneveld AB, Bronsveld W, Thijs LG. Hemodynamic determinants of mortality in human septic shock. Surgery. 1986; 99:140-153.
29. Zhao T, Cheng YN, Tan HN, Liu JF, Xu HL, Pang GL, Wang FS. Site-specific chemical modification of human serum albumin with polyethylene glycol prolongs half-life and improves intravascular retention in mice. Biol Pharm Bull. 2012; 35:280-288.
30. Kaminskas LM, Boyd BJ, Karellas P, Krippner GY, Lessene R, Kelly B, Porter CJ. The impact of molecular weight and PEG chain length on the systemic pharmacokinetics of PEGylated poly l-lysine dendrimers. Mol Pharm. 2008; 5:449-463.
31. Yamaoka T, Tabata Y, Ikada Y. Distribution and tissue uptake of poly(ethylene glycol) with different molecular weights after intravenous administration to mice. J Pharm Sci. 1994; 83:601-606.

(*Received March 10, 2012; Revised March 17, 2012; Accepted March 18, 2012*)

Original Article

DOI: 10.5582/bst.2012.v6.2.89

Protective effect of *Lysimachia christinae* against acute alcohol-induced liver injury in mice

Junming Wang[1,*], Yueyue Zhang[1], Yasu Zhang[2], Ying Cui[1], Ju Liu[3], Binfeng Zhang[4]

[1] *School of Pharmacy, Henan University of Traditional Chinese Medicine, Zhengzhou, China;*
[2] *Graduate School of Medicine, The University of Tokyo, Tokyo, Japan;*
[3] *Xinyang Institute of Food and Drug Control, Xinyang, China;*
[4] *Shanghai R&D Centre for Standardization of Chinese Medicines, Shanghai, China.*

Summary ***Lysimachia christinae* Hance (Primulaceae) is a medicinal plant. The present study was undertaken to investigate protection of *L. christinae* against acute alcohol-induced liver injury in mice, the related mechanism of oxidative stress and its hepatoprotective chemical compound for the first time. Mice were orally administered alcohol at 6 g/kg 2 h after a 75% ethanol extract of *L. christinae* (ET) (100, 200, 400 mg/kg), quercetin (2, 4, 8 mg/kg) isolated from *L. christinae*, or bifendate (150 mg/kg) for seven consecutive days by intragastric administration (*i.g.*) except the normal group. Serum and liver tissue samples were collected 6 h after alcohol administration and the amount of quercetin in ET was analyzed by high-performance liquid chromatography (HPLC) with a diode array detector (DAD). The results showed that alcohol-induced elevated serum alanine transferase (ALT) and aspartate transaminase (AST) activities were significantly reduced by ET (200, 400 mg/kg), quercetin (4, 8 mg/kg) and bifendate (150 mg/kg), respectively. Further analysis demonstrated that lipid peroxidation (LPO) levels significantly decreased, while glutathione amounts, glutathione-s transferase (GST), glutathione peroxidase (GPx), superoxide dismutase (SOD) and catalase (CAT) activities all increased in livers of ET-, quercetin-, and bifendate-treated mice. Besides, amount of quercetin in ET was 1.03%. Taken together, our results indicate that *L. christinae* can protect against acute alcohol-induced liver injury in mice, the potential mechanism can be related to inhibiting liver oxidative stress injury, and its main hepatoprotective compound is quercetin, for the first time.**

Keywords: Ethanol extract, quercetin, hepatoprotective compound, oxidative stress

1. Introduction

Alcohol abuse is one of the main causes of liver disease worldwide and has become a social problem (*1*). Due to the increased frequency of drinking, incidence of alcoholic liver disease has increased in China, becoming another important risk factor for morbility and mortality in addition to viral hepatitis (*2*). However, there is no satisfactory therapy for alcoholic liver disease at present except for the combination of abstinence from alcohol and supportive care (*3*).

There is increasing evidence that oxidative stress plays a vital role in pathogenesis of alcoholic liver disease (*4-7*). During alcohol-induced oxidative stress, reactive oxygen species (ROS) are produced and it is extremely reactive. Such ROS may modify and inactivate lipids, proteins, DNA, and RNA, and thus induce cell dysfunction. To inhibit ROS-induced cell injury, the antioxidant system has been generated in the body. The system includes low-molecular-mass antioxidants such as glutathione, alpha-tocopherol, ascorbic acid and the main antioxidant enzymes such

**Address correspondence to:*
Dr. Jun-Ming Wang, School of Pharmacy, Henan University of Traditional Chinese Medicine, No. 1 Jinshui Road, Zhengzhou 450008, China.
E-mail: mjw98_2010@163.com

as, superoxide dismutase (SOD) and catalase (CAT) (*8*). Generally cellular antioxidants maintain a point of balance between oxidants and antioxidants, and thus prevent the organism from injury induced by ROS.

Lysimachia christinae Hance (Primulaceae), commonly known as "Jinqiancao", is distributed worldwide in temperate climates and is widely found in China (*9,10*). It is one of the herbs commonly used in traditional Chinese medicine for treatment of hepatitis virus, cholecystitis and cholagogic efficiency (*11,12*). A recent study has demonstrated that the water extract of *L. christinae* exhibits a marked anticholecystitis and cholagogic activity in animals (*13*). However, as for its hepatoprotective effect, there is no experimental report up until now. Furthermore, whether the potentially protective effect underlying *L. christinae* against alcohol-induced liver injury is related to the liver antioxidant system has not been known.

The present study was designed to observe the protective effect of *L. christinae* against acute alcohol-induced liver injury, the related mechanism on oxidative stress, and further explore its hepatoprotective chemical compound, for the first time.

2. Materials and Methods

2.1. *Animals*

Kunming (KM) male mice (18-22 g) were purchased from the Experimental Animal Center of Hebei Province (Hebei, China). Animals were given rodent laboratory chow and water *ad libitum*, and maintained under controlled conditions with a temperature of 22 ± 1°C, relative humidity 60 ± 10% and a 12/12 h light/dark cycle (lights on at 7 am). All procedures were in strict accordance with china's legislation on using and caring for laboratory animals and with guidelines established by institute for experimental animals of Henan University of Traditional Chinese Medicine and were approved by the university committee for animal experiments.

2.2. *Reagents*

Bifendate (powdered pill suspended in 0.5% CMC-Na) was purchased from Zhejiang Medicine Co., Ltd., Xinchang Pharmaceutical Factory (Xinchang, China). Bradford protein assay kit was purchased from Sangon Biotech Co., Ltd. (Shanghai, China). Reduced glutathione (GSH), oxidized glutathione (GSSG), and NADPH were purchased from Roche Diagnostics GmbH (Mannheim, German).

2.3. *Plant material and preparation of samples*

L. christinae whole herbs were collected in Henan province and authenticated by Dr. Xiaolong Xie (Pharmacognosy Department, Henan University of Traditional Chinese Medicine, Zhengzhou, China). A voucher specimen (JQC110207) was deposited in the herbarium of School of Pharmacy, Henan University of Traditional Chinese Medicine.

The dried herbs were crushed and preparation of the 75% ethanol extract of *L. christinae* (ET) and quercetin are described as follows.

L. christinae powders (about 1 kg) were soaked in 75% ethanol (w/v = 1:10) and incubated at room temperature for 120 min. The mixture was extracted three consecutive times at 85 ± 5°C with a rotary evaporator 180 min at a time. The combined extraction was centrifuged at 800× g for 10 min, and the supernatant was transferred to a glass container by decanting and concentrated under vacuum with a rotary evaporator under reduced pressure at 45 ± 5°C to about 86 g extracts. The yield of ET was 8.6% from *L. christinae* raw medicinal materials.

Quercetin was isolated from *L. christinae* herbs according to previous literature (*14*). After purification using a silica gel column and gel chromatography, the purity of quercetin was more than 98% as determined by high performance liquid chromatography (HPLC) with diode array detector (DAD).

2.4. *Treatment protocol*

Male mice were divided into several groups of 10 mice each. Mice of treated groups were administered orally with 6 g/kg alcohol 2 h after treatment with ET (100, 200, 400 mg/kg), quercetin (2, 4, 8 mg/kg), or the positive drug bifendate (150 mg/kg) everyday for seven consecutive days by intragastric administration (*i.g.*) except mice in the normal (non-alcohol treated) group. Mice in the normal and control (alcohol alone) groups both received daily oral administration (*p.o.*) of 0.5% CMC-Na (0.2 mL/10 g). Peripheral blood samples of groups were collected 6 h after alcohol administration for determination of serum biomarkers for the protective effect against acute alcohol-induced liver injury, and liver tissues for assay mechanism.

2.5. *Assay for detecting serum biomarkers for liver injury*

The blood samples were obtained from mice of all groups (10 mice per group) for the determination of serum biomarkers for liver injury. The serum alanine amino transferase (ALT) and aspartate amino transferase (AST) were assayed according to the reported methods (*15*).

2.6. *Assay for detecting liver lipoid peroxide (LPO) level*

Liver tissues were homogenized in cold phosphoric acid (PBS). LPO was determined by the previous reported

method (*16*). Malondialdehyde (MDA) was formed as an end product of LPO and served as an index of the intensity of LPO. MDA reacts with total bile acids (TBA) to generate a pink colored product, which has an absorbance at 532 nm. The standard curve for MDA was constructed over the concentration range of 0-40 μM. The level of lipid peroxides was expressed as micromoles of MDA per milligram of protein based on tissue protein concentration measured by the Bradford protein assay kit.

2.7. *Assay for detecting liver glutathione amounts*

Glutathione amount was measured immediately as described in the previous study (*17*). The reaction mixture contained samples, 150 μL of a working solution (0.53 U/mL of glutathione reductase, 40.7 μg/mL of DTNB, 1 mM EDTA in 100 mM sodium phosphate buffer, pH 7.0) and 50 μL of 0.16 mg/mL NADPH solution. The change in absorbance was determined at 412 nm against the reagent blank after standing at room temperature for 30 min and glutathione amounts were determined in comparison with a standard curve. The glutathione amounts of mice livers were calculated based on tissue protein concentration measured by the Bradford protein assay kit.

2.8. *Enzymatic assays*

Tissues were homogenized in cold PBS, and centrifuged at 5,000 × g for 5 min and the supernatant was transferred to new tubes for assay. The liver tissue activities of SOD, CAT, GPx, and GST were determined by previous literature method (*18-21*), respectively, and the results were calculated based on tissue protein concentrations measured by the Bradford protein assay kit.

2.9. *Assay for detecting the amount of quercetin in ET*

Amount of quercetin in ET was measured by HPLC-DAD. The chromatography conditions were used as follows.

Analysis was performed on a Prominence HPLC instrument (Angilent 1200 series) equipped with quaternary pump, DAD, on-line degasser, autosampler, and a column heater compartment. The sample was separated on a Welch Materials XDB-C18 column (4.6 × 200 mm, 5 μm). The mobile phase consisted of methanol and water containing 0.4% (v/v) phosphoric acid with isocratic elution (v/v = 52:48). The flow rate was 0.8 mL/min, and column temperature was set at 25°C. The DAD detector was monitored in the range 200-400 nm, and the on-line UV spectra were recorded at 360 nm.

To obtain a calibration curve of quercetin, purified quercetin (6.13 mg, weighed accurately) was dissolved in 80% methanol in a 10 mL low actinic volumetric flask. This solution was diluted with 80% methanol to obtain standard solutions for the calibration curve in a range of 1.838-29.408 μg/mL on the column, and a 10 μL aliquot was injected. ET was dissolved in 80% methanol and an aliquot (10 μL) was injected into the above HPLC-DAD system. The amount of quercetin in ET was calculated using the calibration curve of quercetin.

2.10. *Statistical analysis*

Data is presented as mean ± standard error of mean (S.E.M.). The differences among experimental groups were compared by one-way ANOVA (analysis of variance) followed by Student Newman Keuls (SNK) ($p < 0.05$) using the SPSS (Statistics Package for Social Science) program Version 11.5.

3. Results

3.1. *Effects of ET and quercetin on serum biomarkers for alcohol-induced liver injury*

Serum ALT and AST activities are liver injury biomarkers and their significant elevation often reflects liver injury (*15*). In the present study, ALT and AST were both found to be elevated significantly in mice treated with alcohol alone (Figures 1A and 1B), demonstrating that acute alcohol-induced liver injury was copied successfully in this study. After ig treatment with ET (200, 400 mg/kg), quercetin (4, 8 mg/kg) and bifendate (150 mg/kg), respectively, for seven consecutive days, such an excessive increase was significantly inhibited (Figures 1B and 1C). These results demonstrate that ET, quercetin isolated from *L. christinae* and bifendate all protect against acute alcohol-induced liver injury.

3.2. *Effects of ET and quercetin on liver LPO level*

MDA is one of the main end products of LPO (*16*). As shown in Figure 2A, MDA amounts increased in livers of mice treated with alcohol alone while ET (200, 400 mg/kg), quercetin (4, 8 mg/kg) and bifendate (150 mg/kg) all inhibited such an excessive increase (Figure 2A), which demonstrated that ET, quercetin, and bifendate could protect against alcohol-induced LPO injury in mice.

3.3. *Effects of ET and quercetin on liver glutathione amounts*

Glutathione is an antioxidant which helps protect cells against ROS such as free radicals and peroxides (*17*). Its excessive exhaustion can induce oxidative stress injury. In the present study, glutathione amounts decreased conspicuously ($p < 0.05$) in alcohol-treated

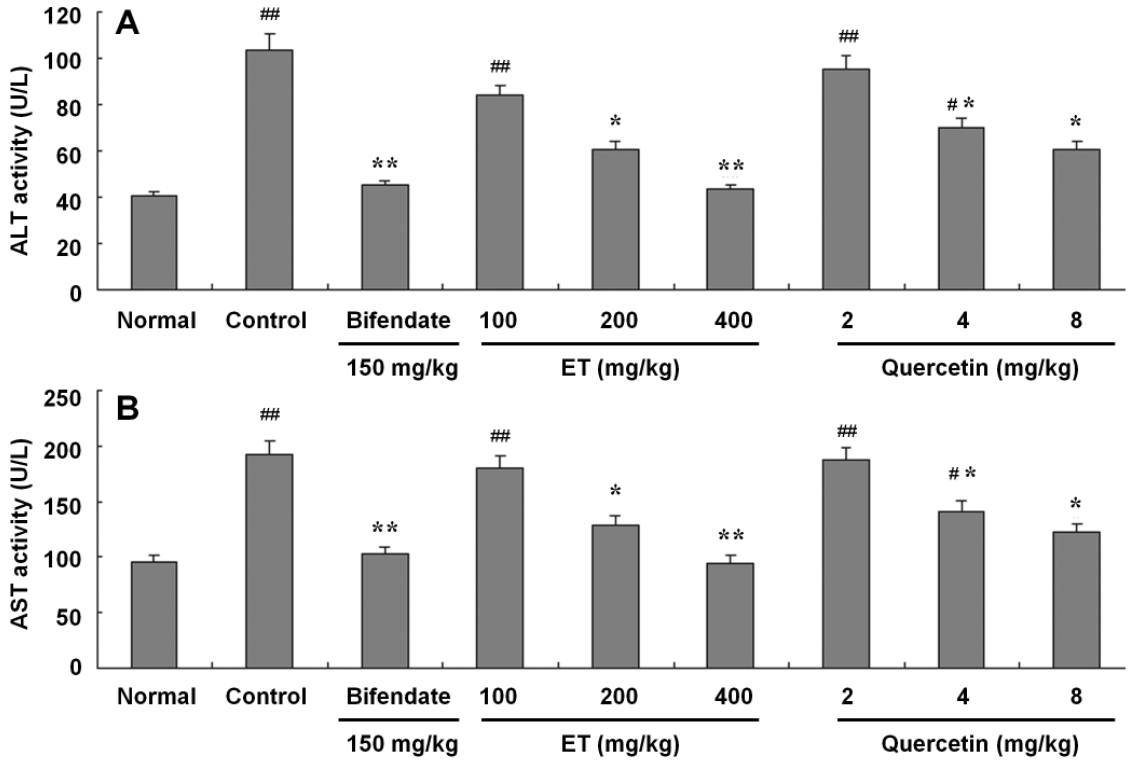

Figure 1. Effects of ET and quercetin isolated from *L. christinae* on the activities of serum ALT and AST in mice. Data are presented as mean ± S.E.M. (n = 10). Significant differences compared with normal (non-alcohol treated) group were designated as $^{\#}p < 0.05$ and $^{\#\#}p < 0.01$ and with control (alcohol alone) as $^{*}p < 0.05$ and $^{**}p < 0.01$.

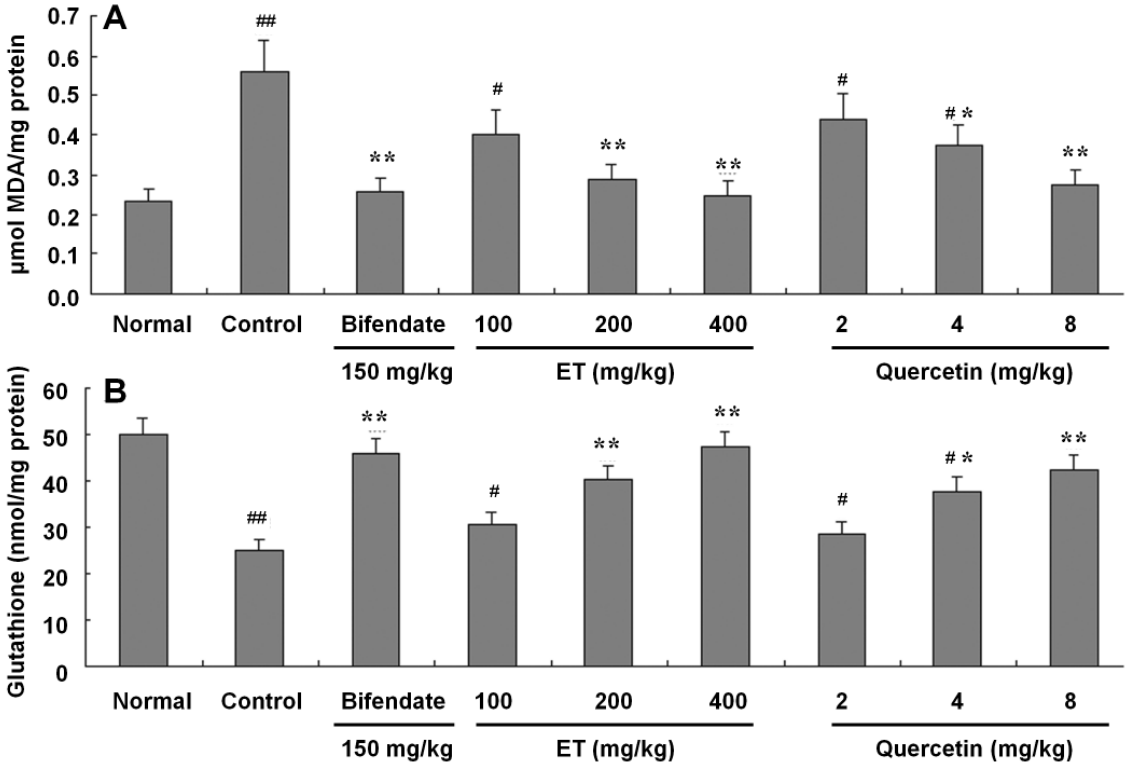

Figure 2. Effects of ET and quercetin isolated from *L. christinae* on the MDA level and glutathione amounts in mice liver tissues. Data are presented as mean ± S.E.M. (n = 10). Significant differences compared with normal (non-alcohol treated) group were designated as $^{\#}p < 0.05$ and $^{\#\#}p < 0.01$ and with control (alcohol alone) as $^{*}p < 0.05$ and $^{**}p < 0.01$.

mice liver, while ET (200, 400 mg/kg), quercetin (4, 8 mg/kg) and bifendate (150 mg/kg) all significantly prevented such a decrease (Figure 2B). The results suggested that ET, quercetin, and bifendate can protect against alcohol destroying the balance between cellular oxidants and antioxidants through inhibiting exhaustion of glutathione amounts and thus can likely protect against liver oxidative stress injury.

3.4. *Effects of ET and quercetin on liver glutathione-related enzymes activities*

GST and GPx are both intracellular glutathione-related enzymes, working with glutathione in participation in the process of oxidative stress injury (*20,21*). Our results showed that alcohol decreased the activities of GST and GPx in mice livers while ET (200, 400 mg/kg), quercetin (8 mg/kg) and bifendate (150 mg/kg) all inhibited such an obvious decease (Figures 3A and 3B), demonstrating that the glutathione-related enzymes could participate in the protection of ET, quercetin, and bifendate against alcohol-induced oxidative stress injury. Our results further confirmed the balance between cellular oxidants and antioxidants was destroyed by alcohol, while ET, quercetin and bifendate could prevent such damage of this balance.

3.5. *Effects of ET and quercetin on liver main antioxidant enzyme activities*

SOD and CAT are both intracellular main antioxidant enzymes, participating in the process of oxidative stress (*18,19*). Our results showed that alcohol decreased the activities of SOD and CAT in livers of mice while ET (200, 400 mg/kg), quercetin (8 mg/kg) and bifendate (150 mg/kg) all inhibited such an obvious decease (Figures 4A and 4B). These results indicate that the main antioxidant enzymes might play a key role in the protection of ET, quercetin, and bifendate against the oxidative stress injury induced by alcohol.

3.6. *Analysis of whether quercetin is the main hepatoprotective compound in ET*

The amount of quercetin in ET was 1.03% as shown by HPLC-DAD analysis. The chemical structure of quercetin is shown in Figure 5A. The standard curve equation of quercetin was $y = 14.634\chi - 0.3958$ (y: Area; χ: concentration of quercetin, μg/mL) and the correlation coefficient was $R^2 = 1$. HPLC chromatograms of quercetin and ET are shown in Figures 5B and 5C, respectively.

Further to confirm that quercetin was the main hepatoprotective compound in ET, we converted the hepatoprotective doses of ET into quercetin, and then compared these converted doses with actual ones of quercetin. According to the above amount of quercetin in ET, the effective doses of ET, 200 and 400 mg/kg, are equivalent to the ones of quercetion, 2.06 and 4.12 mg/kg (4 mg/kg as the actually effective dose of quercetin from this study).

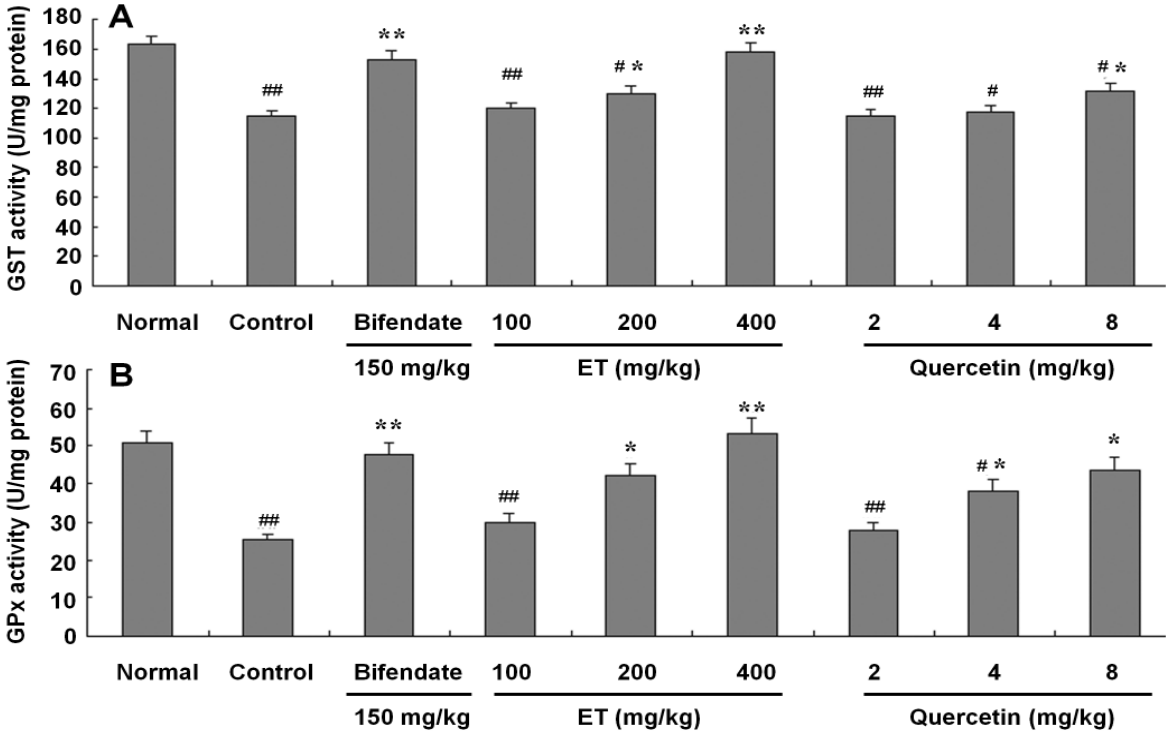

Figure 3. Effects of ET and quercetin isolated from *L. christinae* on liver GST and GPx activities. Data are presented as mean ± S.E.M. ($n = 10$). Significant differences compared with normal (non-alcohol treated) group were designated as $^{\#}p < 0.05$ and $^{\#\#}p < 0.01$ and with control (alcohol alone) as $^{*}p < 0.05$ and $^{**}p < 0.01$.

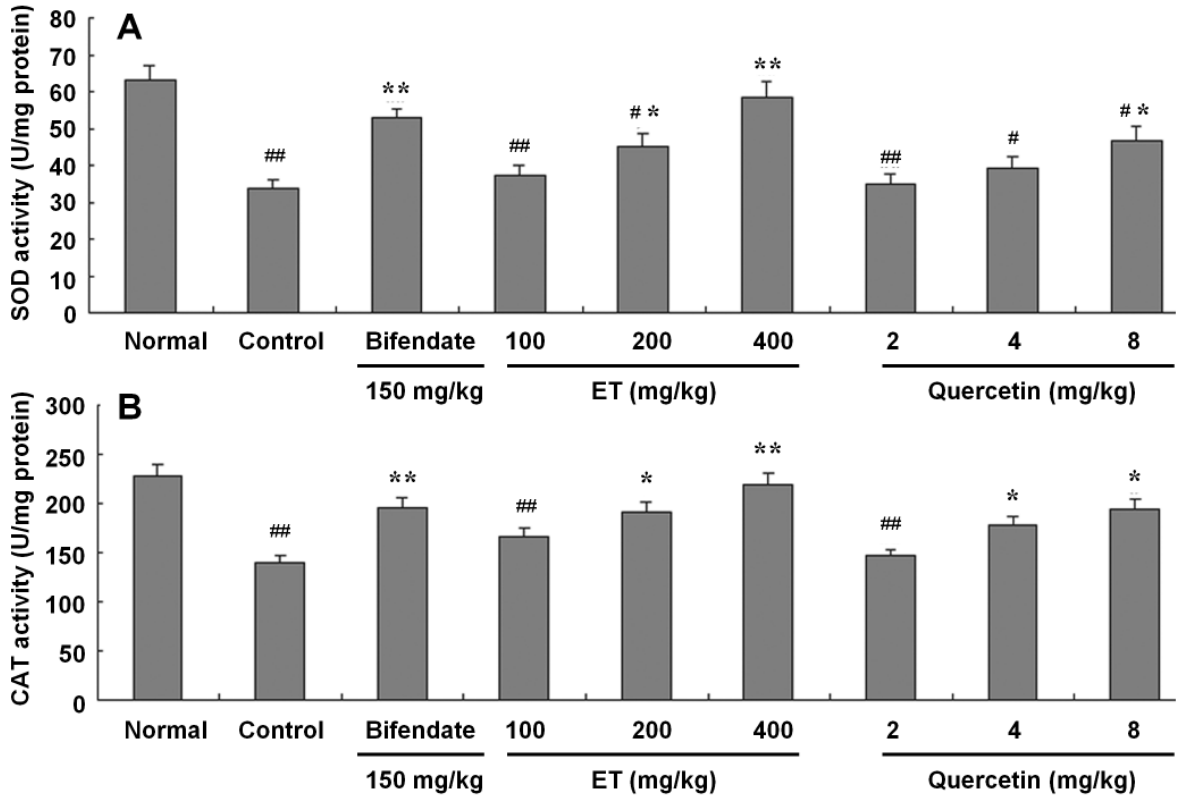

Figure 4. Effects of ET and quercetin isolated from *L. christinae* on liver main antioxidant enzyme activities. Data are presented as mean ± S.E.M. (n = 10). Significant differences compared with normal (non-alcohol treated) group were designated as $^{\#}p < 0.05$ and $^{\#\#}p < 0.01$ and with control (alcohol alone) as $^{*}p < 0.05$ and $^{**}p < 0.01$.

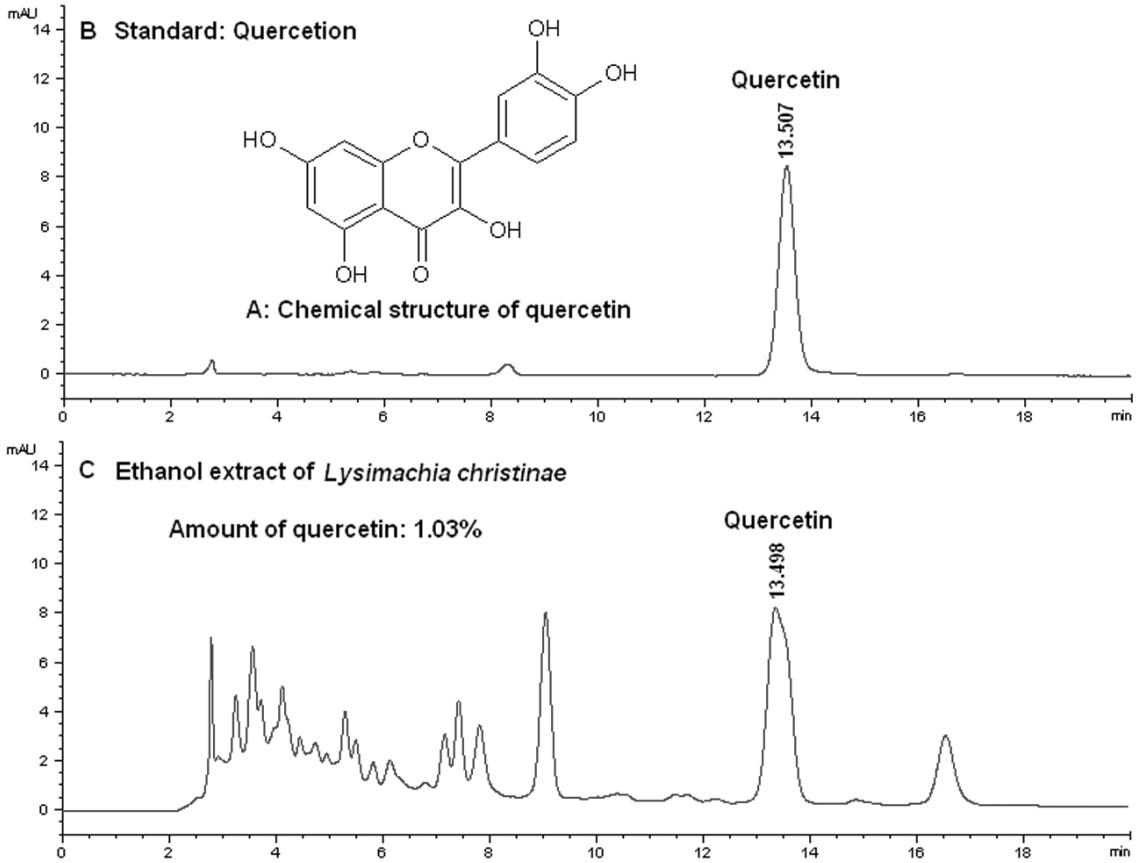

Figure 5. Chemical structure of quercetin, and HPLC chromatograms of ET and quercetin isolated from *L. christinae*. HPLC-DAD procedures are described in "Materials and Methods".

4. Discussion

ALT and AST are reliable biomarkers for liver function (*15*). It has been confirmed that AST can be found in liver, cardiac muscle, skeletal muscle, kidney, brain, pancreas, lung, leukocytes, and erythrocytes, whereas ALT is mainly present in liver (*22*). Significantly elevated levels of serum enzymes such as ALT and AST indicate increased permeability and damage and/or necrosis of hepatocytes (*23*). The results of the present study demonstrate that acute alcohol administration caused liver injury as evidenced by the elevation of serum ALT and AST levels, reflected early biochemical changes in alcoholic liver disease. ET (200, 400 mg/kg), or quercetin (4, 8 mg/kg) pretreatments offered significant protection against acute alcohol-intoxicated mice by attenuating ALT and AST elevation.

The role of oxidative stress in the development of alcoholic liver disease has been investigated since the early 1960s by Diluzio and Hartman (*24,25*), who observed that alcohol administration promoted oxidative breakdown of cell membranes. Studies using the intragastric feeding model have demonstrated that alcohol-induced liver injury was associated with increased LPO, formation of lipid radicals, and decrease of hepatic antioxidant defense, providing the most convincing evidence about the pathogenic role of oxidative stress (*26-29*). Among them, LPO is a free radical-related process (*30*). One of the main end products of LPO is MDA, which is characterized by cross-linking cellular macromolecules such as protein or DNA and induces widespread cellular damage (*31*). The results in Figure 2A showed that ET and quercetin isolated from *L. christinae* significantly inhibited alcohol-induced excessive amounts of MDA, indicating that ET and quercetin can prevent alcohol-induced LPO injury in liver.

SOD and CAT are believed to play key roles in the enzymatic defense of cells against oxidative stress injury. Because peroxisomes have an abundance of proteins, where oxidative stress always happens, CAT is a classical oxidative biomarker. SOD is a metalloenzyme that can convert O_2, produced during oxidative stress, to hydrogen peroxide (*18*). CAT mainly exists in peroxisomes of all aerobic cells and serves to protect the cells against damage from hydrogen peroxide by catalyzing it into molecular oxygen and water without producing toxic free radicals (*19*). Our results showed that ET and quercetin significantly reversed SOD and CAT activities reduced by alcohol, suggesting that they could prevent alcohol-induced oxidative stress injury, while SOD and CAT participated in the protective effect of ET and quercetin against alcohol-induced liver oxidative injury.

Glutathione plays an important role in protecting hepatocytes against exogenous toxins, and there are lots of reports that depletion of cellular glutathione is related to oxidative damage (*32,33*). Our results showed that ET and quercetin isolated from *L. christinae* significantly inhibited the alcohol-induced excessive exhaustion of glutathione amounts, suggesting that glutathione participated in the protective effect of ET and quercetin against alcohol-induced liver oxidative injury.

GST and GPx are both glutathione-related enzymes. Of them, the cytosolic GSTs exist in almost all aerobic species. It can catalyze the conjugation of electrophilic compounds produced during oxidative stress with glutathione (*21*). GPx catalyzes hydrogen peroxide decomposition to the stable form of hydroxides, specifically using reduced glutathione as the electron provider (*20*). In the present study, ET and quercetin significantly elevated the alcohol-induced decrease of GST and GPx activities in livers of mice, which further confirmed that liver glutathione-related enzymes were involved in the protective effects of ET and quercetin isolated from *L. christinae* against alcohol-induced liver oxidative injury.

Flavonoids have been reported to have many bioactivities including antioxidant (*34*), anti-inflammatory (*35*), antitumor (*36*) and so on. The main chemical components in *L. christinae* are flavonoids (*37*). As for the flavonoids in *L. christinae*, quercetin is relatively abundant (*37*) and has been found to have antioxidant activity in the previous study (*38*). However, it was still not clear until now that quercetin is the main hepatoprotective chemical compound of *L. christinae*. In the present study, we found that quercetin could protect against acute alcohol-induced liver injury isolated from *L. christinae* (as was shown in Figure 1B). Further, to determine whether quercetin was the main bioactive ingredient in ET, we converted the hepatoprotective doses of ET into quercetin based on the results of HPLC-DAD analysis. The result indicated that the converted amounts of quercetin were equivalent to the actual ones present in ET, suggesting that quercetin could be the main potential hepatoprotective compound from *L. christinae*.

In conclusion, the present study shows that ET and quercetin isolated from *L. christinae* can protect against alcohol-induced liver injury in mice and the underlying mechanisms may be related to inhibiting liver oxidative stress injury. We have also confirmed that quercetin is the major hepatoprotective component of *L. christinae* for the first time. Further studies are in progress in our laboratory to explore the protection of *L. christinae* against carbon tetrachloride- or drug-induced liver injury.

Acknowledgements

This work was financially supported by Doctoral Research Fund of Henan Chinese Medicine (BSJJ2010-22) and National Natural Science

Foundation of China (30772794).

References

1. Mandayam S, Jamal MM, Morgan TR. Epidemiology of alcoholic liver disease. Semin Liver Dis. 2004; 24:217-232.
2. Li YM. The epidemiology and natural history of alcoholic liver disease. Zhonghua Gan Zang Bing Za Zhi. 2010; 18:171-172. (in Chinese)
3. Frazier TH, Stocker AM, Kershner NA, Marsano LS, McClain CJ. Treatment of alcoholic liver disease. Therap Adv Gastroenterol. 2011; 4:63-81.
4. Adewusi EA, Afolayan AJ. Effect of Pelargonium reniforme roots on alcohol-induced liver damage and oxidative stress. Pharm Biol. 2010; 48:980-987.
5. Faremi TY, Suru SM, Fafunso MA, Obioha UE. Hepatoprotective potentials of Phyllanthusamarus against ethanol-induced oxidative stress in rats. Food Chem Toxicol. 2008; 46:2658-2664.
6. Rukkumani R, Aruna K, Varma PS, Rajasekaran KN, Menon VP. Comparative effects of curcumin and an analog of curcumin on alcohol and PUFA induced oxidative stress. J Pharm Pharm Sci. 2004; 7:274-283.
7. Samuhasaneeto S, Thong-Ngam D, Kulaputana O, Suyasunanont D, Klaikeaw N. Curcumin decreased oxidative stress, inhibited NF-kappa B activation, and improved liver pathology in ethanol-induced liver injury in rats. J Biomed Biotechnol. 2009; 2009:981963.
8. van der Vliet A, O'Neill CA, Cross CE, Koostra JM, Volz WG, Halliwell B, Louie S. Determination of low-molecular-mass antioxidant concentrations in human respiratory tract lining fluids. Am J Physiol. 1999; 276:289-296.
9. Houghton PJ, Hylands PJ, Mensah AY, Hensel A, Deters AM. *In vitro* tests and ethnopharmacological investigations: Wound healing as an example. J Ethnopharmacol. 2005; 100:100-107.
10. Verpoorte R, Choi YH, Kim HK. Ethnopharmacology and systems biology: A perfect holistic match. J Ethnopharmacol. 2005; 100:53-56.
11. Zhou SY, Yao DF, Xu CF, Huang LQ, Zhang SP. Suppressive effect of *Phyllanthus urinaria* L. and *Lysimachia christinae* Hance on hepatitis B surface antigen. Pract J Integr Tradit West Med. 1995; 8:760-761.
12. Yeh TH, Krauland L, Singh V, Zou B, Devaraj P, Stolz DB, Franks J, Monga SP, Sasatomi E, Behari J. Liver-specific β-catenin knockout mice have bile canalicular abnormalities, bile secretory defect, and intrahepatic cholestasis. Hepatology. 2010; 52:1410-1419.
13. Yang X, Wang BC, Zhang X, Liu WQ, Qian JZ, Li W, Deng J, Singh GK, Su H. Evaluation of *Lysimachia christinae* Hance extracts as anticholecystitis and cholagogic agents in animals. J Ethnopharmacol. 2011; 137:57-63.
14. Shen LD, Yao FR. Studies on the chemical constituents of the herb *Lysimachia christinae* Hance. Zhong Yao Tong Bao. 1988; 13:31-34, 63. (in Chinese)
15. Kamei T, Asano K, Nakamura S. Determination of serum glutamate oxaloacetate transaminase and glutamate pyruvate transaminase by using L-glutamate oxidase. Chem Pharm Bull. 1986; 34:409-412.
16. Hogberg J, Larson RE, Kristoferson A, Orrenius S. NADPH-dependent reductase solubilized from microsomes by peroxidation and its activity. Biochem Biophys Res Commun. 1974; 56:836-842.
17. Oh IS, Kim TW, Ahn JH, Keum JW, Choi CY, Kim DM. Use of l-buthionine sulfoximine for the efficient expression of disulfide-containing proteins in cell-free extracts of Escberibia coli. Biotechnol Bioprocess Eng. 2007; 12:574-578.
18. Marklund SL, Marklund G. Involvement of the superoxide anion radical in the autoxidation of pyrogallol and a convenient assay for superoxide dismutase. Eur J Biochem. 1974; 47:469-474.
19. Aebi H. Catalse *in vitro*. Methods enzymol. 1984; 105:121-126.
20. Rotruck JT, Pope AL, Ganther HE, Swanson AB, Hafeman DG, Hoekstra WG. Selenium: Biochemical role as a component of glutathione peroxidase. Science. 1973; 179:588-590.
21. Habig WH, Jakoby WB. Assay for differentiation of glutathione S-transferases. Methods Enzymol. 1981; 77:398-405.
22. Rej R. Aspartate aminotransferase activity and isoenzymes proportions in human liver tissue. Clin Chem. 1978; 24:1971-1979.
23. Goldberg DM, Watts C. Serum enzyme changes as evidence of liver reaction to oral alcohol. Gastroenterology. 1965; 49:256-261.
24. Diluzio NR. Prevention of the acute ethanol-induced fatty liver by the simultaneous administration of antioxidants. Life Sci. 1964; 3:113-118.
25. Diluzio NR, Hartman AD. Role of lipid peroxidation in the pathogenesis of the ethanol-induced fatty liver. Fed Proc. 1967; 26:1436-1442.
26. Rouach H, Fataccioli V, Gentil M, French SW, Morimoto M, Nordmann R. Effect of chronic ethanol feeding on lipid peroxidation and protein oxidation in relation to liver pathology. Hepatology. 1997; 25:351-355.
27. French SW, Wong K, Jui L, Albano E, Hagbjork AL, Ingelman-Sundberg M. Effect of ethanol on cytochrome P450 2E1 (CYP2E1), lipid peroxidation, and serum protein adduct formation in relation to liver pathologypathogenesis. Exp Mol Pathol. 1993; 58:61-75.
28. Polavarapu R, Spitz DR, Sim JE, Follansbee MH, Oberley LW, Rahemtulla A, Nanji AA. Increased lipid peroxidation and impaired antioxidant enzyme function is associated with pathological liver injury in experimental alcoholic liver disease in rats fed diets high in corn oil and fish oil. Hepatology. 1998; 27:1317-1323.
29. Nanji AA, Zhao S, Sadrzadeh SM, Dannenberg AJ, Tahan SR, Waxman DJ. Markedly enhanced cytochrome P450 2E1 induction and lipid peroxidation is associated with severe liver injury in fish oil-ethanol-fed rats. Alcohol Clin Exp Res. 1994; 18:1280-1285.
30. Romero FJ, Bosch-Morell F, Romero MJ, Jareño EJ, Romero B, Marín N, Romá J. Lipid peroxidation products and antioxidants in human disease. Environ Health Perspect. 1998; 106:1229-1234.
31. Hassan L, Bueno P, Ferrón-Celma I, Ramia JM, Garrote D, Muffak K, García-Navarro A, Mansilla A, Villar JM, Ferrón JA. Time course of antioxidant enzyme activities in liver transplant recipients. Transplant Proc. 2005; 37:3932-3935.
32. Carbonell LF, Nadal JA, Llanos MC, Hernández I, Nava E, Díaz J. Depletion of liver glutathione potentiates the oxidative stress and decreases nitric oxide synthesis in a rat endotoxin shock model. Crit Care Med. 2000;

28:2002-2006.
33. Han D, Hanawa N, Saberi B, Kaplowitz N. Mechanisms of liver injury. III. Role of glutathione redox status in liver injury. Am J Physiol Gastrointest Liver Physiol. 2006; 291:G1-G7.
34. Beker BY, Bakır T, Sönmezoğlu I, Imer F, Apak R. Antioxidant protective effect of flavonoids on linoleic acid peroxidation induced by copper(II)/ascorbic acid system. Chem Phys Lipids. 2011; 164:732-739.
35. Funakoshi-Tago M, Nakamura K, Tago K, Mashino T, Kasahara T. Anti-inflammatory activity of structurally related flavonoids, apigenin, luteolin and fisetin. Int Immunopharmacol. 2011; 11:1150-1159.
36. Sun M, Han J, Duan J, Cui Y, Wang T, Zhang W, Liu W, Hong J, Yao M, Xiong S, Yan X. Novel antitumor activities of Kushen flavonoids *in vitro* and *in vivo*. Phytother Res. 2007; 21:269-277.
37. Wang YJ, Sun QS. Chemical constituents of *Lysimachia christinae* Hance. Chinese J Med Chem. 2005; 15:357-359. (in Chinese)
38. Amengual-Cladera E, Nadal-Casellas A, Gómez-Pérez Y, Gomila I, Prieto RM, Proenza AM, Lladó I. Phytotherapy in a rat model of hyperoxaluria: The antioxidant effects of quercetin involve serum paraoxonase 1 activation. Exp Biol Med (Maywood). 2011; 236:1133-1138.

(*Received January 30, 2012; Revised April 8, 2012; Accepted April 12, 2012*)

Case Report

DOI: 10.5582/bst.2012.v6.2.98

Intrahepatic cholangiocarcinoma with intrahepatic biliary lithiasis arising 47 years after the excision of a congenital biliary dilatation: Report of a case

Suguru Yamashita[1], Junichi Arita[1], Takashi Sasaki[2], Junichi Kaneko[1], Taku Aoki[1], Yoshihumi Beck[1], Yasuhiko Sugawara[1], Kiyoshi Hasegawa[1], Norihiro Kokudo[1,*]

[1] *Hepato-Biliary-Pancreatic Surgery Division, Department of Surgery, Graduate School of Medicine, The University of Tokyo, Tokyo, Japan;*
[2] *Department of Gastroenterology, Graduate School of Medicine, The University of Tokyo, Tokyo, Japan.*

Summary **We report a case of intrahepatic cholangiocarcinoma with biliary lithiasis arising 47 years after surgery for a congenital biliary dilatation (CBD). A 62-year-old woman was admitted for the investigation of a liver tumor. She had undergone a choledochoduodenostomy at the age of 15 years for CBD and resection of an extrahepatic bile duct with choledochojejunostomy because of cholangitis at the age of 55 years. An enhanced computed tomography (CT) revealed a liver tumor 50 mm in diameter in the S6 region with surrounding lymph node swelling and intrahepatic metastatic lesions in the S8 region. A drip infusion cholangiographic CT showed biliary lithiases in the left liver. An extended right hepatectomy and lymph node dissection was considered but was abandoned because of suspicions of liver functional insufficiency as a result of biliary lithiasis. She underwent biliary lithotomy through a percutaneous transhepatic cholangioscopy and subsequent systemic chemotherapy.**

Keywords: Intrahepatic cholangiocarcinoma, biliary lithiasis, congenital biliary dilatation

1. Introduction

A significant association between congenital biliary dilatation (CBD) and hepatobiliary malignancies is well known (*1*). According to the literature, 2.5%-28% of CBD cases are associated with malignant biliary tract tumors at the initial presentation (*2*). The cause of this carcinogenesis is presumed to be the reflux of pancreatic juice into the bile duct caused by an anomalous junction of the pancreatobiliary duct. Therefore, for the treatment of CBD, the recommended standard surgical method is the excision of the entire extrahepatic bile duct with a bilioenterostomy to stop the reflux of pancreatic juice, in what is called a "separation-operation". Some patients have been reported to develop intrahepatic cholangiocarcinoma (ICC) at a long interval after treatment as seen in several case reports. Some of these patients have undergone a reoperation to remove the ICC. Ono *et al*. (*3*) investigated the long-term outcomes and late complications after hepaticojejunostomy for a choledochal cyst. In that retrospective study, 56 patients with a choledochal cyst were followed up for more than 10 years after surgery, and two patients (3.6%) and one patient (1.8%) developed ICC and multiple intrahepatic bile duct stones, respectively. However, there have been no reports of ICC with intrahepatic biliary lithiasis in the opposite lobe of the liver arising after the excision of CBD.

2. Case report

A 62-year-old woman was referred to our hospital for the investigation of a large tumor in her liver, detected using computed tomography (CT), after she visited a local hospital complaining of general fatigue, a low-

**Address correspondence to:*
Dr. Norihiro Kokudo, Hepato-Biliary-Pancreatic Surgery Division, Department of Surgery, Graduate School of Medicine, The University of Tokyo, 7-3-1 Hongo, Bunkyo-ku, Tokyo 113-8655, Japan.
E-mail: KOKUDO-2SU@h.u-tokyo.ac.jp

grade fever, and back pain. A physical examination performed upon admission disclosed neither jaundice nor a palpable abdominal tumor. When she was 15 years old, she underwent an anastomosis between a dilated common bile duct and the duodenum for CBD, which was classified as type 1 according to the classification of Todani. However, the patient had continued to suffer from intermittent cholangitis. Although imaging examinations revealed no neoplastic lesions in the biliary tract, her pathologic extrahepatic duct was totally excised using a Roux-en-Y choledojejunostomy and a cholecystectomy when she was 55 years old. The excised gallbladder and extrahepatic bile duct showed evidence of neither carcinoma nor pre-carcinogenic findings. She had been well without any symptoms since her last operation until she felt general fatigue and back pain at the age of 62 years. A laboratory test revealed liver dysfunction, and abdominal ultrasonography and CT scanning showed an ill-defined heterogeneous mass, measuring 50 mm, in the right lateral sector.

The patient's laboratory data upon admission to our hospital showed elevated alkaline phosphatise (1,560 IU/L), gamma glutamyl transpeptidase (303 IU/L), and C-reactive protein (10.65 mg/dL), however, total bilirubin was within the normal range (0.3 mg/dL). Serum albumin was low (2.5 g/dL). As for tumor markers, carcinoembryonic antigen was elevated (46.8 ng/mL) and carbohydrate antigen 19-9 was normal (1 U/mL). The indocyanine green (ICG) retention value at 15 min was 10.1%.

An abdominal enhanced CT examination performed at our hospital revealed an ill-defined tumor, 5 cm in diameter, originating from the right lateral sector of the liver and extending to the porta hepatis (Figure 1). Bile duct dilatation of the right lateral caudate, and left lateral branches was also apparent. Coronal reconstruction of the CT examination data revealed a pancreaticobiliary maljunction and dilatation in the residual intrapancreatic bile duct (Figure 2).

Figure 1. Enhanced abdominal CT showed a dense tumor, 5 cm in diameter, in the right lobe of the liver, extending into the porta hepatis.

Gadoxetic acid disodium-enhanced magnetic resonance imaging (MRI) revealed an intrahepatic metastatic lesion in segment 8 of Couinaud (Figure 3).

Drip infusion cholangiographic (DIC)-CT using meglumine iotroxate revealed diffuse peripheral dilatation of the intrahepatic bile duct in both hemilivers with narrowing proximal portions. In the biliary tracts of the right hepatic lobe, excretion of contrast-enhanced media was not observed. Many intrahepatic biliary stones in segment 2 and 3 were also observed (Figure 4).

The patient was diagnosed as having ICC in the right liver with intrahepatic biliary lithiasis in the left liver arising 47 years after an initial bilioenteric anastomosis for CBD. An extended right hepatectomy with regional lymph node dissection was initially suggested. However, liver volumetry revealed that the future remnant liver corresponded to 40% of the total liver parenchyma, and we suspected that the function of the future remnant left lateral section was insufficient because it was impaired as a result of the numerous intrahepatic biliary stones. Additionally, a hepaticojejunostomy was thought to be inappropriate

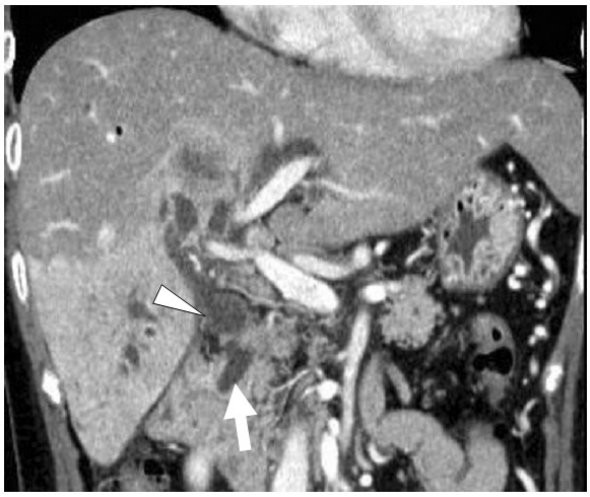

Figure 2. Coronal view CT showed pancreaticobiliary maljunction (white arrow) and dilatation in the residual intrapancreatic bile duct (white arrowhead).

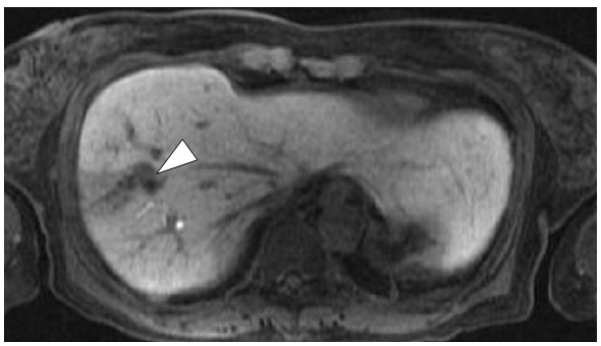

Figure 3. Gadoxetic acid-enhanced MRI showed that there was an intrahepatic metastatic lesion in the right anterior superior segment (white arrowhead).

Figure 4. DIC CT showed that intrahepatic bile ducts in the anterosuperior segment of the right hepatic lobe were dilated (white arrow) and several intrahepatic biliary stones were present in the lateral segment of the left hepatic lobe (white arrowhead).

until all the intrahepatic stones in the future liver remnant, which were thought to be too numerous to remove during surgery, could be removed.

The patient was referred to gastroenterologists to undergo chemotherapy and lithotomy. Following an initial percutaneous transhepatic biliary drainage, the drainage tube was changed several times to a larger-sized one. Then, several lithotomy sessions were performed using a radiological procedure, although several small intrahepatic stones persisted. In parallel with the lithotomy procedures, systemic chemotherapy was planned. The scheduled protocol was as follows: therapy drip infusion of gemcitabine at a dose of 1,400 mg bi-weekly and oral intake of S-1 at a dose of 100 mg/day for 14 days followed by a 14-day rest interval. The systemic chemotherapy was started 12 days after the initial biliary drainage; however, the scheduled therapy was frequently discontinued because of episodes of acute cholangitis or tube dislocation, and gemcitabine was only administered 4 times during 4 months after the initial biliary drainage. A CT scan performed at 5 months after the initial biliary drainage revealed tumor progression in terms of number and size as well as multiple hepatic abscess foci. Although antibiotics were administered, the inflammation did not improve and the patient further developed pulmonary embolization. She died 5 and a half months after the initial biliary drainage, *i.e.*, 7 months after the diagnosis of the intrahepatic cholangiocarcinoma. An autopsy was not performed because of the family's wishes.

3. Discussion

Irwin and Morison described the first reported malignancy associated with CBD in 1944 (*4*). To date, lengthy and repeated reflux episodes of pancreatic juice into the bile duct *via* pancreaticobiliary maljunction have been considered to play an important role in the development of malignant transformations (*5*). Mutations of K-ras and other genes have been implicated, as well as the reflux of pancreatic juice associated with pancreaticobiliary maljunction (*6*). Therefore, once a diagnosis of CBD has been made, early radical surgery is recommended. However, a tendency toward carcinoma development or a precancerous condition in the biliary tree induced by exposure to carcinogens, such as reflux of small intestinal juice, appears to remain after surgery, especially when a pathologic duct is left untouched. Indeed, Kobayashi *et al.* analyzed the relative risks of biliary tract cancer before and after the excision of a congenital choledochal cyst and concluded that the relative risk in patients who underwent this operation was still higher than that of the general population, although it decreased by approximately 50% after surgery (*7*). This result suggested that the epithelium of the residual bile duct wall may have already progressed to a precancerous stage at the time of surgery and that genetic changes may have taken place or continued during the postoperative period. Additionally, biliary-enteric anastomosis is thought to be a possible risk factor for the development of ICC after surgery for benign diseases (*8*). Tocci *et al.* reported that the incidence of ICC after hepaticojejunostomy was 1.9%, with an interval of 11-18 years (*9*). Eleftheliadis *et al.* examined the histological findings of bile duct epithelium obtained by choledochoscopic biopsy from 9 patients at 1-12 years after a choledochoduodenostomy; they detected hyperplasia, pseudopyloric gland metaplasia, and intestinal metaplasia, features that are frequently found in the epithelium adjacent to gallbladder cancer and are regarded as the basis of carcinogenesis (*10*).

Uno *et al.* reported several patients with intrahepatic cholelithiasis developing long after the primary excision of the choledochal cysts (*11*). Some authors have reported a high mutagenic activity of stones from patients with cystic conditions of the biliary tract, a phenomenon that has not been observed in the gallstones of patients without cystic biliary disease (*12*). Postoperative stenosis at the site of a hepaticojejunostomy, congenital remnant stenosis, and repeated cholangitis of the intrahepatic bile duct seem to lead to bile stasis and intrahepatic lithiasis and may be a high-risk factor for carcinogenesis. In the present case, when the patient was diagnosed as having ICC in the right lobe of the liver, multiple intrahepatic bile stones were noted in the opposite lobe of the liver. Thereafter, the patient was thought to be a poor candidate for a radical hepatectomy because the remnant liver volume would be too small, considering the possible insufficient functional reserve of the future liver remnant.

Our search of English and Japanese language

Table 1. Reports of intrahepatic cholangiocarcinoma developing after surgery for congenital biliary dilatation

No.	Age	Gender	Year after resection	Site of cancer development	Treatment	Year	*Ref.*
1	58	F	7	Left lobe	Death before surgery	1972	(*13*)
2	38	F	17	?	Death before surgery	1982	(*14*)
3	33	M	20	Right lobe	Unresected	1992	(*15*)
4	?	?	2	Right lobe	Resected	1994	(*16*)
5	29	M	3	Bilateral lobe	Unresected	1996	(*17*)
6	18	F	2.4	Left lobe	Death before surgery	1999	(*7*)
7	52	F	10	Right lobe	Resected	2000	(*18*)
8	46	M	26	Left lobe	Unresected	2004	(*19*)
9	44	M	34	Left lobe	Resected	2007	(*2*)
10	26	M	26	Left lobe	Resected	2008	(*20*)
11	62	F	47	Right lobe	Unresected	2010	Present case

literature found ten case reports describing ICC after surgery for a congenital choledochal cyst (Table 1). The 11 patients, including our own, consisted of 5 men, 5 women, and 1 unknown patient ranging in age from 18 to 62 years. The present case was the oldest of the reported patients with ICC after the excision of CBD. The median period between the primary operation and the development of ICC was 14.0 years, ranging from 2 to 47 years. The lesions were located in the left hemiliver in 5 patients, the right hemiliver in 4 patients, bilateral hemilivers in 1 patient, and 1 unknown. ICC was resected successfully in only 4 of these patients. Three died of the disease before hepatectomy. Although Ono *et al*. previously reported one case of multiple peripheral lithiases secondary to generation of ICC (*20*), the current report is the first case of ICC with intrahepatic biliary lithiasis in the opposite lobe arising after the excision of CBD to our knowledge. In the former case hemihepatectomy with re-reconstruction by hepaticojejunostomy was successfully performed, while in the present patient, the ICC was not resected because of the appearance of hepatic insufficiency in the future remnant liver volume and biliary lithiasis. As for the difference of the carcinogenic mechanism between this case and past-reported cases, high mutagenic activity of stones could have been associated with the occurrence of the ICC. The postoperative periodic enhanced CT at her local hospital could never detect the intrahepatic biliary lithiasis. Firstly the magnetic resonance cholangiography (MRCP) and DIC CT at our institution revealed numerous biliary lithiasis in the left liver. So it can be said that we should take extra care not to narrow the biliary-enteric anastmosis at the time of the excision of CBD. In addition to the enhanced CT, we may have to sometimes use MRCP or DIC CT to check for the formation of biliary lithiasis.

There is no established effective chemotherapeutic regimen for locally advanced ICC, and we believe that aggressive surgical resection is essential for improving the long-term survival in patients with ICC. In conclusion, careful long-term periodic check-ups should be encouraged for patients with CBD to ensure the early detection of new lesions including malignancy and lithiasis even after definitive surgery, since ICC is characterized by few distinct clinical symptoms until the disease has become severely advanced.

References

1. Todani T, Watanabe Y, Urushihara N, Morotomi Y, Maeba T. Choledochal cyst, pancreatobiliary malunion, and cancer. J Hepatobiliary Panreat Surg. 1994; 1:247-251.
2. Shimamura K, Kurosaki I, Sato D, Takano K, Yokoyama N, Sato Y, Hatakeyama K, Nakadaira K, Yagi M. Intrahepatic cholangiocarcinoma arising 34 years after excision of a type IV-A congenital choledochal cyst: Report of a case. Surg Today. 2009; 39:247-251.
3. Ono S, Fumino S, Shimadera S, Iwai N. Long-term outcomes after hepaticojejunostomy for choledochal cyst: A 10- to 27-year follow-up. J Pediatr Surg. 2010; 45:376-378.
4. Irwin ST, Morison JE. Congenital cyst of common bile-duct containing stones and undergoing cancerous change. Br J Surg. 1944; 32:319-321.
5. Masuhara S, Kasuya K, Aoki T, Yoshimatsu A, Tsuchida A, Koyanagi Y. Relation between K-ras codon 12 mutation and p53 protein overexpression in gallbladder cancer and biliary ductal epithelia in patients with pancreaticobiliary maljunction. J Hepatobiliary Pancreat Surg. 2000; 7:198-205.
6. Matsumoto Y, Fujii H, Itakura J, Matsuda M, Nobukawa B, Suda K. Recent advances in pancreaticobiliary maljunction. J Hepatobiliary Pancreat Surg. 2002; 9:45-54.
7. Kobayashi S, Asano T, Yamasaki M, Kenmochi T, Nakagohri T, Ochiai T. Risk of bile duct carcinogenesis after excision of extrahepatic bile ducts in pancreaticobiliary maljunction. Surgery. 1999; 126:939-944.
8. Strong RW. Late bile duct cancer complicating biliary-enteric anastomosis for benign disease. Am J Surg. 1999; 177:472-474.
9. Tocci A, Mazzoni G, Liotta G, Lepre L, Cassini D, Miccini M. Late development of bile duct cancer in patients who had biliary-enteric drainage for benign disease: A follow-up study of more than 1,000 patients. Ann Surg. 2001; 234:210-214.
10. Eleftheliadis E, Tzioufa V, Kotzampassi K, Aletras H. Common bile duct mucosa in choledochoduodenostomy patients-histological and histochemical study. J

Hepatobiliary Pancreat Surg. 1988; 1:15-20.
11. Uno K, Tsuchida Y, Kawarasaki H, Ohmiya H, Honna T. Development of intrahepatic cholelithiasis long after primary excision of choledochal cysts. J Am Coll Surg. 1996; 183:583-588.
12. Bull P, Guzman S, Nervi F. Mutagenic activity in stones from a patient with a congenital choledochal cyst. J Cancer Res Clin Oncol. 1984; 107:61-63.
13. Gallagher PJ, Millis RR, Mitchinson MJ. Congenital dilatation of the intrahepatic bile ducts with cholangiocarcinoma. J Clin Pathol. 1972; 25:804-808.
14. Chaudhuri PK, Chaudhuri B, Schuler JJ, Nyhus LM. Carcinoma associated with congenital cystic dilation of bile duct. Arch Surg. 1982; 117:1349-1351.
15. Cohen GP, O'Donnell C. Malignant change within surgically drained choledochal cysts. Australas Radiol. 1992; 36:219-221.
16. Scudamore CH, Hemming AW, Teare JP, Fache JS, Erb SR, Watkinson AF. Surgical management of choledochal cysts. Am J Surg. 1994; 167:497-500.
17. Joseph VT. Surgical techniques and long-term results in the treatment of choledochal cyst. J Pediatr Surg. 1990; 25:782-787.
18. Goto N, Yasuda I, Uematsu T, Kanemura N, Takao S, Ando K, Kato T, Osada S, Takao H, Saji S, Shimokawa K, Moriwaki H. Intrahepatic cholangiocarcinoma arising 10 years after the excision of congenital extrahepatic biliary dilation. J Gastroenterol. 2001; 36:856-862.
19. Suzuki S, Amano K, Harada N, Tanaka S, Hayashi T, Suzuki M, Hanyu F, Hirano H. A case of intrahepatic cholangiocarcinoma arising 26 years after excision of congenital biliary dilatation. Jpn J Gastroenterol Surg. 2004; 37:416-421. (in Japanese)
20. Ono S, Sakai K, Kimura O, Iwai N. Development of bile duct cancer in a 26-year-old man after resection of infantile choledochal cyst. J Pediatr Surg. 2008; 43: E17-E19.

(*Received February 15, 2012; Revised March 23, 2012; Accepted April 4, 2012*)

BST
BioScience Trends

Guide for Authors

1. Scope of Articles

BioScience Trends is an international peer-reviewed journal. BioScience Trends devotes to publishing the latest and most exciting advances in scientific research. Articles cover fields of life science such as biochemistry, molecular biology, clinical research, public health, medical care system, and social science in order to encourage cooperation and exchange among scientists and clinical researchers.

2. Submission Types

Original Articles should be well-documented, novel, and significant to the field as a whole. An Original Article should be arranged into the following sections: Title page, Abstract, Introduction, Materials and Methods, Results, Discussion, Acknowledgments, and References. Original articles should not exceed 5,000 words in length (excluding references) and should be limited to a maximum of 50 references. Articles may contain a maximum of 10 figures and/or tables.

Brief Reports definitively documenting either experimental results or informative clinical observations will be considered for publication in this category. Brief Reports are not intended for publication of incomplete or preliminary findings. Brief Reports should not exceed 3,000 words in length (excluding references) and should be limited to a maximum of 4 figures and/or tables and 30 references. A Brief Report contains the same sections as an Original Article, but the Results and Discussion sections should be combined.

Reviews should present a full and up-to-date account of recent developments within an area of research. Normally, reviews should not exceed 8,000 words in length (excluding references) and should be limited to a maximum of 100 references. Mini reviews are also accepted.

Policy Forum articles discuss research and policy issues in areas related to life science such as public health, the medical care system, and social science and may address governmental issues at district, national, and international levels of discourse. Policy Forum articles should not exceed 2,000 words in length (excluding references).

Case Reports should be detailed reports of the symptoms, signs, diagnosis, treatment, and follow-up of an individual patient. Case reports may contain a demographic profile of the patient but usually describe an unusual or novel occurrence. Unreported or unusual side effects or adverse interactions involving medications will also be considered. Case Reports should not exceed 3,000 words in length (excluding references).

News articles should report the latest events in health sciences and medical research from around the world. News should not exceed 500 words in length.

Letters should present considered opinions in response to articles published in BioScience Trends in the last 6 months or issues of general interest. Letters should not exceed 800 words in length and may contain a maximum of 10 references.

3. Editorial Policies

Ethics: BioScience Trends requires that authors of reports of investigations in humans or animals indicate that those studies were formally approved by a relevant ethics committee or review board.

Conflict of Interest: All authors are required to disclose any actual or potential conflict of interest including financial interests or relationships with other people or organizations that might raise questions of bias in the work reported. If no conflict of interest exists for each author, please state "There is no conflict of interest to disclose".

Submission Declaration: When a manuscript is considered for submission to BioScience Trends, the authors should confirm that 1) no part of this manuscript is currently under consideration for publication elsewhere; 2) this manuscript does not contain the same information in whole or in part as manuscripts that have been published, accepted, or are under review elsewhere, except in the form of an abstract, a letter to the editor, or part of a published lecture or academic thesis; 3) authorization for publication has been obtained from the authors' employer or institution; and 4) all contributing authors have agreed to submit this manuscript.

Cover Letter: The manuscript must be accompanied by a cover letter signed by the corresponding author on behalf of all authors. The letter should indicate the basic findings of the work and their significance. The letter should also include a statement affirming that all authors concur with the submission and that the material submitted for publication has not been published previously or is not under consideration for publication elsewhere. The cover letter should be submitted in PDF format. For example of Cover Letter, please visit http://www.biosciencetrends.com/downcentre.php (Download Centre).

Copyright: A signed JOURNAL PUBLISHING AGREEMENT (JPA) form must be provided by post, fax, or as a scanned file before acceptance of the article. Only forms with a hand-written signature are accepted. This copyright will ensure the widest possible dissemination of information. A form facilitating transfer of copyright can be downloaded by clicking the appropriate link and can be returned to the e-mail address or fax number noted on the form (Please visit Download Centre). Please note that your manuscript will not proceed to the next step in publication until the JPA Form is received. In addition, if excerpts from other copyrighted works are included, the author(s) must obtain written permission from the copyright owners and credit the source(s) in the article.

Suggested Reviewers: A list of up to 3 reviewers who are qualified to assess the scientific merit of the study is welcomed. Reviewer information including names, affiliations, addresses, and e-mail should be provided at the same time the manuscript is submitted online. Please do not suggest reviewers with known conflicts of interest, including participants or anyone with a stake in the proposed research; anyone from the same institution; former students, advisors, or research collaborators (within the last three years); or close personal contacts. Please note that the Editor-in-Chief may accept one or more of the proposed reviewers or may request a review by other qualified persons.

Language Editing: Manuscripts prepared by authors whose native language is not English should have their work proofread by a native English speaker before submission. If not, this might delay the publication of your manuscript in BioScience Trends.

The Editing Support Organization can provide English proofreading, Japanese-English translation, and Chinese-English translation services to authors who want to publish in BioScience Trends and need assistance before submitting a manuscript. Authors can visit this organization directly at http://www.iacmhr.com/iac-eso/support.php?lang=en. IAC-ESO was established to facilitate manuscript preparation by researchers whose native language is not English and to help edit works intended for international academic journals.

4. Manuscript Preparation

Manuscripts should be written in clear, grammatically correct English and submitted as a Microsoft Word file in a single-column format. Manuscripts must be paginated and typed in 12-point Times New Roman font with 24-point line spacing. Please do not embed figures in the text. Abbreviations should be used as little as possible and should be explained at first mention unless the term is a well-known abbreviation (*e.g.* DNA). Single words should not be abbreviated.

Title Page: The title page must include 1) the title of the paper (Please note the title should be short, informative, and contain the major key words); 2) full name(s) and affiliation(s) of the author(s), 3) abbreviated names of the author(s), 4) full name, mailing address, telephone/fax numbers, and e-mail address of the corresponding author; and 5) conflicts of interest (if you have an actual or potential conflict of interest to disclose, it must be included as a footnote on the title page of the manuscript; if no conflict of

interest exists for each author, please state "There is no conflict of interest to disclose"). Please visit Download Centre and refer to the title page of the manuscript sample.

Abstract: A one-paragraph abstract consisting of no more than 250 words must be included. The abstract should briefly state the purpose of the study, methods, main findings, and conclusions. Abbreviations must be kept to a minimum and non-standard abbreviations explained in brackets at first mention. References should be avoided in the abstract. Key words or phrases that do not occur in the title should be included in the Abstract page.

Introduction: The introduction should be a concise statement of the basis for the study and its scientific context.

Materials and Methods: The description should be brief but with sufficient detail to enable others to reproduce the experiments. Procedures that have been published previously should not be described in detail but appropriate references should simply be cited. Only new and significant modifications of previously published procedures require complete description. Names of products and manufacturers with their locations (city and state/country) should be given and sources of animals and cell lines should always be indicated. All clinical investigations must have been conducted in accordance with Declaration of Helsinki principles. All human and animal studies must have been approved by the appropriate institutional review board(s) and a specific declaration of approval must be made within this section.

Results: The description of the experimental results should be succinct but in sufficient detail to allow the experiments to be analyzed and interpreted by an independent reader. If necessary, subheadings may be used for an orderly presentation. All figures and tables must be referred to in the text.

Discussion: The data should be interpreted concisely without repeating material already presented in the Results section. Speculation is permissible, but it must be well-founded, and discussion of the wider implications of the findings is encouraged. Conclusions derived from the study should be included in this section.

Acknowledgments: All funding sources should be credited in the Acknowledgments section. In addition, people who contributed to the work but who do not meet the criteria for authors should be listed along with their contributions.

References: References should be numbered in the order in which they appear in the text. Citing of unpublished results, personal communications, conference abstracts, and theses in the reference list is not recommended but these sources may be mentioned in the text. In the reference list, cite the names of all authors when there are fifteen or fewer authors; if there are sixteen or more authors, list the first three followed by *et al.* Names of journals should be abbreviated in the style used in PubMed. Authors are responsible for the accuracy of the references. Examples are given below:

Example 1 (Sample journal reference):
Inagaki Y, Tang W, Zhang L, Du GH, Xu WF, Kokudo N. Novel aminopeptidase N (APN/CD13) inhibitor 24F can suppress invasion of hepatocellular carcinoma cells as well as angiogenesis. Biosci Trends. 2010; 4:56-60.

Example 2 (Sample journal reference with more than 15 authors):
Darby S, Hill D, Auvinen A, *et al.* Radon in homes and risk of lung cancer: Collaborative analysis of individual data from 13 European case-control studies. BMJ. 2005; 330:223.

Example 3 (Sample book reference):
Shalev AY. Post-traumatic stress disorder: diagnosis, history and life course. In: Post-traumatic Stress Disorder, Diagnosis, Management and Treatment (Nutt DJ, Davidson JR, Zohar J, eds.). Martin Dunitz, London, UK, 2000; pp. 1-15.

Example 4 (Sample web page reference):
Ministry of Health, Labour and Welfare of Japan. Dietary reference intakes for Japanese. *http://www.mhlw.go.jp/houdou/2004/11/h1122-2a.html* (accessed June 14, 2010).

Tables: All tables should be prepared in Microsoft Word or Excel and should be arranged at the end of the manuscript after the References section. Please note that tables should not in image format. All tables should have a concise title and should be numbered consecutively with Arabic numerals. If necessary, additional information should be given below the table.

Figure Legend: The figure legend should be typed on a separate page of the main manuscript and should include a short title and explanation. The legend should be concise but comprehensive and should be understood without referring to the text. Symbols used in figures must be explained.

Figure Preparation: All figures should be clear and cited in numerical order in the text. Figures must fit a one- or two-column format on the journal page: 8.3 cm (3.3 in.) wide for a single column, 17.3 cm (6.8 in.) wide for a double column; maximum height: 24.0 cm (9.5 in.). Please make sure that the symbols and numbers appeared in the figures should be clear. Please make sure that artwork files are in an acceptable format (TIFF or JPEG) at minimum resolution (600 dpi for illustrations, graphs, and annotated artwork, and 300 dpi for micrographs and photographs). Please provide all figures as separate files. Please note that low-resolution images are one of the leading causes of article resubmission and schedule delays. All color figures will be reproduced in full color in the online edition of the journal at no cost to authors.

Units and Symbols: Units and symbols conforming to the International System of Units (SI) should be used for physicochemical quantities. Solidus notation (*e.g.* mg/kg, mg/mL, mol/mm^2/min) should be used. Please refer to the SI Guide www.bipm.org/en/si/ for standard units.

Supplemental data: Supplemental data might be useful for supporting and enhancing your scientific research and BioScience Trends accepts the submission of these materials which will be only published online alongside the electronic version of your article. Supplemental files (figures, tables, and other text materials) should be prepared according to the above guidelines, numbered in Arabic numerals (*e.g.*, Figure S1, Figure S2, and Table S1, Table S2) and referred to in the text. All figures and tables should have titles and legends. All figure legends, tables and supplemental text materials should be placed at the end of the paper. Please note all of these supplemental data should be provided at the time of initial submission and note that the editors reserve the right to limit the size and length of Supplemental Data.

5. Submission Checklist

The Submission Checklist will be useful during the final checking of a manuscript prior to sending it to BioScience Trends for review. Please visit Download Centre and download the Submission Checklist file.

6. Online Submission

Manuscripts should be submitted to BioScience Trends online at http://www.biosciencetrends.com. The manuscript file should be smaller than 5 MB in size. If for any reason you are unable to submit a file online, please contact the Editorial Office by e-mail at office@biosciencetrends.com.

7. Accepted Manuscripts

Proofs: Galley proofs in PDF format will be sent to the corresponding author via e-mail. Corrections must be returned to the editor (proof-editing@biosciencetrends.com) within 3 working days.

Offprints: Authors will be provided with electronic offprints of their article. Paper offprints can be ordered at prices quoted on the order form that accompanies the proofs.

Page Charge: Page charges will be levied on all manuscripts accepted for publication in BioScience Trends ($140 per page for black white pages; $340 per page for color pages). Under exceptional circumstances, the author(s) may apply to the editorial office for a waiver of the publication charges at the time of submission.

(*Revised October 2011*)

Editorial and Head Office:
Pearl City Koishikawa 603
2-4-5 Kasuga, Bunkyo-ku
Tokyo 112-0003 Japan
Tel: +81-3-5840-8764
Fax: +81-3-5840-8765
E-mail: office@biosciencetrends.com

BioScience Trends

JOURNAL PUBLISHING AGREEMENT (JPA)

Manuscript No.:

Title:

Corresponding Author:

The International Advancement Center for Medicine & Health Research Co., Ltd. (IACMHR Co., Ltd.) is pleased to accept the above article for publication in BioScience Trends. The International Research and Cooperation Association for Bio & Socio-Sciences Advancement (IRCA-BSSA) reserves all rights to the published article. Your written acceptance of this JOURNAL PUBLISHING AGREEMENT is required before the article can be published. Please read this form carefully and sign it if you agree to its terms. The signed JOURNAL PUBLISHING AGREEMENT should be sent to the BioScience Trends office (Pearl City Koishikawa 603, 2-4-5 Kasuga, Bunkyo-ku, Tokyo 112-0003, Japan; E-mail: **office@biosciencetrends.com**; Tel: **+81-3-5840-8764**; Fax: **+81-3-5840-8765**).

1. Authorship Criteria

As the corresponding author, I certify on behalf of all of the authors that:

1) The article is an original work and does not involve fraud, fabrication, or plagiarism.
2) The article has not been published previously and is not currently under consideration for publication elsewhere. If accepted by BioScience Trends, the article will not be submitted for publication to any other journal.
3) The article contains no libelous or other unlawful statements and does not contain any materials that infringes upon individual privacy or proprietary rights or any statutory copyright.
4) I have obtained written permission from copyright owners for any excerpts from copyrighted works that are included and have credited the sources in my article.
5) All authors have made significant contributions to the study including the conception and design of this work, the analysis of the data, and the writing of the manuscript.
6) All authors have reviewed this manuscript and take responsibility for its content and approve its publication.
7) I have informed all of the authors of the terms of this publishing agreement and I am signing on their behalf as their agent.

2. Copyright Transfer Agreement

I hereby assign and transfer to IACMHR Co., Ltd. all exclusive rights of copyright ownership to the above work in the journal BioScience Trends, including but not limited to the right 1) to publish, republish, derivate, distribute, transmit, sell, and otherwise use the work and other related material worldwide, in whole or in part, in all languages, in electronic, printed, or any other forms of media now known or hereafter developed and the right 2) to authorize or license third parties to do any of the above.

I understand that these exclusive rights will become the property of IACMHR Co., Ltd., from the date the article is accepted for publication in the journal BioScience Trends. I also understand that IACMHR Co., Ltd. as a copyright owner has sole authority to license and permit reproductions of the article.

I understand that except for copyright, other proprietary rights related to the Work (*e.g.* patent or other rights to any process or procedure) shall be retained by the authors. To reproduce any text, figures, tables, or illustrations from this Work in future works of their own, the authors must obtain written permission from IACMHR Co., Ltd.; such permission cannot be unreasonably withheld by IACMHR Co., Ltd.

3. Conflict of Interest Disclosure

I confirm that all funding sources supporting the work and all institutions or people who contributed to the work but who do not meet the criteria for authors are acknowledged. I also confirm that all commercial affiliations, stock ownership, equity interests, or patent-licensing arrangements that could be considered to pose a financial conflict of interest in connection with the article have been disclosed.

Corresponding Author's Name (Signature):

Date: